

BHANDER LIMESTONE OF BUNDI, RAJASTHAN- QUALITY ASSESSMENT FOR CEMENT INDUSTRY

A THESIS

*Submitted in fulfilment of the
requirements for the award of the degree*
of
DOCTOR OF PHILOSOPHY
in
EARTH SCIENCES

By

MOHAMMAD IMRAN



DEPARTMENT OF EARTH SCIENCES
INDIAN INSTITUTE OF TECHNOLOGY ROORKEE
ROORKEE-247 667 (INDIA)

NOVEMBER, 2003

551.07

I M R

CANDIDATE'S DECLARATION

I hereby certify that the work, which is being presented in the thesis, entitled "**Bhander Limestone of Bundi, Rajasthan – Quality Assessment for Cement Industry**" in fulfillment of requirement for the award of the degree of Doctor of Philosophy and submitted in the Department of Earth Sciences, Indian Institute of Technology, Roorkee is an authentic record of my own work carried out during a period from November 1997 to November 2003 under the supervision of Dr. A. K. Awasthi, Professor, Department of Earth Sciences, Indian Institute of Technology, Roorkee, Dr. D. C. Srivastava, Professor, Department of Earth Sciences, Indian Institute of Technology, Roorkee and Dr. S. P. Ghosh, Ex-Director General, National Council for Cement and Building Materials, Ballabgarh.

The matter presented in this thesis has not been submitted by me for the award of any other degree of this or any other Institute.


20/11/03

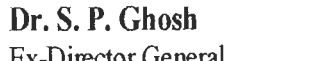
Date : 20. 11. 2003

MOHAMMAD IMRAN

This is to certify that the above statement made by the candidate is correct to the best of my knowledge.



Dr. D. C. Srivastava
Professor
Department of Earth Science
IIT Roorkee
Roorkee 247667, India

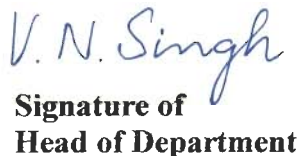

Dr. S. P. Ghosh
Ex-Director General
National Council for Cement
and Building Materials
Ballabgarh 121004, India

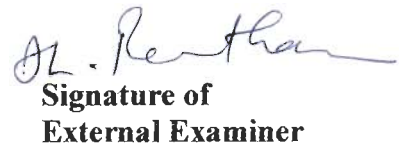

20/11/03

Dr. A. K. Awasthi
Professor
Department of Earth Science
IIT Roorkee
Roorkee 247667, India

The Ph.D. Viva-Voce examination of MOHAMMAD IMRAN, Research Scholar, has been held on


14/8/04
D.C. Srivastava
Signature of
Supervisor(s)


V. N. Singh
Signature of
Head of Department


**Signature of
External Examiner**

ACKNOWLEDGEMENT

I feel great pleasure in expressing my profound and sincere gratitude to Dr A K Awasthi, Professor in Geology, Department of Earth Sciences, Indian Institute of Technology, Roorkee for his thought provoking ideas, constant support, guidance, cheerful encouragement and help at every stage of this research work. It would not have been possible for me to complete this thesis without his cooperation and involvement.

I am grateful to my co-guides Dr D C Srivastava, Professor in Geology, Department of Earth Sciences, Indian Institute of Technology, Roorkee and Dr S P Ghosh, Ex-Director General, National Council for Cement and Building Materials, New Delhi for their encouragement and suggestions at every available opportunity.

I express my sincere gratitude to Shri Shiban Raina, Director General, National Council for Cement and Building Materials, New Delhi, for his encouragement, motivation and support during the course of this research work.

I express my deep and heartfelt thanks to Shri Anurag Srivastava and Shri Amit Sahay for their continued co-operation, support and help during the course of this work.

I sincerely acknowledge the co-operation of all my colleagues in National Council for Cement and Building Materials during the course of this research work. My special thanks are due to Shri N L Murthy, , Shri B S Roy, Dr S K Handoo, Dr V P Chatterjee, Dr Pankaj Srivastava, Shri N K Sharma, Shri R N Sharma, Dr M M Ali, Shri C K Sharma, Dr V K Mathur , and Shri S C Sharma for their help, support and cooperation from time to time.

My heartfelt thanks are due to Mrs P Awasthi and Dr Amita Srivastava for their moral support, encouragement and help during my stay at Roorkee.

I sincerely acknowledge the untiring efforts and patience of Miss Poornika Rishi in typing the manuscript of the thesis efficiently.

And above all, my sincere and heartfelt gratitude to my loving wife Shaheen Neha, wonderful sons Naved and Ramiz and my parents for their continued encouragement, co-operation, motivation and patience throughout the course of this research work.



Mohammad Imran

ABSTRACT

In the Bundi district of Rajasthan (Western India), a large tract of barren land occupied by vast surface exposures of limestone occurs conspicuously. This poorly and sparsely inhabited calcareous rock bearing terrain, with little cultivation, forms the locale of this study. This investigation aims at assessing the possible use of these limestones as raw material for manufacturing cement, the demand of which is continually increasing with the increasing developmental activities in the adjoining and nearby areas. Geographically, the area of study is located 10 km northwest-of the Bundi city along the National Highway No. 12.

Geologically, these 'limestones' known as the Bhander Limestone, belong to and form a part of the uppermost unit of the Vindhyan Supergroup, (Upper Proterozoic -Lower Cambrian?). Lithologically, this area exhibits limestone along with sandstone and shales. These units have been mapped on the basis of False Colour Composite (FCC) using IRS-LISS III Satellite data and field investigations.

The Great Boundary Fault, which defines the western boundary between Achaean meta-sediments and the Vindhyan Supergroup, passes just north of the area of study. The rocks in this area occur in the form of non-plunging anticlinally folded structure, with ENE-WSW axis. Pink shales forming low land occupy the core of the fold. The overlying pink to grey coloured limestone exhibits gently undulating topography and the youngest pink, pale grey, red brown to white coloured sandstone forms ridge like topographic feature.

Bhander Limestone

The calcareous sediments of the Bhander Limestone, locally called Lakheri Limestone, are characterized by pink, blue-grey, light grey, green and dark grey

colours. Petrographic studies indicate that they are micritic in nature. Based on physical characteristics, petrography, stratification and internal structures, the Bhandar limestone in this area can be classified into the following four Lithounits.

Lithounit A

The oldest Lithounit A consisting of pink to red coloured limestone lies over the Ganurgarh Shales (pre-Bhandar Limestone) and has gradational contact with it. This argillaceous limestone is composed of micrite (as per classification of Bissell and Chilingar 1967) with 10% or more admixture of terrigenous sediments. Intramicrudite occurs in the form of lenses of flat pebble breccia. Thin sections studies under microscope show abundant horizontal fenestrae and bird's eye structures filled with sparry calcite.

The features such as horizontal fenestrae, bird's eye structures, appreciable content of terrigenous admixture, general absence of algal mats, presence of micrite rich channels of small dimensions and predominant pink colour of sediments collectively indicate high to low supratidal depositional environment for Lithounit A.

Lithounit B

This blue to grey coloured calcareous Lithounit occurs above the Lithounit A with sharp contact. It also has in it some coarse grained beds with discontinuous lateral extent and generally devoid of sedimentary structures except for occasional symmetrical, straight crested ripple marks. These limestones show alternate dark and light coloured laminations. The calcareous beds, micritic in nature, show mud cracks suggesting their sub-aerial exposures. At places it exhibits profuse small domal stromatolites.

The features such as profuse development of algal mats, mud cracks, graded bedding, high energy conditions, reversal of current direction within the channels in

this Lithounit, suggest its deposition in the high intertidal flat zone and in the transitional zone onto the supratidal flat.

Lithounit C

Overlying the Lithounit B, this Lithounit mainly comprises fine-grained sediments in the form of calcareous shales with occasional lenses of calcareous siltstones. The shales are mostly olive coloured, but occasionally bright green. They are generally splintery in nature. The fine-grained nature of sediments together with the thin lamination and general absence of current and wave formed structures indicate suspension deposits of low energy depositional environment for this Lithounit.

Lithounit D

Overlying the Lithounit C, this dark grey to black coloured Lithounit 'D' is the youngest Lithounit. It consists of laminated to thin-bedded limestones, which are mainly micritic in nature. Palisade structure is common but ripple laminations, flaser bedding and symmetrical ripple marks also occur occasionally in this unit.

The abundance of micrite, absence of features of intermittent exposures, black colour of sediments and presence of algal mats suggests mainly the protected, shallow, sub-tidal environment, in which this unit was deposited.

Spectral Response of Lithounits

From what has been said above, it is apparent that each Lithounit of the Bhandar Limestone was born in its own depositional environment, which is characteristically indicated by the physical imprints, bio-indicators and chemical make up of sediments deposited in it. If this is so, then each Lithounit should have its own spectral response to various electromagnetic waves and therefore can be differentiated from one

another. With this premise an attempt was made to identify various calcareous Lithounit of the Bhandar Limestone using remote sensing data. The pixel values of IRS-LISS III data were determined for bands 2, 3, 4 and 5 in the wavelength range of 0.52 – 0.59 (Green), 0.62 – 0.68 (Red), 0.77-0.86 (Near Infrared) and 1.55 – 1.70 (SWIR) respectively. These Lithounits could not be differentiated in the band 2, 3 and 4. However, in Linear Contrast Image of band 5 of Short-Wave Infrared in wavelength range of 1.55 to 1.70 μ m, the Lithounits A, B and D with average pixel values of 152, 140 and 127 respectively, can be identified to some extent.

Bhandar Limestone as Raw Material for Cement

Portland cement - a commonly used binding substance is composed mainly of silicates, aluminates and ferro-aluminates of lime. Limestone is the major raw material required for the manufacturing of cement, besides other additives such as laterite, bauxite, red ochre etc. As per norms evolved by the National Council for Cement and Building Materials (India), compositionally, a limestone should have CaO between 44 and 52%, SiO₂ less than 14% and MgO less than 3.5% so as to qualify for use as raw material for cement manufacturing.

In order to assess the quality of the Bhandar Limestone for cement manufacturing, 160 representative limestone samples were collected from the area of study, covering different Lithounit. The samples were powdered to – 160 mesh size and analyzed for CaO, SiO₂, Al₂O₃, Fe₂O₃, MgO and Loss on Ignition (LOI), besides other minor constituents such as Na₂O, K₂O, SO₃, Cl, P₂O₅ and Mn₂O₃.

X Ray Fluorescence (XRF) technique and the Wet chemical analyses following IS-1727-1967 and Standard method evolved by National Council for Cement and Building Materials (NCB) were carried out

The comparison of chemical composition for various Lithounits of Bhander Limestone with the NCB prescribed specifications for cement grade limestone suggests the following:

- (i) The limestones of the Lithounits B and D qualify for use directly in the cement manufacturing. Lithounit D has highest CaO and lowest SiO₂ as compared to other Lithounits B, A and C and it therefore provides the best variety of cement grade limestone.
- (ii) The limestone of Lithounit B qualifies for direct use as raw material for cement.
- (iii) The calcareous unit A is marginally sub-grade and can only be used, if blended with Lithounit D.
- (iv) The argillaceous unit- C does not qualify for cement manufacturing.

In view of this, the limestone of the area has been classified into three categories - High Grade (CaO >48%, SiO₂ <10%), Acceptable Grade (CaO 44-48%, SiO₂ 10-12%) and Sub Grade (CaO 42-44%, SiO₂ 13-16%).

The Sub-Grade Limestone can be upgraded with the High Grade Limestone of the Lithounit D. In addition to limestone, raw materials rich in Fe₂O₃ and Al₂O₃ are also required in small quantities for the manufacturing of cement for which laterite, bauxite and red ochre are found to occur in plenty in the nearby areas namely Pratapgarh near Chittorgarh and Iswal near Udaipur, located at a distances of 220 and 280 kms. from this area respectively.

Raw Mix Design for Cement

Limestones, laterite / bauxite and red ochre are the important raw materials required for manufacturing cement. The proportion of each of these depending upon their chemical composition plays important role in the production of cement of desired quality.

In order to optimally utilize the High Grade Limestone of Lithounit D with the Sub-Grade or blendable grade limestone of Lithounit A, several raw mix proportions were worked out along with red ochre and laterite or bauxite. Amongst the many possible proportions of these constituents, two types of Raw Mix Designs have optimally been worked out, conforming to the prescribed specifications for production of desired quality of cement, one with High Grade limestone as 12%, Sub Grade limestone as 85% laterite 2.0% and red ochre 1.0% and the other one with 12% High Grade limestone, 86% Sub Grade limestone alongwith red ochre and bauxite as 1% each.

The theoretically worked out proportions were used to calculate the potential composition of kiln feed and clinker. The moduli values (ratios of oxide components in clinker) and phase compositions of resultant clinker were then calculated and compared with the standard values prescribed for cement manufacturing. The Moduli values and phase composition, thus calculated, were found to be well within the prescribed standard ranges for cement manufacturing.

Laboratory Experiments

With a view to test the efficacy of the above mentioned theoretically optimized Raw Mix Designs, laboratory experiments were conducted. The samples as per proposed designs of the two types of raw mixes were prepared from weighted average quantities of raw materials. These were ground in a ball mill to a fineness of 170 mesh size. The nodules thus prepared were fired in electric furnace at 1350°, 1400° and 1450°C temperatures. The resultant clinkers were analyzed for free lime content. The free lime content in clinker nodules based on Type 1 and Type 2 designs, were

determined as 0.3 and 0.9% respectively and are less than maximum permissible limit of 1%, implying thereby proper burning of raw mixes.

The Cement was then prepared on laboratory scale by grinding the laboratory fired nodules clinkers with 5% gypsum. The cements thus prepared for both type 1 and type 2 designs were tested for setting time, compressive strength and Le-Chatelier and autoclave expansion tests as per standard procedures. The initial and final setting time for the first and second cement samples are 55, 190 minutes and 50, 180 minutes respectively. The 28 days strength of the cements prepared was found to be 51 N/mm² and 51.8 N/mm² respectively, which are well above the minimum prescribed limit of 35 N/mm². Thus these and likewise the other properties of laboratory made cement conform to Indian Standard specification for Portland cement, thereby validating theoretically worked out proportions of various constituents in both types of Raw Mix Designs.

Feasibility of Setting of Cement Plant

With a view to assess the feasibility of setting of a cement plant in the area, an attempt has been made to estimate the quantum of limestone, the cost of Cement manufacturing and other related expenditures. In this area, on a conservative side, the possible reserve of limestone of Lithounits A, B and D have been worked out to be of the order of 69.5, 437.5 and 96.8 million tonnes respectively. Taking 1.5 as limestone consumption factor, the calcareous Lithounits A, B and D are good enough to manufacture 403 million tonnes of cement.

The cost to manufacture cement has been estimated as Rs. 1670/- per tonne at current rate. The profit margin as per current selling price of Rs 2100/- per tonne has been worked out to be Rs. 430/- per tonne. On the basis of this, it is concluded that prima facie, on techno-economic basis, an eco - friendly 2 to 3 million tonne per annum capacity cement plant can be setup in the area. The barren area with well

exposed limestone outcrops and negligible soil overburden, sparse habitation, little landuse, and availability of road and rail transport facilities, further make this limestone terrain attractive for such a venture.

As a spin off advantage, the proposed cement plant can utilize the industrial wastes of lead-zinc slag of Hindustan Zinc Ltd. Chittorgarh, fly ash from the Thermal Power Plant at Kota, Phospo Gypsum from fertilizer plant at Kota and low grade gypsum from Bikaner, located at distances of 250 km, 60km, and 300 km respectively to produce Pozzolana cement and slag cement.

In conclusion, it is surmised that the calcareous Lithounits B, A and D of the Bhander limestone, locally known as Lakheri Limestone, deposited in the physico chemical environment ranging from low energy to tidal (intertidal to supratidal), are quality wise and quantity wise good enough to be used as raw material for commercial manufacturing of Portland cement by an environmentally friendly cement plant in this area which is characterized by easy availability and workability of limestone, besides transport facilities. In addition, the proposed plant can also be put to use the industrial wastes of other nearby factories to manufacture Pozzolana and slag cements.

Contents

Page No.

Candidate's Declaration

Acknowledgement

Abstract

1.	INTRODUCTION	1
1.1	Background	1
1.2	The Area of Study	3
1.3	Scope of the Present Investigations	4
2.	GEOLOGICAL FRAMEWORK	7
2.1	Review of Previous Literature	7
2.2	Regional Geological Set up	7
2.3	Geology of Bundi Area	8
2.4	Structures	13
	2.4.1 Major Structures	13
	2.4.2 Minor Structures	14
2.5	Spectral Signatures of Various Geo- elements	17
	2.5.1 Ground Reflectance Data	17
	2.5.2 IRS – LISS III Satellite Data	18
	2.5.3 Landuse Pattern	20
3	QUALITY PREREQUISITES OF CEMENT GRADE LIMESTONE – A REVIEW	23
3.1	Introduction	23
3.2	Mineralogical Constituents of Raw Materials and Their Role in Cement Manufacturing	24
	3.2.1 Impact of Mineral Constituents of Calcium Carbonate	24
	3.2.2 Impact of Mineral Constituents of MgO	25
	3.2.3 Impact of Mineral Constituents of Silica and Silicates on Burnability and Clinker Properties	26

3.3	Chemical Parameters	26
	3.3.1 Major Oxides	29
	3.3.2 Minor Constituents in Cement Production And Their Effects	30
3.4	Physical Properties of Raw Materials and Their Role in Cement Preparation	32
	3.4.1 Natural Moisture Content	33
	3.4.2 Strength Parameters	33
3.5	Summary	33
4	BHANDER LIMESTONE – ITS LITHOUNITS, PETROGRAPHY AND DEPOSITIONAL ENVIRONMENT	35
4.1	Introduction	35
4.2	Lithounits of Bhander Limestone	36
	4.2.1 Lithounit A	37
	4.2.2 Lithounit B	47
	4.2.3 Lithounit C	56
	4.2.4 Lithounit D	59
4.3	Spectral Response of Lithounits	64
4.4	Summary	66
5.	EVALUATION OF BHANDER LIMESTONE AS SOURCE OF CEMENT	69
5.1	Introduction	69
5.2	Geochemical Analysis	69
	5.2.1 Determination of Loss on Ignition	70
	5.2.2 Determination of Silica	70
	5.2.3 Determination of Calcium Oxide and Magnesium Oxide	71
5.3	X – Ray Fluorescence Spectrometry	76
5.4	Strength Parameters	77
5.5	Assessment of Limestone Reserves	77
	5.5.1 Categorization of Reserves	78
	5.5.2 Method of Reserves Estimation	79
5.6	Technical Classification of Bhander Limestone	81
5.7	Estimate of Block Capital Cost and Cost of Production of Cement	81

5.7.1	Estimate of Block Capital Cost	81
5.7.2	Estimate of Cost of Production	82
5.8	Summary	84
6	RAW MIX DESIGN FOR OPTIMAL UTILIZATION OF MARGINAL GRADE LIMESTONE	85
6.1	Introduction	85
6.2	Burnability of the Selected Raw Mixes	90
6.3	Preparation and Evaluation of Bulk Clinker	90
6.4	Chemical Analysis of Clinker	91
6.5	Optical Microscopic Studies of Clinker	91
6.6	Preparation and Evaluation of Ordinary Portland Cement	92
6.7	Setting Time of Cement	93
6.8	Compressive Strength	93
6.9	Soundness	93
6.10	Summary	93
7	SUMMARY AND CONCLUSIONS	99
	ANNEXURE – I	111
	ANNEXURE – II	119
	REFERENCES	123

LIST OF FIGURES

<u>Sl. No.</u>	<u>Contents</u>	<u>Page No.</u>
1.1	Geological Map of the Vindhyan Basin	2
1.2	Geographical and Geological Location of the Study Area	3
2.1	Geological Map of the Area	9
2.2	Ground Reflectance of Shale, Sandstone and Limestone of the Area	18
2.3	Pixel Values of Various Lithologies in Raw Images of Different Bands of IRS-LISS-III Satellite Data	19
2.4	Geological Map of the Study Area Generated from IRS-LISS-III Satellite Data	21
4.1	Lithounit- A Showing Wavy and Discontinuous Laminae	41
4.2	Lithounit A Showing Intraformational Breccia	41
4.3	Vertical Section of Lithounit A Showing Intraformational Breccia	42
4.4	Lithounit A Showing Silty Micrite	42
4.5	Photomicrograph Showing Clusters of Quartz and Magnetite in the Carbonate Matrix of Lithounit A	43
4.6	Photomicrograph Showing Three Sets of Calcite Micro Veins Cutting Across Each Other in the Carbonate Matrix of Lithounit A.	43
4.7	Photomicrograph Showing Poorly Developed Lamination Planes of Magnetite and Quartz Grains in the Carbonate Matrix of Lithounit A.	44

4.8	Photomicrograph Showing Predominant Magnetite Grains Along with Minor Quartz Grain in the Carbonate Matrix of Lithounit A.	44
4.9	Photomicrograph Showing Discontinuous Micro Vein of Quartz and Calcite in Lithounit A.	45
4.10	Photomicrograph Showing Cluster of Quartz of Varying Sizes in the Carbonate Matrix in Lithounit A.	45
4.11	Photomicrograph Showing Clusters of Magnetite, Quartz and Secondary Calcite in Lithounit A.	46
4.12	Photomicrograph Showing Clusters of Quartz in the Carbonate Matrix in Lithounit A.	46
4.13	Vertical Section of Lithounit B Showing Distinct Laminae of Micritic Limestone	52
4.14	Lithounit B Showing Trough Cross Bedding With Truncated Top and Asymptotic Bottom	52
4.15	Photomicrograph Showing Laminated Planes of Calcite With Scattered Quartz, Hematite and Magnetite Grains in Lithounit B	53
4.16	Photomicrograph Showing Formation of Secondary Calcite in its Initial Stage with Scattered Quartz Grains in Lithounit B	53
4.17	Photomicrograph Showing veins of secondary calcite grains with euhedral grain boundaries are developed in the carbonate matrix in Lithounit B	54
4.18	Photomicrograph of Well Sorted and Homogeneously Distributed Calcite Grains Along With Magnetite (black) and Quartz (dark blue) Grains in Lithounit B	54
4.19	Photomicrograph Showing Clusters of Calcite and Dolomite Depicting the Grain Size Variation	

	in the Limestone in Lithounit B	55
4.20	Photomicrograph Showing Clusters of Secondary Calcite and Dolomite in the Carbonate Matrix in Lithounit B	55
4.21	Photomicrograph Showing Well Sorted and Homogeneously Distributed Calcite Grains with Poorly Oriented Magnetite Grains in Lithounit B	56
4.22	Lithounit C Showing Parallel Lamination in Jointed Olive Shale	57
4.23	Kink Folds in Lithounit C	58
4.24	Kink Folds in Splintery Olive Shales of Lithounit C	58
4.25	Lithounit D Consisting of Thinly Bedded Micritic Limestone	60
4.26	Vertical Section of Thickly Bedded Micritic Limestone of Lithounit D	60
4.27	Domal Structure in Thick to Thinly Bedded Lithounit D of Micritic Limestone	61
4.28	Photomicrograph Showing Well Sorted and Homogeneously Distributed Calcite Grains with Micro Fractures in Lithounit D	61
4.29	Photomicrograph Showing Three Sets of Discontinuous Calcite Veins Cutting Across Each Other Within Fine Grained Lamination Plane of Lithounit D	62
4.30	Photomicrograph Showing Well Sorted and Homogeneously Distributed Calcite Grains in Lithounit D. Black Grains Represent Magnetite	62
4.31	Photomicrograph Showing Discontinuous Micro Veins of Calcite in the Carbonate Matrix in Lithounit D	63

4.32	Photomicrograph Showing Well Sorted and Homogeneously Distribute Calcite Grains Relatively Finer in size in Lithouint D	63
4.33	Map Showing Lithounits of Bhander Limestone in the Study Area	65
4.34	Pixel Values of Limestone Lithounits (In Linear Contrast Image of IRS-LISS-III Satellite Data)	66
6.1	Sources of Additives, Lignite(Fuel), Industrial and Mining WastesWith Respect to Study Area	87
6.2	Photomicrograph of RM-1 Showing Clusters of C₂S Surrounded by Lath Shaped C₃S Grains On the Periphery, 50x	95
6.3	Photomicrograph of RM-1 Showing Transformation of C₂S in C₃S, Rounded C₂S Grains and Lath Shaped Grains with Inclusions, 100x	95
6.4	Photomicrograph of RM-1 Showing Fused Grains of C₃S, Rounded C₂S Grains and Clustered Interstitial Matters,	96
6.5	Photomicrograph of RM-1 Showing Transformation of Clinker Phases,	96
6.6	Photomicrograph of CL-1 Showing Hexagonal and pseudo hexagonal Grains of C₃S	97
6.7	Photmicrograph showing C₃S alongwith Clusters of C₂S	97
6.8	Photomicrograph showing homogeneous Distribution of C₂S and C₃S,	98
6.9	Photomicrograph Showing pseudo-Hexagonal Alite grains	98

LIST OF TABLES

<u>Sl. No.</u>	<u>Contents</u>	<u>Page No.</u>
2.1	Lithostratigraphy of Lower Bhander Sub group In the Area (after Prasad, 1984)	9
3.1	Dependence of Reactivity of Calcite on Crystallinity and Grain Size of Limestone	25
3.2	Chemical Specifications of Cement Grade Run-of-Mine Limestone (NCB- Norms modified, 2000)	28
4.1	Petrographic Analysis of Lithounit A	38
4.2	Petrographic Analysis of Lithounit B	48
5.1	Chemical Constituents (%) of Limestone Samples of Lithounit A	72
5.2	Chemical Constituents (%) of Limestone Samples of Lithounit B	73
5.3	Chemical Constituents (%) of Lithounit C (Olive Shale) of Bhander Limestone	74
5.4	Chemical Constituents (%) of Limestone Samples of Lithounit D	75
5.5	Permissible Difference in Chemical Analysis of Components	76
5.6	Minor Chemical Constituents in Bhander Limestone of Study Area	76
5.7	Strength Parameters of Limestone of Bundi Area	77
5.8	Estimation of Limestone Reserves in Bundi area	80
5.9	Estimated Capital Cost for 1 MTPA Cement Plant	82
5.10	Estimates of Production Cost	83

6.1	Average Chemical Composition of Bhander Limestone and Corrective Materials Used for Raw Mix Design	86
6.2	Raw Mix Proportions using Laterite and Red Ochre	88
6.3	Modulii values and phase composition of various Raw Mix Design	88
6.4	Design parameters of cement Raw Mixes and resultant clinker along with potential phase composition using bauxite	89
6.5	Burnability studies of Raw Mixes prepared	90
6.6	Mineral Phase analysis of clinker samples by optical microscopy	91
6.7	Performance of ordinary Portland cement prepared In laboratory	92
6.8	Performance of Ordinary Portland cement prepared In Laboratory	92
7.1	Average chemical composition of lithounits of Bhander Limestone	104
7.2	Categories of limestone based on chemical Parameters	105
7.3	Minor constituents in Bhander Limestone	106
7.4	Raw Mix Proportion for Cement Production	107
7.5	Principal Modulii Values and Phase Composition of Raw Mixes	107
7.6	Bhander Limestone and its Assessment for Cement Manufacturing	110

CHAPTER 1

INTRODUCTION

1.1 Background

Portland cement makes up about 98 percent of the world's cement production used for construction purposes. Though India ranks second in production of cement after China, its per capita consumption of 100 kg is much below the world's average of 270 kg. In order to meet the ever-increasing demand of cement with rising developmental activities, there is scope for setting up new cement units. Portland cement is mainly composed of silicates, aluminates and ferro-aluminates of lime, hence the limestone of requisite quality is the basic raw material for cement making. The availability of potential limestone deposits for Greenfield cement projects has been restricted by environmental considerations, viz. forest cover, Coastal Regulation Zone, rapid urbanization etc. There is, therefore, an urgent need to explore more and more limestone deposits suitable for cement production, in order to cater to the requirement of Cement Industry.

In India, a thick pile of sedimentary rocks belongs to what is geologically known as Vindhyan Supergroup. These rocks consist dominantly of limestone, shale and sandstone and are found to occur north of Narmada-Son rivers and east of the Aravalli mountain (Fig. 1.1). Although the Vindhyan rocks have been studied from various angles by many workers such as Oldham (1856), Medicott (1860), Mallet (1869), Hackett (1881), Heron (1917, 1922, 1936), Coulson (1927), Prasad (1975, 1980, 1981, 1984), Iqbaluddin et al., (1978), Soni et al. (1987), Srivastava et al. (1998, 1999) for more than hundred years or so, little investigations have been done on the quality assessment of these limestones for their use in the Cement Industry.

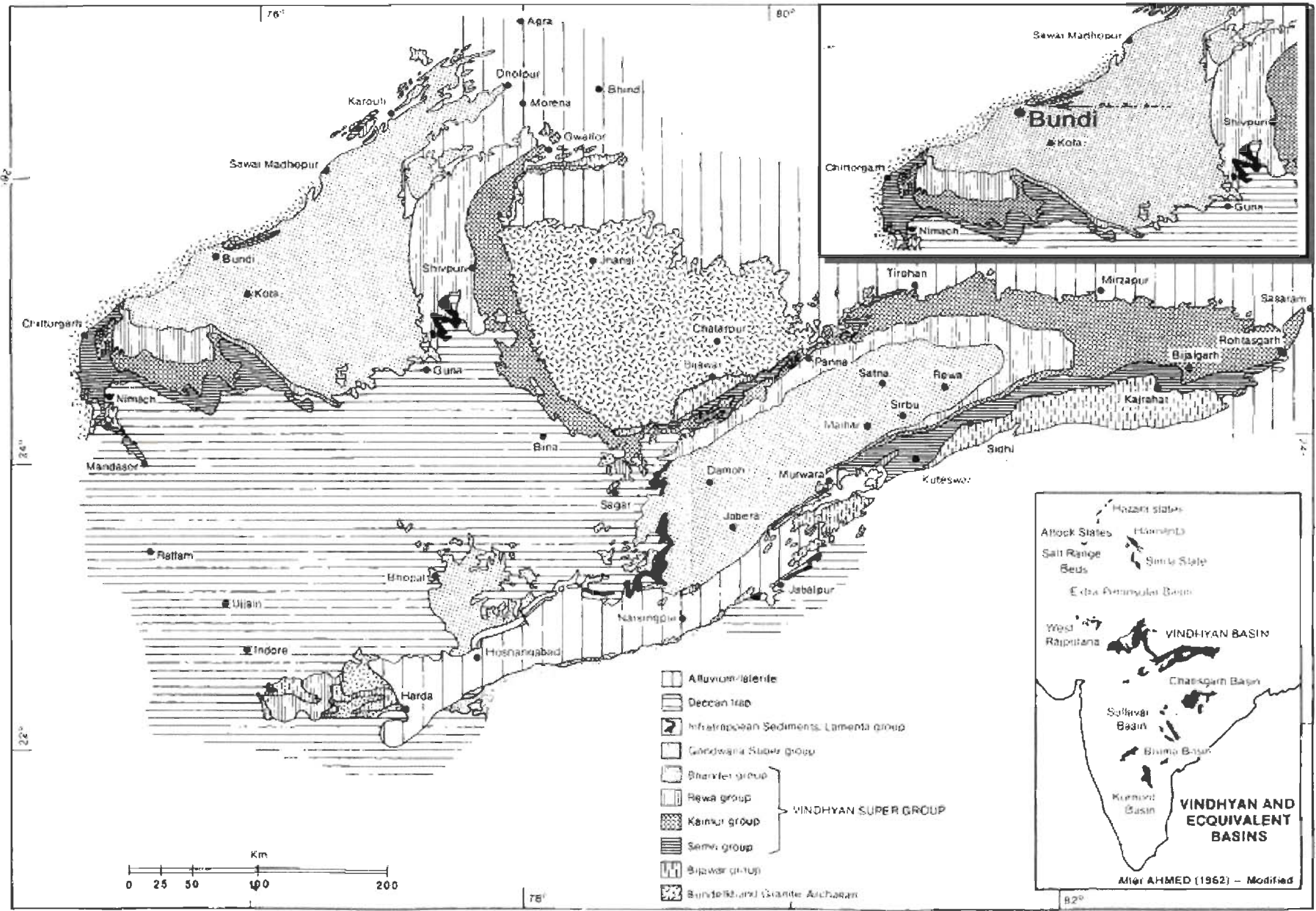


Fig. 1.1 : GEOLOGICAL MAP OF THE VINDHYAN BASIN (After Soni et.al. 1987)

The present study is an attempt in this direction to evaluate these limestone deposits for their possible use by Cement Industry, and explore the possibility of using simpler, quicker and cost effective approach of remote sensing, which may help in identifying cement quality limestone in this and adjoining areas.

1.2 The Area of Study

The area of study is located around Satur Village, 10 km northeast of Bundi city of Rajasthan, along the National Highway No. 12. The study area is located between latitude $25^{\circ}25'$ to $25^{\circ}30'N$ and longitude $75^{\circ}30'$ to $75^{\circ}40'E$ and falls on Survey of India Toposheet No 45 O/11. The location of the study area is shown in the Fig. 1.2. This particular area has been selected because it occupies various varieties of limestone associated with shales and sandstone. The Bhander Group, being the youngest, occupies the largest exposed area in the Vindhyan formation. The rocks have little overburden of soil or other rocks and therefore, provide good opportunity for radiometric and satellite observations of barren outcrops.

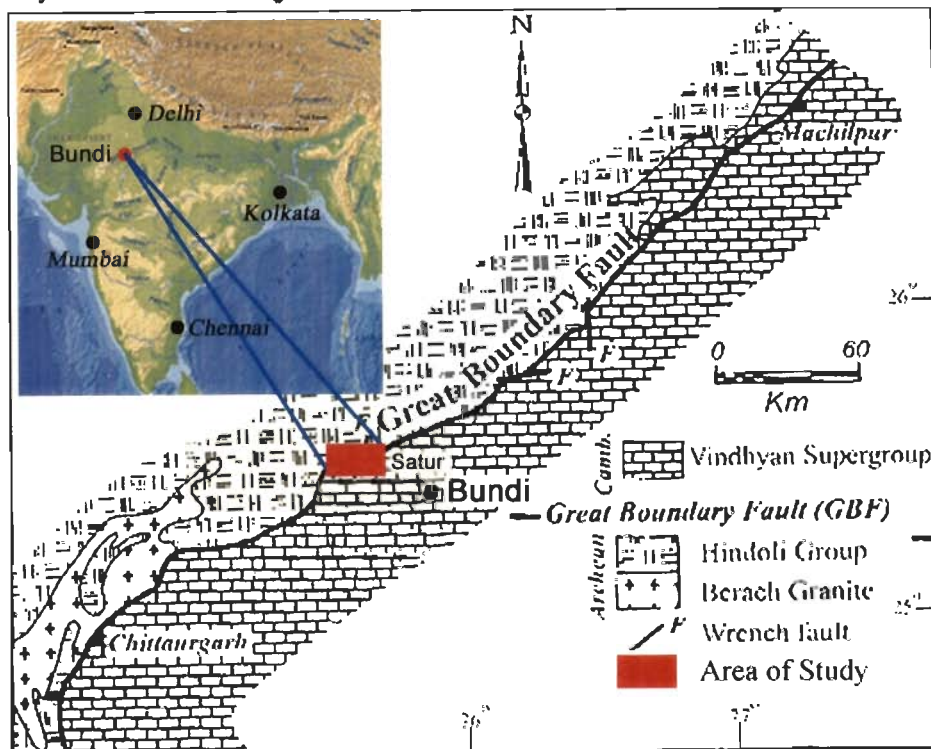


Fig. 1.2 Geographical and Geological Location of the Study Area
(after Srivastava et al. 1998)

Physiographically, the area consists of gently undulating topography with high ridges of sandstone having maximum elevation of 498 meters above the mean sea level and low lying elongated domal shaped hillocks of limestone at elevation ranging between 349 m and 300 meters, above the mean sea level. The general topographic relief of the area is 198 meters. However, in the limestone bearing terrain, it is only 43 m.

The area is sparsely vegetated with thorny bushes, shrubs and small trees. The cultivated fields were confined to Ganurgarh shale formation, at the core of anticline. Extreme weather conditions are prevalent in the area with lowest temperature recorded in winter as 1° to 2°C and in summer between 42° to 48°C. Rainfall is generally scanty and the relative humidity recorded by hygrometer during fieldwork varies between 45 % - 80 %.

The area is, by and large, dry with few seasonal streams that are activated during rainy season. The dendritic drainage pattern was observed in limestone terrain. The ground water table observed in the dug wells is 15-20 m below the ground level.

1.3 Scope of the Present Investigations

The present work has been carried out to study and explore the possibility of use of limestone for cement manufacturing. A multi-disciplinary approach has been adopted involving field investigation, remote sensing techniques and laboratory analyses. The studies are broadly listed below :-

- a. Geological mapping of the area based on IRS-LISS-III Satellite Data and field traverses.
- b. Petrographic analyses and depositional environment of the Bhandar Limestone.

- c. Chemical analyses of the sediments pertinent to the Cement Industry.
- d. Identification of cement grade limestones and their spectral signatures in IRS LISS-III Satellite Data.
- e. Designing of the raw material mixes for the optimum use of limestone in cement manufacturing.
- f. Preparation of clinker and cement in the laboratory and testing them for their quality.
- g. Feasibility of setting up of a cement plant.

CHAPTER 2

GEOLOGICAL FRAMEWORK

2.1 Review of Previous Literature

Various facets of Vindhyan Basin have been studied in detail by a galaxy of workers. Probably the pioneering efforts in this direction were that of David Hiram Williams (West, 1981) who studied the Vindhyan rocks of “Keymore” range to the west of the Son river in the early part of 1848 while searching for coal. In 1854, Oldham also examined parts of the Vindhyan formation and gave a summary of his observations to the Asiatic Society in 1856 (West, 1981).

Oldham proposed the name Vindhyan, establishing the threefold division of “Keymore” (now spelled as Kaimur), Rewah and Bhandar “Series”, which have since been called upper Vindhyan. Medicott (1859) studied the Vindhyan of Son valley and classified them as Lower Vindhyan. Captain Dangerfield (1823), Franklin (1829) Jacquoment (1841) have discussed the nature of Vindhyan rocks during the course of search for diamonds in Panna area. The earliest comprehensive study of the Vindhyan system as a whole, based on the work on eastern part of the range, was however, brought out by Mallet in 1869. Hackett (1881) studied the Vindhyan of Rajasthan. Some of the important workers who have made significant contributions to the regional geology of the Vindhyan of Rajasthan include Coulson (1927), Heron (1917, 1922, 1936), Prasad (1975, 1976, 1980, 1981, 1984), Sinha-Ray et al. (1985, 1986, 1998), Ramasamy (1995), Tiwary (1995) and Srivastava et al. (1998, 1999).

2.2 Regional Geological Set-up

Rocks of the Vindhyan Super Group are found to occur mainly to the east, northeast, southeast of Aravalli mountains and north of Narmada-Son Lineament (Fig. 1.1). Vindhyan rocks of Rajasthan form the western part of the main Vindhyan

Basin, where they attain a thickness of about 3200 m, covering an area of about 24000 Sq Km (Prasad 1984).

The Vindhyan Supergroup consists of a group of rocks comprising conglomerate, sandstone, shale, limestone, porcellanite and basic effusions occupying a large basin, which is extending from Dehri On Son to Hoshangabad and from Chittorgarh to Agra (Fig. 1.1). At different horizons, these rock units show variation in general characters such as grain size, compactness, interbedding etc. However, these variations do not have a definite norm or trend.

The Vindhyan rocks are inferred to have been laid down in a shallow marine environment characterised by intermittent periods of subaerial exposures and euxinic conditions (Prasad, 1981). However, Kale and Phansalkar (1985) suggested an outer shelf environment of deposition for majority of Vindhyan rocks with some intervening formation having been deposited in shore or lagoonal environment.

Stratigraphically, the Vindhyan Super Group have been divided into two groups - the Lower Vindhyan and the Upper Vindhyan. The rocks of the Lower Vindhyan Group are predominantly calc-argillaceous marine sediments. The lithology of the Lower Vindhyan in a complete section of 1500 m in Chittorgarh area from the Basal stage up to Rohtas Stage is represented approximately by 40% sandstone, 35% limestone, 20% shale and the rest 5% by chert and pyroclastics. The rocks of the Upper Vindhyan Group consist mainly of arenaceous sediments with calcareous and argillaceous intercalations.

2.3 Geology of Bundi Area

The study area consists of Lower Cambrian sedimentary sequence juxtaposed to the Great Boundary Fault (GBF) in western India (Fig. 2.1). The lithology of the study area comprises Ganurgarh shale, Lower Bhandar limestone

Samaria shale and lower Bhander sandstone. The geology of the area is shown in the Fig, 2.1, Table 2.1.

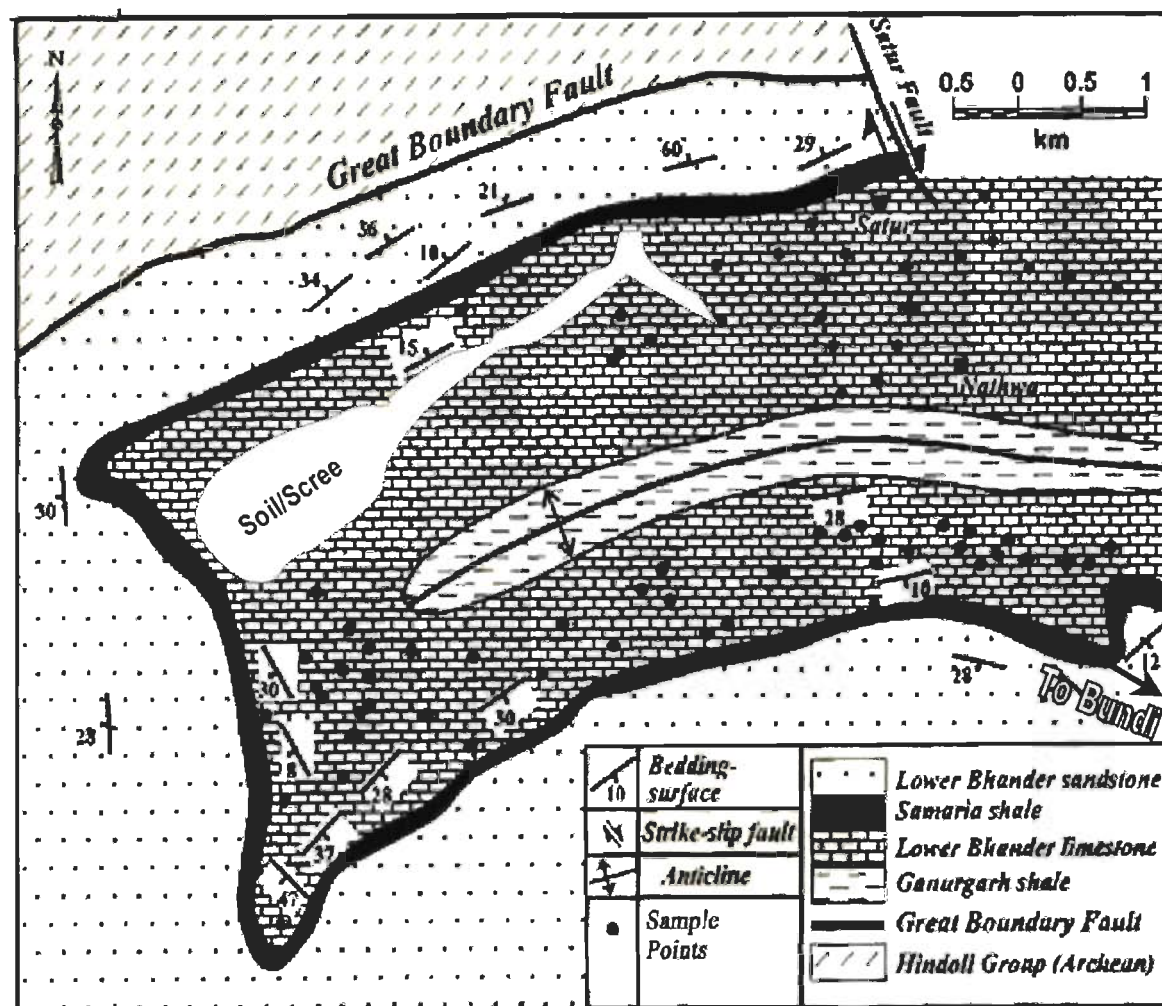


Fig. 2.1 : Geological Map of the Area (modified after Srivastava et al. 1999)

Table- 2.1 : Lithostratigraphy of Lower Bhander Subgroup in the area (after Prasad, 1984)

Group	Formation
Lower Bhander Sub Group (805 m)	Lower Bhander Sandstone (200 m)
	Samaria Shale (90 m)
	Lower Bhander Limestone (180 m) (Lakheri Limestone)
	Ganurgarh shale (180 m)

2.3.1 Lower Bhander Subgroup

The Lower Bhander consists of Ganurgarh Shale, Lower Bhander Limestone (Lakheri Limestone), Samaria Shale, Lower Bhander Sandstone, Sirbu Shale Formations and the Upper Bhander comprises Upper Bhander Limestone (Maihar Limestone) and Dholpura (Upper Bhander) shale Formations. The latter are exposed only in northeastern part of the area, viz in Lakheri – Kamleshwarji (25°46' ; 76°20') and Chhan (25° 55' ; 76° 28') – Kandher area and further northeast. Lower Bhander has the maximum extent and expanse amongst the upper Vindhya in the area. Lakheri (“Lower Bhander”) Limestone with characteristic ash grey colour, intraformational breccia at the base and non – stromatolitic nature, is the marker horizon. Sirbu Shale has scarce exposures due to its softness, is horizontally disposed, and consists of bands of grey and pink stromatolitic limestone intercalation. Bundi Hills (Lower Bhander Sandstone) constitute the Bundi Hills, which are the landmark with cuesta landform and associated scarp faces facing south. Structurally, Lower Bhanders maintain uniformity, because wherever faulted, they are missed or exposed in as a block. Samaria Shale underlying the Bundi Hill Sandstone always occur on the up dip slopes of this sandstone and is characterised by a siliceous dolomitic limestone horizon, pale yellow in colour, feebly stromatolitic and occurring as girdle around or as a hogback - like lenses.

Ganurgarh Shale

Ganurgarh shale is dark red or reddish brown, greyish green, purple, friable splintery and jointed. It is generally ferruginous and at places arenaceous, micaceous and calcareous towards the top. The ripple marks and the mud cracks are very common. Occasionally it is intercalated by lenticular and impersistent thin bands of limestone and dolomite varying in thickness from few centimeters to a meter. These reddish, pink coloured calcareous, laminations and lenses are argillaceous in nature.

Lower Bhandar (Lakheri) Limestone

Overlying the Ganurgarh shale with sharp contact, the Lower Bhandar limestone is typically ash grey to pink coloured persistent horizon, characterised by beds (0.1 to 0.6 m thick) of intraformational conglomerates and breccia at its base. Its thickness varies from about 30 m in southern part to about 150 m in the northern part. The thickness of individual beds of the limestone varies from 1.5 cm to 1.0 m.

Following the code of stratigraphic nomenclature, the name Lakheri Limestone was given by Prasad (1976, 1981) after the well known town Lakheri in Bundi District in place of Lower Bhandar Limestone.

The lower Bhandar (Lakheri) limestone is generally ash grey, bluish grey, chocolate, pink, reddish brown or purple. It is non-crystalline, massive and breaking with sub-conchoidal fractures or splitting along thin film of argillaceous parting. The argillaceous partings are 1cm to over 50 cm thick, more common in the lower part and also between reddish or pinkish limestone to grey limestone, which is characteristic of this limestone. There are one or two more pinkish coloured limestone bands in some parts. Polygonal suncracks are seen in the grey limestone on surfaces of the upper beds.

Intraformational conglomerate and breccia occurring in basal part consist of elongated, randomly oriented pellets of calcilutites set in argillaceous carbonate mud. Some pellets are oval and vary in thickness from less than a centimeters. Some have sharp edges and are even rectangular. Differential weathering and often staining of the pellets bring out the character of the beds. This type of rock seen elsewhere also with the other limestone units, but this peculiar structure is seen only on the weathered surfaces whereas the intraformational conglomerate seen at the base exhibit the feature even on breaking. Micro-laminations are observed in the arenaceous band in the lower portion. Backwash ripple marks have been observed in limestone at a few places.

Samaria Shale

Samaria shale overlies the non-stromatolitic Lakheri Limestone, ("Lower Bhander Limestone"). The Samaria shale is greenish, reddish brown, purplish and also pale yellow with dirty white banding. It is hard, fissile, jointed and ferruginous at places. Suncracks have also been observed at some places.

Samaria shale comprises a thin impersistent, impure dolomitic limestone member, siliceous and faintly stromatolitic at places. The shale always occur as a narrow strip of 0.1 to 0.5 km. It has maximum width near Samaria Kalan, the type area, where it is about 6 km wide. It is thinly bedded, the individual beds are a cm to a few cm thick, the total thickness of the formation varies from 40 m in Mandalgarh area, 90 m in Satur-Bundi-Gaindoli area to 130-135 m in Samaria Kalan, Talwas, Indergarh and Phalodi areas. In Satur, Samaria Kalan and Bhainsrorgarh areas stromatolitic limestone occur at about the middle of the sequence. Thin lenticular non-stromatolitic limestone with chert intercalation also occurs in Keshopura-Talwas-Indergarh area, apart from stromatolitic limestone, which also occurs as girdle all along the slope below the Bundi Hill Sandstone (Lower Bhander Sandstone).

Bundi Hill Sandstone

The Bundi Hill sandstone overlies conformably the Samaria shale. The sandstone is generally pale, pink, grey, red brown to white in colour, fine to medium grained, compact, ferruginous and occasionally micaceous in lower part and quartzitic in upper. Frequent cross bedding and ripple marks are seen and exhibits ball and pillow structures. Towards the central part the sandstone bears mega cross bedding. It consists essentially of quartz in a siliceous compact, at times impregnated with iron oxide cement, dark brown blotchings are common. It is thin to thickly bedded (0.1 to 2.0 m) and is sub-horizontally disposed with rolling

attitudes away from the basin margin where it is very much affected by the Great Boundary Fault, because this formation is in faulted contact with pre-Aravali slate and phyllite.

The total thickness of this sandstone varies but not exceeding 250 m. In the western and southern limbs in Ladpura-Mandalgarh-Nayagaon Haripura area, there are two shale members, Lower 5.30 m and upper 15-30 m, subdividing the sandstone horizon into Lower sandstone (10-20 m), Middle sandstone (30-40 m) and Upper sandstone (30-130 m).

Under the microscope, the sandstone is found to be composed of well rounded to sub-rounded grain of quartz in ferruginous and siliceous cement. The cementing material is mostly secondary quartz, though some amount of carbonate is also seen in between the quartz grains.

2.4 Structures

2.4.1 Major Structures

The Great Boundary Fault (GBF), which is the most conspicuous tectonic lineament in the Precambrian terrain of Western India having strike length of more than 400 km in between Chittorgarh in the Southwest to Machilpur in the Northeast is passing through the study area (Fig. 1.2). For much of its length, the Great Boundary Fault defines the boundary between Archean metasediments of the Hindoli Group and the lower Cambrian sedimentary sequence of the Vindhyan supergroup (Prasad 1984). Towards the central sector of GBF near Satur (study area), the upper Vindhyan sedimentary sequence is folded into a macroscopic, non-plunging kink fold that trends ENE-WSW (Satur anticline, Coulson 1927). The limb traces and axial trace of the Satur anticline parallel the Great Boundary Fault, and a dextral strike slip fault offsets this anticline near Satur village (Fig. 2.1) (Srivastava et al.1998; 1999). The Great Boundary Fault is defined by local

development of brecciation, ferruginisation, intense fracturing, development of slicken sides and truncation of beds.

Morphotectonically, the wrench faults are expressed by straight drainage channels, depressions and at a few places by the development of minor fault line scarps. Structurally these are characterised by shifts in trends and lithology along strike slip components of the faults.

The morphotectonic expression of faulting is not present along the entire length of fault partly because the faulting has been controlled by brittle-ductile transition failure (Griggs and Handson, 1960 in Turner & Weiss, 1963) and partly due to the fact that the morphology of fault plane has been eroded by deep erosion, due to which basement rocks occur on up-throw side of the fault.

2.4.2 Minor Structures

(i) Planar Structure

The planer structures observed in the area are bedding and foliations.

(a) Bedding (S_0)

This is the most common planer structure observed in the area. This is well defined by thin shaly or colour lamination within the limestone bands. The thickness of laminae varies from a few mm to a cm. The general strike of the bedding in the southern limb is almost ENE-WSW with a gentle (20°) to moderate (40° - 50°) dip due north as well as south.

(b) Foliation

Two types of foliations have been observed within the limestone bands of this area. An earlier generation foliation (S_1), which is quite well developed, mostly parallel to the axial plane of minor folds. The general attitude is almost

ENE-WSW, almost parallel to the strike of the bedding and dipping steeply either to the south or north.

The other foliation S_2 , which is rarely observed, appears as fracture cleavage and is defined by discrete fractures. This cleavage (S_2) is incongruous with first generation folds but congruous with the major second-generation fold. The general strike is almost north south and dipping steeply towards east.

(ii) Linear Structure

The linear structures observed in the area are the hinge lines (axis) of the minor folds plunging gently towards either east or west. Another set of linear structures observed in the area appears as thin lines on bedding plane (stripes). These are the intersections of the fracture cleavage with the bedding plane and are moderately to steeply dipping either towards north or south.

(a) Minor Folds

Two orders of minor folds of first generation have been noticed. The first order minor folds are 'S', 'M' and 'Z' shaped in section and are close to tight in nature. These are congruous with respect to first generation major fold and are termed as second order folds. The second order folds of its generation have also folded the bedding plane and are mostly antiforms or synform open to close in nature. These are doubly plunging folds.

The second generation minor folds are Z shaped in plan as seen on the southern limb of the southwesterly closing major structure of the area. These are congruous with respect to the major anticlinorium structure.

(b) Kink Folds

The mesoscopic kink folds developed congruently with the macroscopic kink fold (Satur anticline). These mesoscopic kink folds have been observed on both the limbs as well as in the hinge zone of Satur anticline. They are however, best observed in the thinly bedded (centimeter scale) Lower Bhandar Limestone formation (Fig. 2.1). Kink bands in the study area are mostly exposed as monoclines, but examples of conjugate pairs are also common. The geometry of the conjugate kinks varies from symmetric to asymmetric, and although both the fold hinge lines are essentially of a non plunging type, their angular divergence in map view, can range from 0° to 20° . Most of the kink bands either exhibit an orthorhombic symmetry or a monoclinic symmetry that approaches an orthorhombic symmetry (Srivastava et al. 1999).

External and internal foliation and kink plane is defined by the bedding surfaces and axial surface of the kink folds, respectively. In most of the kink bands, the external foliation is sub-horizontal to shallowly dipping, and the kink axes plunges at shallow angles ($<20^{\circ}$) towards ENE WSW.

The deflection of foliation across the kink bands invariably implies a thrust type of movement on the kink planes. All the kink bands can be classified into two sets that correspond to conjugate pairs and imply top-to-the NNW and top-to-the SSE sense of movement, respectively. The relative sense of slip on kink planes is always antithetic to the sense of slip on the internal foliation within the kink bands. Layer-parallel slip during the formation of the kinks is implied by the shear offset of the prescribing markers (e.g. vertical views and stylolites) along the shallowly dipping bedding surfaces.

A characteristic geometrical feature of these conjugate pair of kink bands in the parallelism between the kink plane in one set and the internal foliation in the

complementary set. In this respect, these conjugate kink bands are geometrically similar to conjugate pairs of brittle-ductile shear zone, where the en-echelon veins within either set are parallel to the shear zone boundary in the complementary set (Srivastava et al. 1999).

2.5 Spectral Signatures of Various Geo-elements

2.5.1 Ground Reflectance Data

Analysis of solar reflectance spectra obtained by using broad band (half-band pass of greater than 50 nm) interference filters has been extensively employed as a remote sensing method for mapping regional geology and identifying large hydrothermal and geothermal patterns (Hunt and Salisbury, 1970, 1971; Rowan and Kahle, 1982). The feasibility of routine remote identification of specific alteration minerals has been demonstrated using airborne high resolution spectro radiometers (Goetz et al. 1982; Collings and Chang, 1982). These workers have, however, stressed the need for insitu ground measurements of reflectance to allow accurate calibration of the remote sensing data. (Imran et al. 1989, 1991, 1992; Imran and panda, 1995)

In-situ spectral signatures of limestone terrain of the test site were determined in different wavelength ranges of electromagnetic spectrum using the instrument Ground Truth Radiometer designed by Space Application Center (Indian Space Research Organization), Ahmedabad. The equipment enables collection of reflectance data in the range of 485 to 837 nm compatible to 4 bands of TM, IRS and three bands of SPOT satellite data. The data was normalised by eliminating the effects due to varying intensity and inclination of the incident radiation, cloud covers, surface orientation of the object and height of the instrument using GTR calibration plate which is uniformly coated with barium sulphate. The ground reflectance data of sandstone, shale and limestone was

used for broad lithological discrimination in IRS bands 1, 2, 3 and 4 in the wavelength ranges of 485, 555, 650 and 815 Nm (Fig. 2.2).

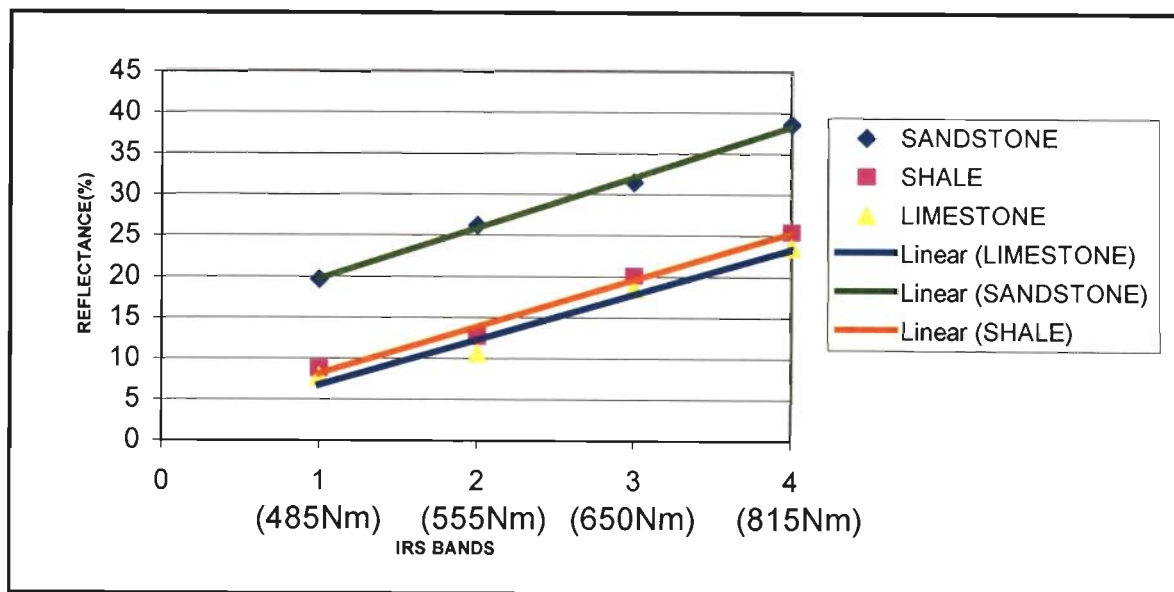


Fig. 2.2 : Ground Reflectance of Shale, Sandstone and Limestone of the Area

2.5.2 IRS LISS-III Satellite Data

The cloud free digital data of IRS-LISS III (Path/Row: 95/54) dated 1-12-1998 was processed. The digital data was converted into a valid image format from the raw format with the help of header information that describes the format of data, size and orientation of image and the file storage format. The output image file formed after image translation is segregated into all its bands. The bands of image were used in generating Standard False Color Composite (SFCC) using green, red and infrared bands.

Base map of the study area was generated from Survey of India (SOI) topographic map of 1: 50,000 scale by digitizing prominent landmarks including surface drainage features, transportation network etc. In order to remove the geometric distortion, remote-sensing data was geo-referenced to the base map. Ground control points were taken at the junction of road and drainage intersection.

The FCC image was registered to base map by converting image co-ordinates to real world co-ordinates. The pixel values of observation points were recorded. The observation points that are covered by more than one pixel, average pixel value was recorded. The pixel values of observation points were correlated with the geochemistry of shale, sandstone and limestone. It was observed that the pixel values in band 5 of Short Wave Infrared (1.55 - 1.70 μm) were showing contrast to differentiate shale, sandstone and limestone as compare to band 2, 3 and 4 in the wavelength range of 0.52 to 0.86 (Fig. 2.3).

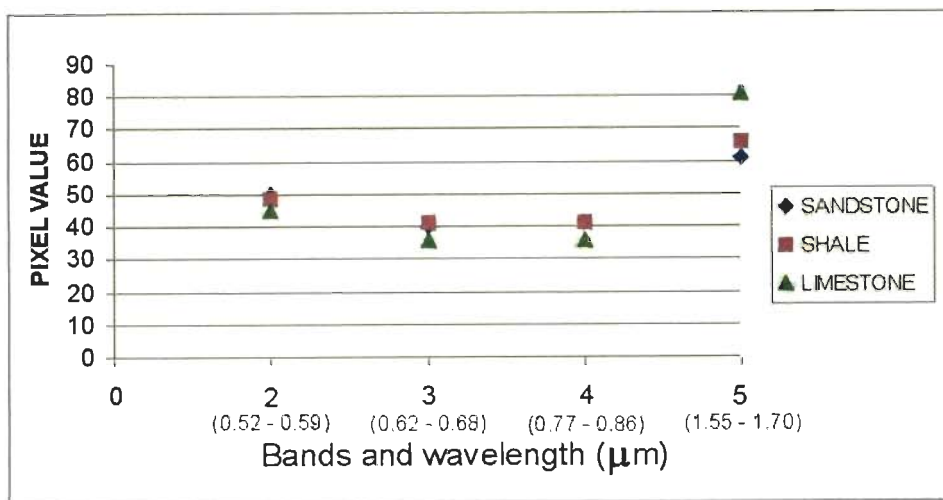


Fig. 2.3 : Pixel Values of Various Lithologies in Raw Images of Different Bands of IRS LISS-III Satellite Data

The synoptic view enabled lithological discrimination, identification of major and minor structures, drainage pattern and drainage density of the area. The most conspicuous structure evident in the FCC is box type anticlinal folded limbs of sandstone ridge. In addition to this, abundant limestone outcrops have also been observed. The limestone could easily be differentiated from the sandstone due to relatively low relief and typical dendritic drainage pattern. The Lower Shale (Ganurgarh Shale) being softer is most susceptible to weathering and erosion and has lowest relief as compared to sandstone and limestone. It also absorbs lot of moisture and as evident from the FCC, supports good cultivation at the core of anticline. The Upper Shale (Samaria Shale) stratigraphically sandwiched between

sandstone and limestone along the foothills of sandstone ridge could not be differentiated in the FCC due to inconsistent and thin exposure. Other major structures, the Great Boundary Fault separating Vindhya from the older Aravalli. Local folds and faults could also be identified in the FCC. The road network, water bodies cultivated fields and habitats were also clearly visible in the FCC. The geological map generated from IRS LISS-III data is shown on Fig. 2.4. The observations were re-confirmed through limited field checks during ground truth studies.

2.5.3 Landuse Pattern

The standard FCC generated with the help of IRS-LISS III satellite data was also studied for interpretation of landuse pattern (Fig. 2.4). It was observed that the area is without any significant cultivation. The vegetation was also insignificant. The sandstone ridges and undulating limestone outcrops were almost barren. The cultivated fields were confined to Ganurgarh shale formation in the core of anticline. No perennial source of water has been observed in the area. However, some of the palaeo channels suggest a few seasonal streams that might be activated during rainy season. The area was found to be sparsely habitated. All these features make the study area ideal for open cast mining.

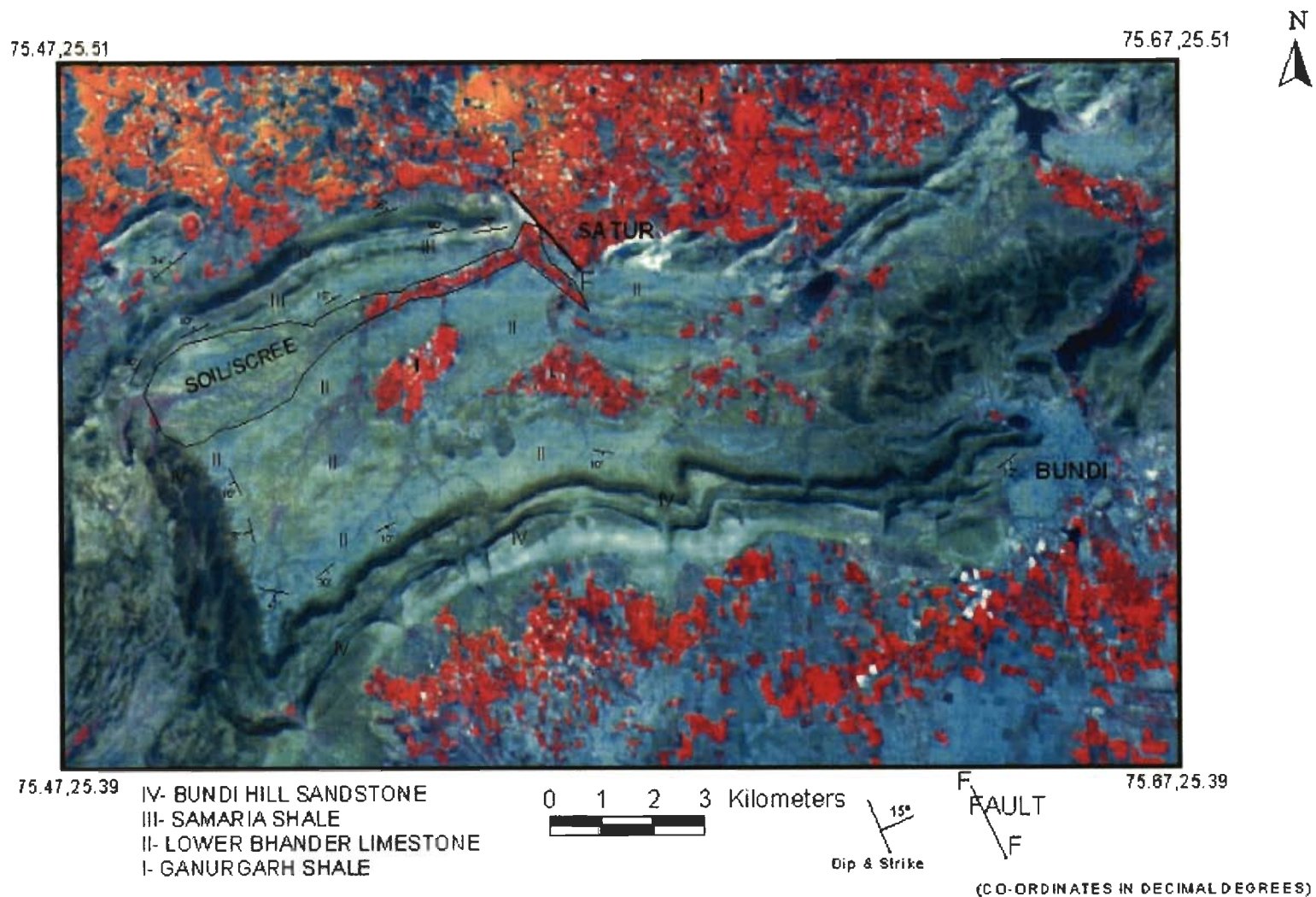


Fig. No. 2.4 Geological Map of the Study Area generated from IRS LISS-III Satellite Data

CHAPTER 3

QUALITY PREREQUISITES OF CEMENT GRADE LIMESTONE - A REVIEW

3.1 Introduction

In its widest sense, the word cement includes an infinite variety of adhesive and building materials ranging from the clay need to bind stone, upto the modern rapid hardening cements. In its most restricted sense, the word cement always means Portland cement that makes up about 98 percent of the world cement production used for construction purpose. The principal raw material required in the manufacture of Portland cement is limestone low in magnesia (Ghosh and Imran, 1986).

The chemical composition of limestone for use of cement manufacture shall be such that it yields a raw mix of appropriate composition in combination with argillaceous components and under certain conditions with corrective materials. The specifications for different types of cement being different, no rigorous independent specification of cement grade limestone is possible (Imran, 1998).

Portland cement is an active combination of silicates, aluminates and ferro-aluminates of lime, obtained by the preliminary grinding and mixing of the requisite quantities of lime usually in the form of carbonates, silica, iron oxide and alumina, burning the mixture to incipient vitrification and grinding the resulting clinker to a fine powder with a small percentage of gypsum to adjust the setting time. The name Portland cement was coined by Joseph Aspdin in 1824 based on the resemblance of the colour and quality of cement to Portland stone - a limestone quarried in Dorset, UK (Lea 1998).

Portland cement clinker is a hydraulic material, which shall consist of at least two third by mass of calcium-silicate $(\text{CaO})_3\cdot\text{SiO}_2$ and $(\text{CaO})_2\cdot\text{SiO}_2$, the remainder containing aluminium oxide (Al_2O_3), iron oxide (Fe_2O_3) and other oxides. The ratio of $\text{CaO} / \text{SiO}_2$ by mass should not be less than 2. The content of magnesium oxide (MgO) should not exceed 5% by mass.

3.2 Mineralogical Constituents of Raw Materials and Their Role in Cement Manufacturing

The importance of mineralogical constituents of raw materials are increasingly realised in cement manufacture. Depending on the mineral form in which carbonate, silica or other constituents are present, their grindability and burnability shows distinct and wide variation with consequent effect on the manufacturing operations.

3.2.1 Impact of Mineral Constituents of Calcium Carbonate

The dissociation of CaCO_3 in carbonate rocks depends, besides their chemical composition, on their textural and micro-structural features. Holocrystalline calcite, marble and crystalline limestone dissociates at higher temperature than fine grained, organogenic, pelitic-amorphous or chemically precipitated (chemogenic) varieties. These differences reflect upon the temperatures at which CaO appears from breakdown of CaCO_3 and subsequently loses its initial reactivity due to recrystallisation and lattice compaction. It has also been experimentally established that the rate of dissociation and reaction temperature are directly related to grain size (Table 3.1).

Table 3.1 : Dependence of Reactivity of Calcite on Crystallinity and Grain Size of Limestone

Crystallinity	Grain Size (mm)	Rate of Dissociation	Reaction Temperature ($^{\circ}\text{C}$)
Very coarse grained crystalline limestone/marble	1.0	Lowest	Highest (around $870^{\circ}\text{C} - 900^{\circ}\text{C}$) ↑ Lowest ($780^{\circ}\text{C} - 820^{\circ}\text{C}$)
Coarse grained limestone/Marble	1.0 - 0.5	↓	
Medium grained limestone/marble	0.5 - 0.25		
Fine grained limestone	0.25 - 0.1		
Very fine grained limestone	0.1 - 0.01		
Microcrystalline limestone/chalk	< 0.01	Highest	

A perusal of Table 3.1 shows that with decreasing grain size of limestone, the rate of dissociation increases with decreasing reaction temperature. The dissociation of calcite proceeds more intensively in particles obtained by grinding holocrystalline limestone as a result of presumed partial breakdown of crystal lattice. The dissociation is accelerated by the impurities, especially the argillaceous matters and mineralizing substances (Boyuton 1979).

3.2.2 Impact of Mineral Constituents of MgO

The MgO in limestone can be present in the form of magnesium silicates, dolomites, magnesites, ankerite, brucite etc. Each of these minerals have their own stability and break-down temperature of lattice structure, eg., dolomite $\text{Ca, Mg}(\text{CO}_3)$ $700^{\circ} - 750^{\circ}\text{C}$ Ankerite $\text{Ca}(\text{Mg, Fe}) (\text{CO}_3)_2 - 700^{\circ}\text{C}$, Magnesite (MgCO_3) $- 660^{\circ}\text{C}$, Magnesian siderite $\text{Mg, Fe} (\text{CO}_3)_2 - 580^{\circ}\text{C}$. These dissociation characteristics are further influenced by the presence of Al_2O_3 , SiO_2 , Iron oxide etc. It has been observed that under identical conditions of fine grinding and rapid cooling, the presence of magnesian silicates ensures even distribution of the fine (1 to 5 μm) periclase crystals whereas limestone with dolomite or magnesite are prone to yield coarser crystals of periclase, (25 to 30 μm) which causes delayed

expansion. If ankerite, magnesite and magnesian siderite are present, free MgO will appear at much lower temperature of 700⁰, 660⁰ and 580⁰ C, and the ultimate clinker will have larger periclase grains. Therefore, besides the amount of MgO present, the mineral form in which it occurs is also equally important for its behaviour and effect on clinker properties (Ali et al. 1998 and Lea 1998).

3.2.3 Impact of Mineral Constituents of Silica and Silicates on Burnability and Clinker Properties

The mineralogical nature and dispersion characteristics of silica have a strong bearing on the reactivity of cement raw mix. It has been experienced from actual experiments in raw mix design that on increase of silica content in the raw mix by only 1.5 percent (in the form of free quartz) reduces the C3S content of the raw mix by about 20% (the CaO variation has been kept within 0.25 percent). Silicates react more readily than free silica or uncombined silica such as quartz, flint and chert. It has been widely accepted that the reactivity of different forms of silica with calcium oxide increases in the following order:

β – Quartz → Chalcedony → Opal → -Cristobelite → α - Tridymite
Silica in feldspars → Amorphous silica → Silica of granulated slag from dehydrated and vitrified matter

3.3 Chemical Parameters

The chemical parameters are the most vital factors in selecting limestone for cement manufacture. It is the ultimate deciding factor for judging the suitability of raw material components, while mineralogical, granulometric and physical characteristics are to be taken into consideration for optimization of process parameters and quality control. No independent specifications of chemical composition for the individual components in a raw mix can be prescribed, as the

ultimate aim is to obtain a clinker of appropriate composition from a suitable combination of raw materials of easy techno-economic availability.

The desired limits of cement clinker composition are CaO 62 to 67%, SiO₂ 20 to 24%, Al₂O₃ 4 - 7%, Fe₂O₃ 2 - 5%, others which include specific limits of minor constituents ranging from 1.5 to 4 %. Based on the above compositional requirements of a cement clinker, the broad chemical specification of cement grade limestone has been formulated (Table 3.2) in the Norms evolved by National Council for Cement and Building Materials (NCB). It is important that these specifications should take into consideration, the scope of adding the appropriate argillaceous and/or ferruginous components for satisfying the moduli values of raw mix.

Table 3.2 : Chemical Specifications of Cement Grade Run-of-Mine Limestone (NCB Norms modified in 2000)*

Chemical Components of Cement Grade Run-of-Mine Limestone	Acceptable Range for Ordinary Portland Cement (%)	Acceptable and Preferable Ranges of Moduli Values
CaO	44-52	$\text{LSF} = \frac{\text{CaO}}{2.8 \text{ SiO}_2 + 1.65 \text{ Al}_2\text{O}_3 + 0.35 \text{ Fe}_2\text{O}_3}$ <p>Should be $\geq 0.66 \leq 1.02$ Preferable 0.85 – 0.95 (LSF = Lime Saturation Factor)</p>
MgO	Max 3.5	
SiO ₂	To satisfy the LSF and silica modulus of the raw mix	
Al ₂ O ₃		
Fe ₂ O ₃		
Mn ₂ O ₃	0.5	<p>Silica Modulus (M_S) =</p> $\frac{\text{SiO}_2}{\text{Al}_2\text{O}_3 + \text{Fe}_2\text{O}_3}$ <p>Should be $> 1.7 < 3.5$ (Preferable 2.2 to 2.6)</p>
R ₂ O(K ₂ O+Na ₂ O)	0.6	<p>Alumina Modulus (M_A) =</p> $\frac{\text{Al}_2\text{O}_3}{\text{Fe}_2\text{O}_3}$ <p>Should be $> 0.66 < 2.5$ (Preferable 1.5 to 2.5)</p>
S as SO ₃	0.6 – 0.8	
P ₂ O ₅	0.6	<p>Hydraulic Modulus (H_M)</p> $= \frac{\text{CaO}}{\text{SiO}_2 + \text{Al}_2\text{O}_3 + \text{Fe}_2\text{O}_3}$ <p>Should be $> 1.7 < 2.3$ (Preferable around 2)</p>
Cl	<0.05	

* NCB - National Council for Cement and Building Materials, New Delhi

Any change in chemical composition of the raw materials have profound effect on the process, fuel consumption and quality of clinker. The change in CaO, SiO₂, Al₂O₃ or Fe₂O₃ contents in a raw mix has consequent effects on raw material burning and clinker quality (Chatterjee 1979).

3.3.1 Major Oxides

(i) CaO Content

The Lime Saturation Factor (LSF) is the measure of free CaO content in clinker. A high CaO limestone will give high LSF and the clinker will have plenty of Calcium Tri-silicate (C3S), less Calcium-Bi-silicate (C2S) and more free lime. Generally, about 7% increase of CaO in raw mix gives 14.2 percent increase on the potential Calcium Tri-silicate (C3S) and 11.6 percent decrease in C2S. A higher LSF requires more fuel to drive off CO₂ gas, i.e. increase of burning temperature and retention time in the burning zone.

On the contrary, with low-lime limestone, a low LSF raw mix will give low C3S, plenty of C2S and no free lime; this also requires more fuel. The appropriate CaO content and LSF value of raw mix should give a low lime Calcium Tri-aluminate (C3A) 9 to 11 percent, Calcium Tetra-aluminoferrite (C4AF) 12 percent and C2S as balance, not exceeding 20 to 25 percent (Albats 1997).

(ii) SiO₂ content

High silica content of raw mix and high silica modulus reduces the liquid phase and increases clinker burning temperature (Basbanyagre 1997, Moranville et al. 1992). A low silica modulus increases the liquid phase, improves burning and formation of coating in the kiln, which reduces fuel consumption. A high silica raw mix produces high free lime, unless the silica is in a very fine state. Such a raw mix has a tendency to remove the coating from the kiln lining.

When the limestone has high silica and low alumina and iron oxide, it is preferable to add alumina, when silica is low and alumina is high, it is preferable to add iron oxide as additives.

(iii) Al_2O_3 Content

Both Al_2O_3 and Fe_2O_3 act as flux in the kiln and govern the sintering temperature at which they combine with Ca and Si oxides. They reduce the clinkering temperature and fuel consumption, increase the liquid phase and kiln production, help to produce high C3S clinker with too much free CaO, and improve grindability of clinker. If the alumina content is too low in a raw mix, without free quartz, the amount of flux due to Fe_2O_3 content is so large that the clinker becomes very viscous causing sticking and balling (Mehta 1980).

(iv) Fe_2O_3 Content

Bogue (1970) has shown that the viscosity of the liquid phase is decreased by adding iron oxide to the raw mix. Increase in Fe_2O_3 tends to markedly decrease the free CaO thereby improve the burnability at a temperature of 1275°C , while liquid is usually formed at 1300°C . A high Fe_2O_3 content compared to Al_2O_3 gives rise to ball formation. There is a belief that large Fe_2O_3 content cause ring formation, while some investigations showed that minerals like muscovite, illite and feldspar containing alkalies also cause such rings in the kiln (Gouda 1979).

3.3.2 Minor Constituents in Cement Production and Their Effects

Besides Ca, Si, Al, Fe and to some extent Mg, the raw materials may contain various sulphates, alkalies, phosphate, manganese, chloride etc., which have their own individual good or bad effects on the process and clinker quality, depending upon their concentration. It is necessary to highlight the mode of occurrence and effects of some commonly occurring minor constituents such as sulphates, alkalies, phosphates and chloride (Kakali 2003).

(i) Sulphates

The IS specifications allow 2.75 percent SO_3 content in finished cement, which includes SO_3 in clinker as well as that contributed by gypsum. In raw materials, SO_3 is available from gypsum ($\text{CaSO}_4 \cdot 2\text{H}_2\text{O}$) in clay or limestone, or pyrite, marcasite (FeS_2) in clay or limestone. If limestone contains SO_3 as gypsum, this SO_3 gets fully transferred to clinker; whereas if pyrite / marcasite is the source, the SO_3 goes mainly into the gas stream. In small amounts SO_3 acts as mineralizer, but presence in excess leads to lowered strength of cement. The SO_3 has a beneficial effect, when alkalis are also present in the raw mix, as it forms stable alkali sulphates and prevents ring formation (IS-269 1989 and Wajdowiez 1994).

(ii) Alkalies

Alkali oxides are undesirable in raw material, as they retard clinker reaction and promote ring formation in the kiln. Excessive alkalies reduces the cement strength and accelerates setting time. Cement with more than 1% alkalies in concrete gives rise to reaction with reactive aggregates such as opal, chalcedony or amorphous silica. The source of alkalies in raw materials are feldspar (KAlSi_3O_8) and muscovite or illite (alkali-bearing clay minerals) in clays etc. The maximum limit of R_2O in clinker may be tentatively fixed at 1.2. In fixing the maximum tolerable limit of alkalies in a raw mix, one should be guided by the fact that by maintaining molecular ratio of combinable SO_3 to total alkalies around 1.5, the formation of stable sulphates (K_2SO_4 or Na_2SO_4) and the individual bad effects of both can be mitigated (Wajdowiez 1994).

(iii) Phosphates

Phosphate has varying effect on clinker quality (Boynton 1979). Small quantities of P_2O_5 improve the quality of cement, acts as mineralizer in firing, and

help in reducing fuel consumption. However, excessive P_2O_5 content causes retardation of setting, hardening and decrease in strength. With above 2% P_2O_5 , there is breakdown of C3S and formation of free lime. Although the limit of P_2O_5 is shown as 0.6%, recent studies indicates that it is desirable to keep P_2O_5 within 0.25% (unpublished reports of NCB).

(iv) Chlorides

Presence of chloride in the raw mix promotes formation of rings and objectionable coatings in the dry-process kiln. The source of chlorides are mostly the clays, shales or occasionally limestone. The limits for chlorides in raw materials for dry-process suspension preheater kilns were earlier considered to be 0.05%, but it has still been lowered down to 0.015 to 0.02% at present (Shah 2003).

(v) Manganese

Manganese compounds generally play the role of flux, similar to Fe_2O_3 and Mn_2O_3 content. Its presence, upto 4% in cement, has not been found to effect the properties adversely. However, because of the fact that Mn_2O_3 concentration above 0.5% in the raw mix makes the clinker dark or blue, it is desirable to limit it to 0.5%.

3.4 Physical Properties of Raw Materials and Their Role in Cement Preparation

The physical properties of cement raw materials, which have significant effect on the manufacturing process, are natural moisture content, crushability and grindability.

3.4.1 Natural Moisture Content

Moisture content of raw material plays an important role in deciding whether the cement manufacturing process should be wet or dry. In the past, when fuel conservation was not so important, if the raw materials contained 15 to 18 percent moisture, the decision used to be to go for the wet process. At present, since dry process is opted for towards fuel economy, raw materials with high moisture content (upto 7%) can also be used for dry process, which will involve installation of dryers (or a battery of dryers), and utilizing all the kiln waste gases. In case of Bhandar limestone of Bundi area, the natural moisture content is found to be negligible, hence it can be used for cement manufacture using dry process technology.

3.4.2 Strength Parameters

The strength parameters of limestone are very important for their amenability to crushing and grinding and corresponding energy consumption. The strength parameters are generally given by hardness, crushing strength, shatter index, crushability and grindability. The above parameters are extremely variable in limestone and depends on variations in grain size, nature of cementing material, porosity, degree of weathering, natural moisture content etc. Since each of these properties vary in different types of limestone, they modify the strength properties in different ways.

3.5 Summary

Portland cement is an active combination of silicates, aluminates and ferro aluminates of lime, obtained by the preliminary grinding and mixing of the requisite quantity of lime usually in the form of carbonates, silica, iron oxide and alumina. The calcareous components generally required for Portland cement are in the form of limestone. In case limestone is poor in iron and alumina bearing minerals, bauxite, red ochre and iron ore are also required. The broad chemical prerequisites

required in the limestone for cement manufacturing are CaO 44 – 52 % SiO₂ < 14% and MgO < 3.5 %

In addition mineralogical, granulometric and some minor constituents in the form of impurities in the limestone such as Na₂O, K₂O, Cl, SO₃, P₂O₅ and MnO₂ together with its physical properties namely crushability and grindability affect the treatment, processing and ultimate manufacturing of cement. The dissociation of CaCO₃ in carbonate rocks depends, beside their chemical composition, on their textural and microstructural features. With decreasing crystallinity and grain size, the rate of dissociation increases and the reaction temperature decreases. The mineralogical nature and dispersion characteristics of silica and MgO have a strong bearing on the reactivity of cement raw mix. The increase of silica content in the raw mix only 1.5 % in the form of free quartz, reduces the C3S content of the raw mix by about 20 %. The reactivity of different forms of silica increases from beta quartz, opal, and cristoballite to amorphous silica.

In short ideally a limestone should be fine grained, organogenic, pelitic-amorphous or chemically precipitated (chemogenic) for cement manufacturing. It should have reactive silica and low crushability and grindability. However, in nature such characters of limestone are rare and therefore, deviation in these characters require effective corrective treatment.

CHAPTER 4

BHANDER LIMESTONE - ITS LITHOUNIT, PETROGRAPHY AND DEPOSITIONAL ENVIRONMENT

4.1 Introduction

The limestone is a sedimentary rock consisting essentially of carbonates, mainly calcite and dolomite, but small amounts of iron bearing carbonates may also occur. Many of the commonly occurring limestones contain organic, detrital and chemically precipitated material in varying proportions. Both calcite (hexagonal CaCO_3) and aragonite (Orthorhombic CaCO_3) are present in modern limestone accumulations. However, since aragonite is more easily dissolved or converted to calcite, it is absent in ancient limestones such is the case of Bhander limestone. The changes and the ease with which carbonates re-crystallise during diagenesis, may result in losing its characteristic features, resulting in uncertainties to its mode of origin, especially for ancient limestone.

Limestone can be formed in lakes, lagoons and in the sea. However, their greatest development is in the sea bottoms, mostly at depths of less than a few hundred meters. In fact, limestone containing algal mats and stromatolites indicate shallow water littoral or even supra-tidal origin. The most favourable place for large accumulations of chemically precipitated limestone is one characterized by climatically stable, warm, shallow, relatively sluggish water with slow but continuous subsidence of the sea bottom. The limestone formed by chemical precipitation of the solution rich in bicarbonate form of the calcium $\text{Ca}(\text{HCO}_3)_2$ are well bedded, thick and uniform and may be fine grained. They may show laminations extensively uniform in nature. They often break with an even, conchoidal fracture and with sharp edges. The rocks are dense with low porosity.

A thorough knowledge about the mode of origin, mode of occurrence, structural peculiarities are essential for prospecting, exploration, exploitation and optimal utilisation of limestone deposits.

4.2 Lower Bhander Limestone

The field investigations indicate that the Lower Bhander Limestones (locally known as Lakheri Limestone) overlies transitionally the Ganurgarh shales and underlies the Bundi Hill Sandstone to which it merges upwards. In this study, an attempt has been made to present the investigations made on the Lower Bhander Limestone for their field character, mineralogical, granulometric, petrological and palaeo-depositional environment, which may help in compositional characterization and to evaluate their possible use in the Cement Industry. In the present study, broadly the classification of the Limestones by Folk (1962) has been followed with some modification in the usage of the term micrite as per classification of Bissel and Chilingar (1967) in view of size of carbonate grains upto 50 μm .

Based on field investigations, the Bhander Limestone basically occurs as calcareous rock sequence of various colours, with an intervening argillaceous unit above the basal calcareous unit. Stratigraphically, it has been divided into four mapable Lithounit A (oldest), B, C and D (youngest) on the basis of lithology, colour, stratification, spatial relationship and internal structures.

The distribution of minerals, granulometry and microstructural features were studied in Image Analysing System using the software Image Pro Plus and Materials Pro Plus. Percent distribution of minerals was determined by counting 3000 grains of various minerals present in each of representative samples. Granulometric analyses of various mineralogical phases were done. Average grain size analyses of calcite were done by counting 1500 grains each, whereas for quartz, 1000 grains were considered. Maximum and minimum grain sizes of

phases were determined using Image Pro Plus. Micro-structural variations were studied with the help of Materials Pro Plus.

4.2.1 Lithounit A

Lithounit A overlies Ganurgarh shale with a transitional contact and consists of pink argillaceous limestone that varies in thickness from 5 to 50 cm. The upper part shows wavy and discontinuous laminae, measuring 10 to 15 cm in lateral extent (Fig. 4.1). The limestone is micritic in nature and contains 10% or more terrigenous sediments mainly clay and silt. The clastic components of silts are quartz and fine micaceous flakes.

Intraformational lenses of about 7 to 20 cm thick occur as intramicrudite in the upper part of this Lithounit. It contains sub-angular to sub-rounded, poorly sorted, 3 mm to 6 cm long flat pebbles of red coloured limestones. It consists of intraclasts and matrix both of which are composed of similar red micrite and hence appear identical. The intraclasts range in size from a fraction of centimeter to more than a centimeter and are poorly sorted and loosely packed. Their shape is variable and ranges from irregular to elongated with rounded edges (Fig. 4.2, 4.3 and 4.4).

Petrography

Petrographic investigations under microscope indicate that the main mineralogical constituents of Lithounit A are calcite, with some quartz, magnetite, and hematite (Fig. 4.5). Based on modal counts of 1500 grains in each of the samples, the calcium carbonate (CaCO_3) is found to be the dominant minerals (73%) followed by quartz (12%) and magnetite (11%) (Table 4.1). The calcite is microcrystalline and the limestone can be classified as micrite.

Table 4.1: Petrographic Analysis of Limestone of Lithounit A

Name of the Mineral	Quantity (%)	Grain Size (μm)		
		Minimum	Maximum	Average
Calcite	73	20	160	85
Quartz	12	15	210	90
Magnetite	11	--	--	--
Hematite	4	--	--	--

Granulometric studies were done using Image Analysing System and measuring 1000 to 1500 grains in each of thin sections. The size of calcite grains varies from 20 μm to 160 μm with an average size 85 μm . The rock has attained red, pink colour due to ferruginous component in the micrites. Quartz grains show signs of corrosion due to surrounding micrites. Three sets of micro veins of calcite are seen that are indicative of structural weak planes present in this rock. Two of them are parallel and third one is developed obliquely (Fig. 4.6).

Subhedral to anhedral quartz grains are randomly scattered, which ranges in size from 15 μm to 210 μm with an average of 90 μm (Table 4.1). Fine grains of magnetite and hematite are also uniformly distributed in the rock (Fig. 4.7 to 4.12).

Depositional Environment

The main constituent of this Lithounit is red argillaceous silty micritic limestone, which shows abundant horizontal fenestrae and bird's eye structures and contains appreciable amount of terrigenous admixture, interpreted as to representing deposition on supratidal flats. Horizontal fenestrae and bird's eye structures are reported to be highly characteristic of recent supratidal sediments and result from desiccation and shrinkage of lime mud and because of prolonged exposure (Shinn, 1968; Shinn, et. al., 1969; Akhtar, 1973, 1975, 1976).

Absence of algal mats in the lower part of Lithounit A and their occasional appearance towards the top suggests that the greater part of the deposition of this Lithounit took place under conditions not suited to the growth of algal mats. This indicates deposition in high supratidal environment and prolonged exposures. Laminae appearing in the upper part of this Lithounit have been interpreted as due to the work of algal mats. The appearance of algal mats towards the top of this Lithounit is suggestive of a gradual transition from a high to a low supratidal environment where occasional flooding permitted algal growth.

The upper part of Lithounit A, consisting of lenses of flat pebble breccia (intramicrudite) is interpreted as localized high energy deposit by small, very shallow gullies. The composition of pebbles suggests that they have been derived locally from the associated argillaceous, micritic limestones. The generally horizontal to sub-horizontal arrangement of pebbles is suggestive of their deposition from suspension following upon flooding. Low-energy conditions of the deposition are further indicated by the presence of micrite as matrix in between the flat pebbles. The small size of breccia lenses and their deposition under low energy conditions are together suggestive of their origin in small gullies which, observed on modern tidal flats generally exist in the high tidal flat zone but may sometimes extend into the low supratidal zone. These small gullies arise from repeated branching of tidal channels in the landward direction, and have been reported 1.5 to 4.5 m wide and less than 1.5 m deep (Shinn et al., 1969). Flood tide is spent force by the time it reaches these gullies through the trunk channel, and that is why low-energy conditions and high mud content are obtained within such gullies (Van Straaten, 1961).

The presence of intraclasts and micrite matrix in the intramicrudite suggests the case of textural inversion and indicates that intraclasts did not originate by current action because currents, strong enough to generate intraclasts are capable of winnowing any lime mud present. Since flat pebbles of Lithounits A do not

appear to be current formed in all probability, they were derived from brecciated crusts. When the flats were flooded, flat pebbles floated to adjacent gullies where they were deposited from suspension alongwith lime mud.

Non existence of mud polygons and brecciated crusts from this Lithounit is noteworthy and probably reflects the fact that their chance of rapid burrial and preservation are poor on supratidal flats. The restricted occurrence of flat pebbles within small channels of Lithounit A suggests that while fragments lying on the ancient supratidal flat were disintegrated, those which reached the nearby gullies could be preserved.

The features such as horizontal fenestrae, bird's eye structures, appreciable content of terrigenous admixture, general absence of algal mats, presence of micrite in the channels of small dimensions and predominant pink to red colour of the sediments collectively indicate high to low supratidal environment for Lithounit A.

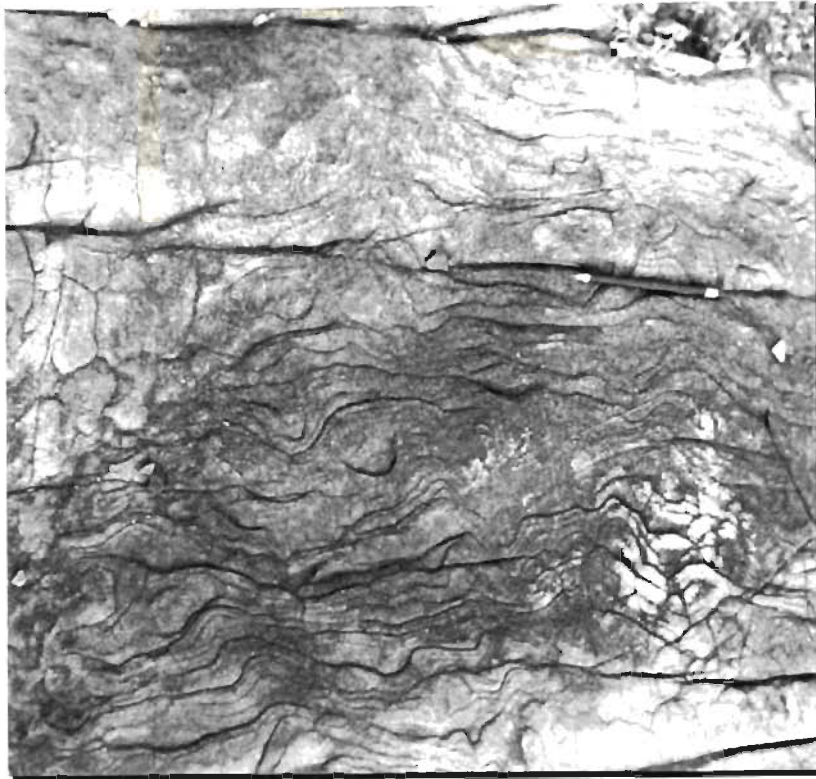


Fig. 4.1 : Lithounit A Showing Wavy and Discontinuous Laminae



Fig. 4.2 : Lithounit A Showing Intraformational Breccia

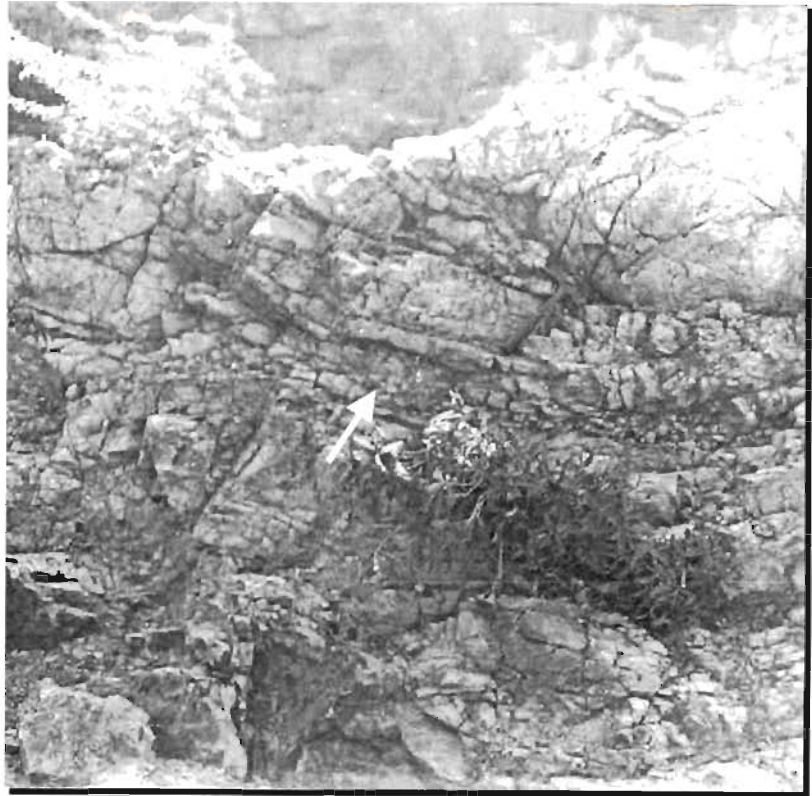


Fig. 4.3 : Vertical Section of Lithounit A Showing Intraformational Breccia

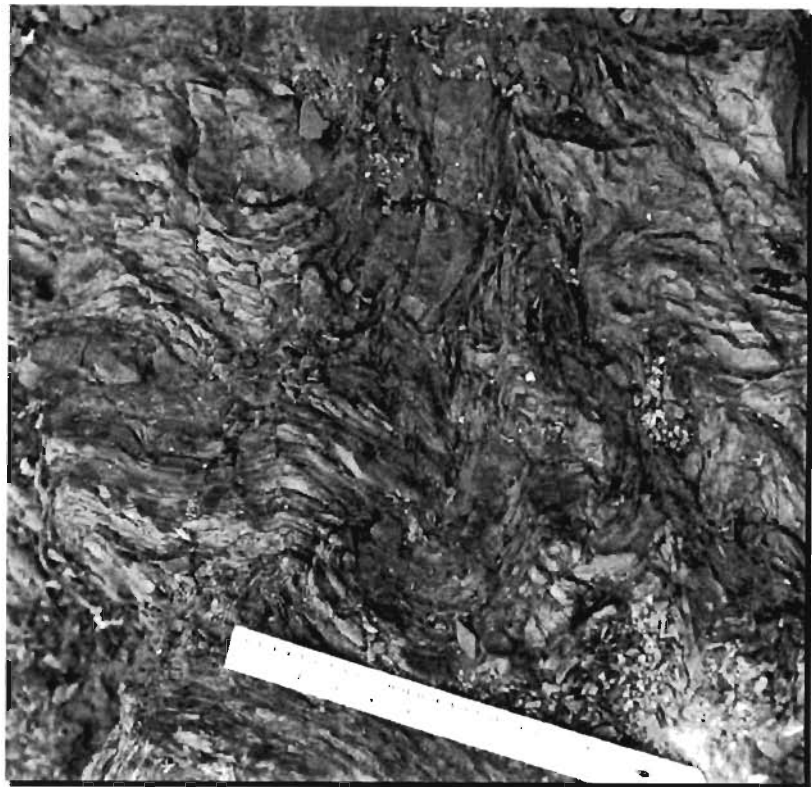


Fig. 4.4 : Lithounit A Showing Silty Micrite

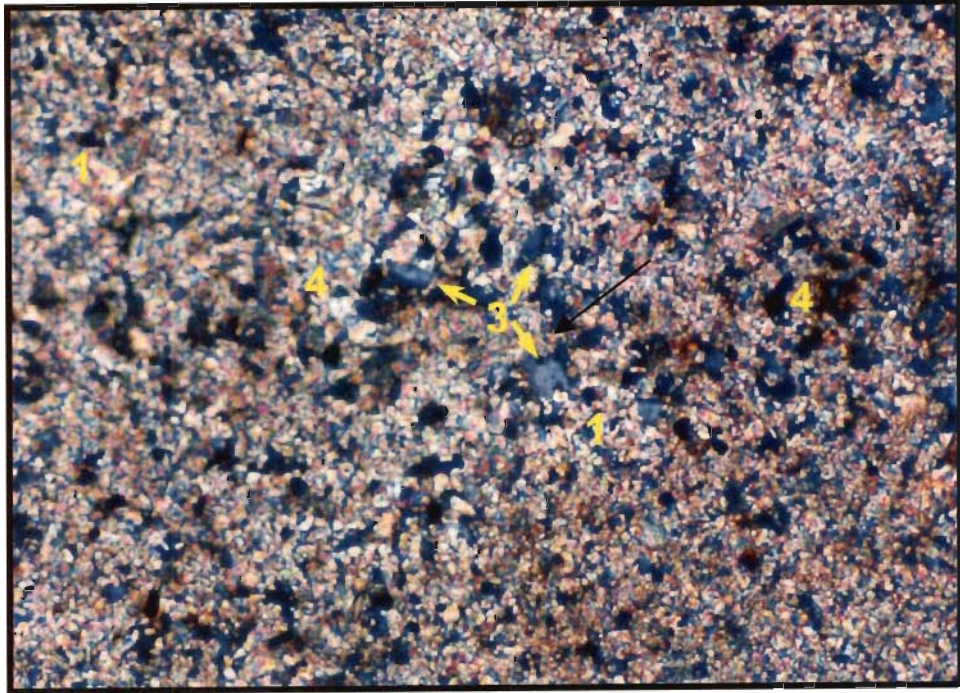


Fig. 4.5 : Photomicrograph Showing Clusters of Quartz and Magnetite in the Carbonate Matrix of Lithounit A (100 x, x - nicols)

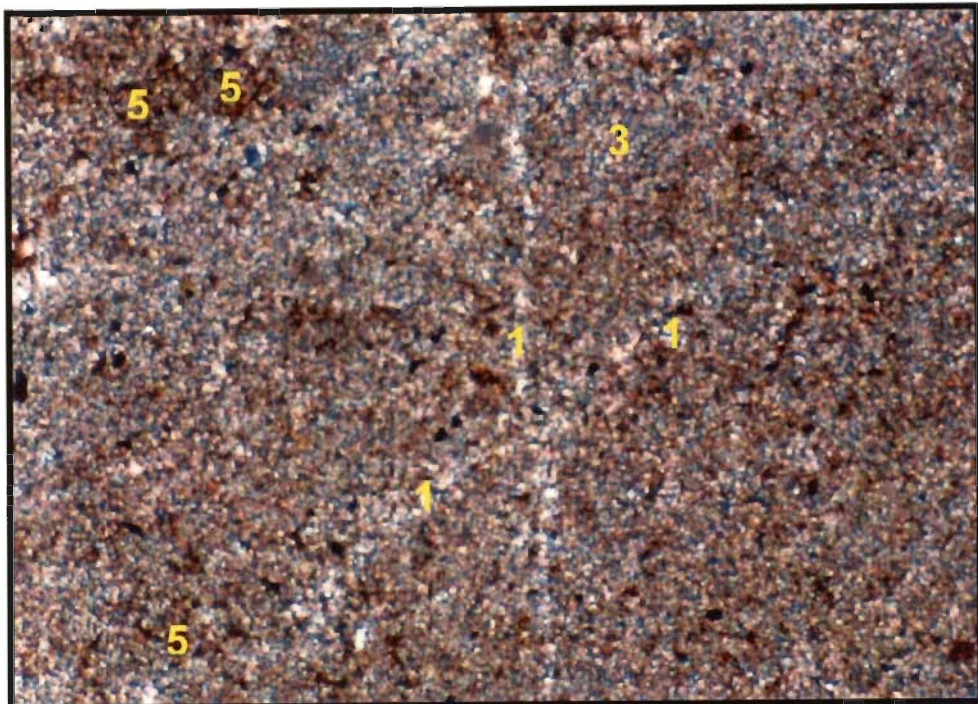


Fig. 4.6 : Photomicrograph Showing Three Sets of Calcite Micro-Veins Cutting Across Each Other in the Carbonate Matrix of Lithounit A. Patches of Iron-Oxide Minerals are also present (100 x, x - nicols)

1 - CALCITE; 2 - DOLOMITE; 3 - QUARTZ; 4 - MAGNETITE; 5 - HEMATITE

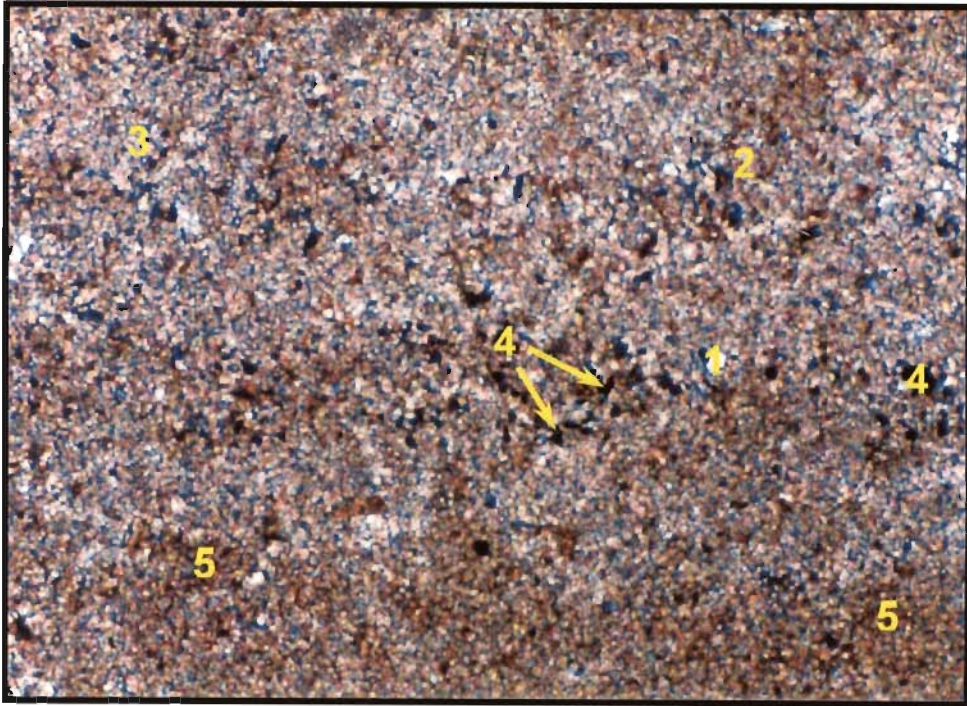
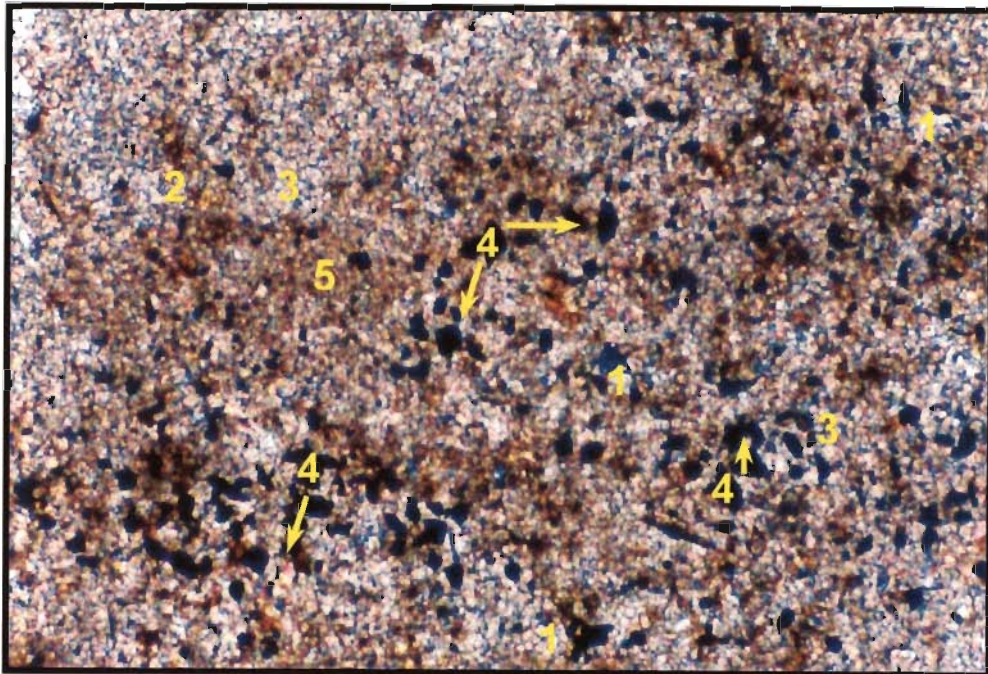


Fig. 4.7 : Photomicrograph Showing Poorly Developed Lamination Planes of Magnetite and Quartz Grains in the Carbonate Matrix of Lithounit A



**Fig. 4.8 : Photomicrograph Showing Predominant Magnetite Grains along with Minor Quartz Grains in the Carbonate Matrix of Lithounit A
Variation in Calcite Grains is also depicted (100 x, x - nicols)**

1 - CALCITE; 2 - DOLOMITE; 3 - QUARTZ; 4 - MAGNETITE; 5 - HEMATITE

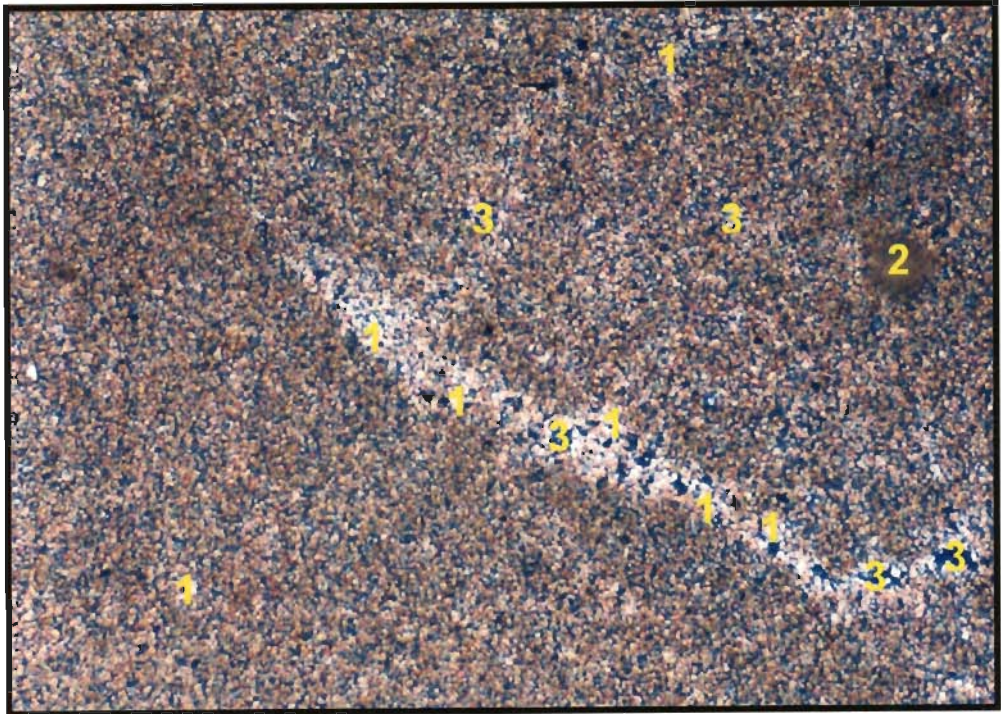


Fig. 4.9 : Photomicrograph Showing Discontinuous Micro Vein of Quartz and Calcite in Lithounit A. (100 x, x - nicols)

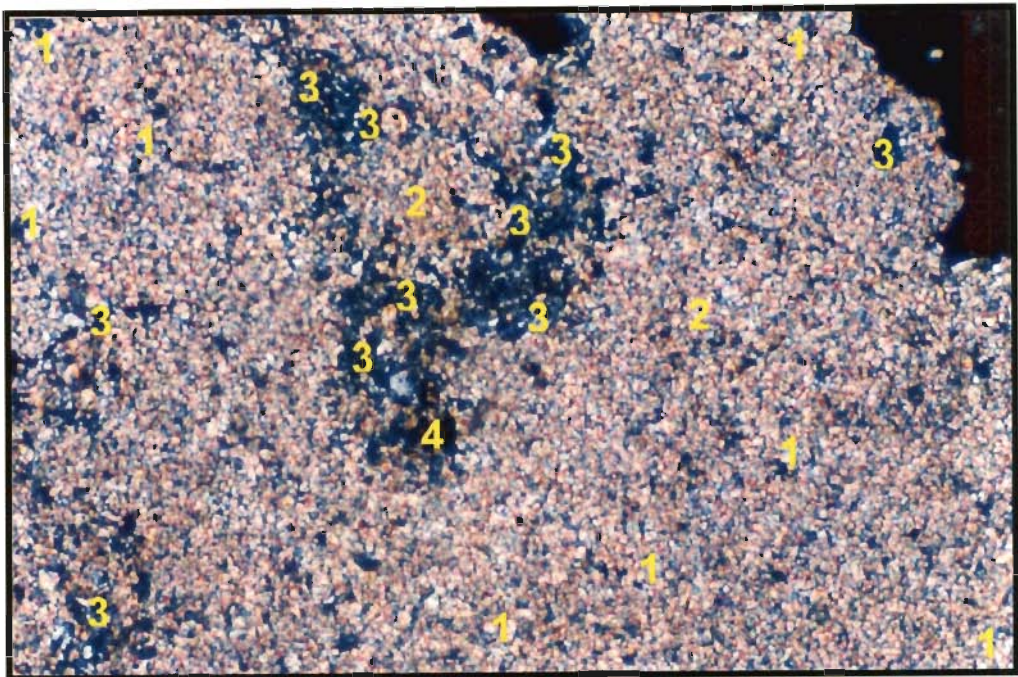


Fig. 4.10 : Photomicrograph Showing Cluster of Quartz of Varying Sizes in the Carbonate Matrix of Lithounit A. (100 x, x - nicols)

1 - CALCITE; 2 - DOLOMITE; 3 - QUARTZ; 4 - MAGNETITE; 5 - HEMATITE



Fig. 4.11 : Photomicrograph Showing Clusters of Magnetite, Quartz and Secondary Calcite in Lithounit A. Scattering of Quartz is also seen (50 x, x - nicols)

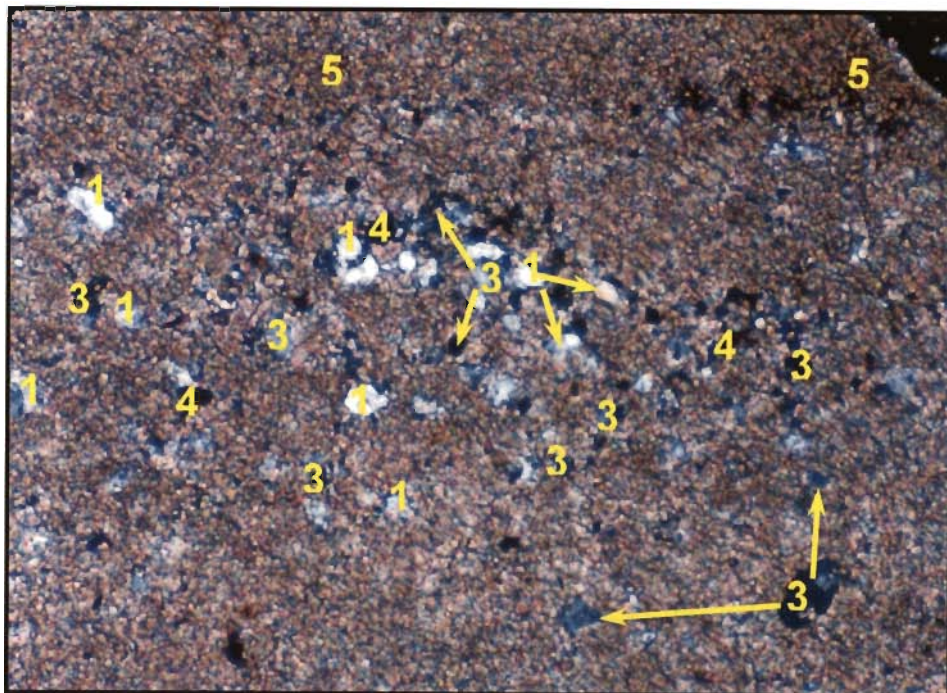


Fig. 4.12 : Photomicrograph Showing Clusters in the Carbonate Matrix of Lithounit A. (50 x, x - nicols)

1 - CALCITE; 2 - DOLOMITE; 3 - QUARTZ; 4 - MAGNETITE; 5 - HEMATITE

4.2.2 Lithounit B

Overlying the Lithounit A, Lithounit B comprised of alternate laminae of blue-grey micritic limestones (Fig. 4.13). They are wavy and discontinuous, and extend laterally from a few tens of centimeters to a few tens of meters. Lithounit B is generally devoid of sedimentary structures except for occasional trough cross bedding (Fig. 4.14), symmetrical straight crested ripple marks with wavelengths of 3-14 cm, rhombic ripple marks measuring 5 cm along long axes, mud cracks and small domal stromatolites. Intraformational breccia lenses within this Lithounits are 20-30 cm thick and contain flat pebbles of laminated micritic limestones. The pebbles range in length from a fraction of a centimeter to 12 cm. They are generally poorly sorted, and sub angular to sub rounded. Their orientation is highly variable, flat lying in some beds, imbricate in others, and standing on edge in some others. On the bedding plane a crude preferred orientation of elongated pebbles is sometimes noticeable

Petrography

This limestone is essentially micritic with few intraclasts and minerals like quartz, magnetite and hematite (Fig. 4.15 and 4.16). The limestone shows organic matter rich banding which is fairly continuous. The presence of organic matter imparts the grey colour to this limestone. The micrites show iron leaching along the grain boundaries. Micrites also show signs of dissolution and re-precipitation as is evident by presence of relatively coarser micritic grains in random orientation and containing impurities. Quartz and iron oxide grains are irregularly distributed and are anhedral to subhedral. Secondary calcite veins with euhedral grains of well sorted calcite along with magnetite and quartz are also observed (Fig. 4.17 and 4.18)

Graded micrite occurs in Lithounit B as interlaminated blue micritic limestone. Microscopic studies indicate that it is mostly composed of 0.25 mm to

more than millimetre thick micrite laminae, which under high magnification show a delicate, normal size grading of their constituent particles. This micrograded bedding is marked by the relative amount of light transmitted through the base and top of the laminae. The base comprising coarser grains appears somewhat transparent as compared to the darker top where much of the light is cut off by cryptograined calcite. Medium to coarse silt-sized terrigenous quartz and mica occur at the base of laminae. Dolomite occurs in this micro facies as anhedral to euhedral, equigranular crystals ranging in size from 50 to 150 μm (Fig. 4.19 and 4.20). It is mostly concentrated along the top of the laminae where it consists of intergrown anhedral crystals forming a more or less continuous dolomite layer. From the top, dolomitization decreases downward until at the base only a few single anhedral crystals are seen floating in micrite. Graded micrite contains 5 to 30% dolomite by volume. Well sorted and evenly distributed calcite grains with poorly oriented magnetite grains are also observed (Fig. 4.21)).

Modal analysis indicates that in these limestone, calcite (CaCO_3) forms about 80% alongwith the 10% quartz and 8% magnetite (Table 4.2). Granulometric studies show that the grain size of calcite ranges from 15 μm to 360 μm with average size of 90 μm and the quartz grain vary in size from 20 μm to as large as 480 μm , with average grain size as 110 μm

Table 4.2 : Petrographic Analysis of Lithounit B

Name of the Mineral	Quantity (%)	Grain Size (μm)		
		Minimum	Maximum	Average
Calcite	80	15	360	90
Quartz	10	20	480	110
Magnetite	8	--	--	--
Hematite	2	--	--	--

Depositional Environment

The laminated micritic limestone of Lithounit B exhibits small-scale domal stromatolite indicating algal activities. This structure, consisting of vertical flutings within a lamina, resembles “palisade” structure described by Davies (1970 a, b) from recent algal mat sediments. Davies believes that such structure is formed “by vertical algal filaments growing upward through sediment laminae”, and it marks “the position of a zone of active filament growth”. An organic, rather than a mechanical control on deposition is suggested by the encrusting relationship of laminae, which pinch and swell without compensating for relief on the underlying surface.

Graded bedding is observed in thin sections of the laminated micrite limestone. It is a common feature of Recent algal mat sediments as reported by Black (1933), Ginsburg et al., (1954), Shinn et al., (1969) and Davies (1970 a). Each graded lamina in the algal mat sediments most probably represents deposition during one tidal pulse (Roehl, 1967, and Davies 1970 a).

By analogy with modern environments (Logan et al. 1964, Kendall and Skipwith, 1968, Davies, 1970 a, b and Friedman et al., 1973) the laminated micrite of Lithounit B, interpreted as algal-mat sediments, were most probably deposited in the low supratidal – high intertidal zone in a rather protected basin. A subtidal environment of algal mats (Gebelein, 1969; Newmann et al., 1970 and Friedman et al., 1973) is contradicted by the common presence of feature such as mud cracks, suggesting intermittent exposure.

The small lenses of flat pebble breccia (intrasparudite) interbedded with the laminated micritic limestones of Lithounit B are interpreted as deposits of small, shallow tidal channels crossing high intertidal flats. This interpretation is based on (1) their close association with the inferred tidal flat deposits (laminated micritic limestones) (2) pebble imbrication oriented at 180° in superjacent beds

indicating reversals of current direction and by implication, flood and ebb tide currents and (3) size grading of pelletoidal intraclasts which is most probably a result of decreasing current velocities during a single tidal pulse.

The intrasparite matrix of the flat pebble breccia indicates that within the channels, currents were strong enough to winnow lime mud (Folks, 1962) and deposit well-rounded and well-sorted pelletoidal intraclasts. Strong currents are also attested to by the frequent edgewise arrangements of flat pebbles. The identical composition of the majority of the pebbles and the matrix strongly suggests that the former were generated by powerful currents, which ripped up partly lithified intrasparite from the ancient channel bed. Thus, it is evident that most of the pebbles originated within the channels by current action and were re-deposited there.

Flat pebble breccia of Lithounit B differs genetically from that of Lithounit A, though both suggest deposition indicating in small shallow channels. In the case of Lithounit A, brecciated surfaces of supratidal flat provided pebbles of micrite, which were floated to the adjacent gullies and deposited therefrom, suspension along with lime mud. On the other hand, current action was responsible for the generation and redeposition of a large majority of flat pebbles, composed of intrasparite, within the channels of Lithounit B. However, some intraclasts, composed of micrite might have originated on the flats and floated to channels. The flat pebbles on Lithounit 'B' are bigger than those in Lithounit A, breccia lenses of the two Lithounits also differ in size since the maximum thickness of lenses increases from 20 cm in Lithounit A to 30 cm in Lithounit B. This indicates an increase in the size of the channels from Lithounit A to Lithounit B. The comparatively higher energy conditions and larger size of the channels of Lithounit B are suggestive of their relatively basinward location. Thus in all probability, Lithounit B was deposited in a zone lying seaward, in which Lithounit A was formed. Since the Lithounit A has been interpreted as high to low supratidal flat deposit, it follows that the Lithounit B was formed in the high intertidal zone.



It can thus be concluded that features such as profuse development of algal mats, graded bedding, high energy conditions and reversals of current direction within the channels collectively suggest that Lithounit B was deposited in the high intertidal flat zone and in the transitional zone onto the supratidal flat.



Fig. 4.13 : Vertical Section of Lithounit B Showing Distinct Laminae of Micritic Limestone



Fig. 4.14 : Lithounit B Showing Trough Cross Bedding with Truncated Top and Assymptotic Bottom

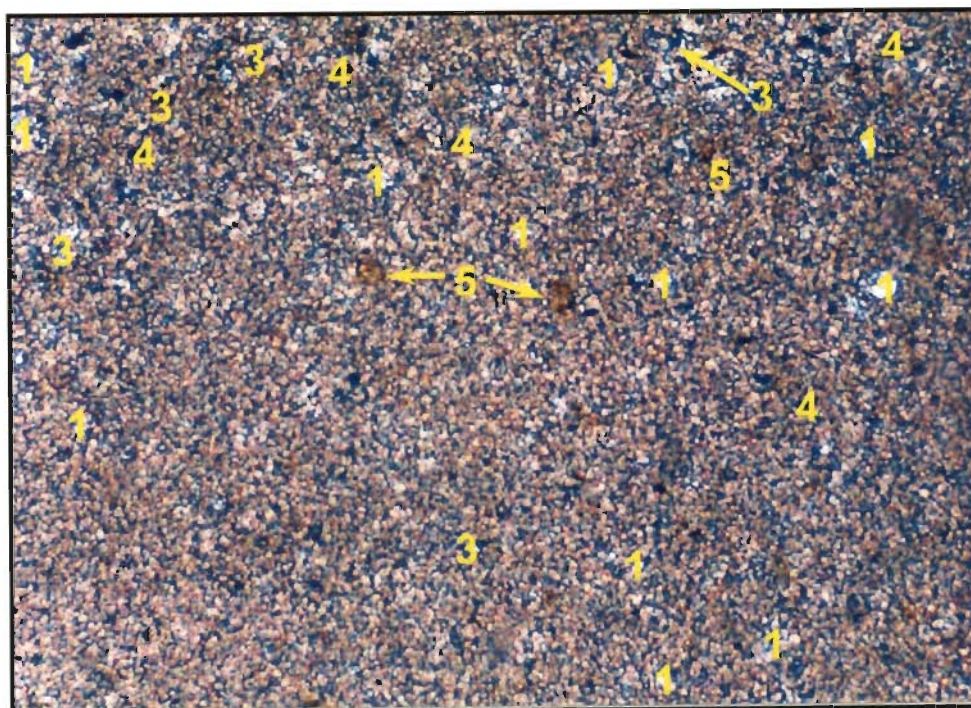


Fig. 4.15 : Photomicrograph Showing Laminated Planes of Calcite With Scattered Quartz, Hematite and Magnetite Grains in Lithounit B. (50 x, x - nicols)



Fig. 4.16 : Photomicrograph Showing Formation of Secondary Calcite in its Initial Stage with Scattered Quartz Grains in Lithounit B. (50 x, x - nicols)

1 - CALCITE; 2 - DOLOMITE; 3 - QUARTZ; 4 - MAGNETITE; 5 - HEMATITE

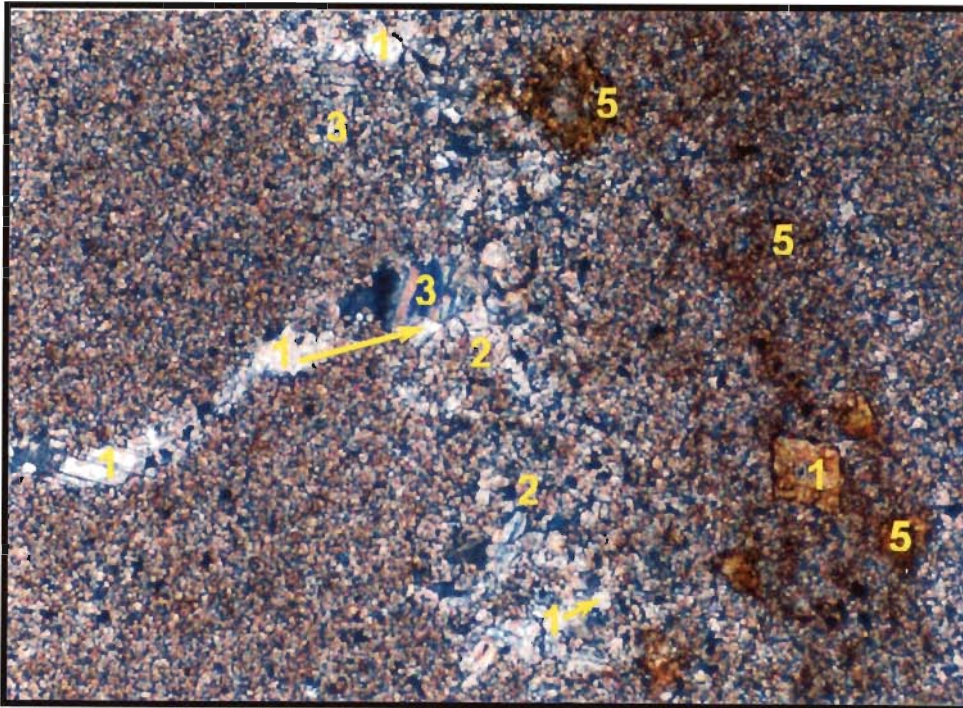


Fig. 4.17 : PhotomicrographS veins of Secondary Calcite Grains with Euhedral Grains Developed in the Carbonate Matrix of Lithounit B (50 x. x - nicols)



Fig. 4.18 : Photomicrograph Showing Well Sorted and Homogeneously Distributed Calcite Grains alongwith Magnetite (black) and Quartz (dark blue) Grains in Lithounit B. (50 x, x - nicols)

1 - CALCITE; 2 - DOLOMITE; 3 - QUARTZ; 4 - MAGNETITE; 5 - HEMATITE

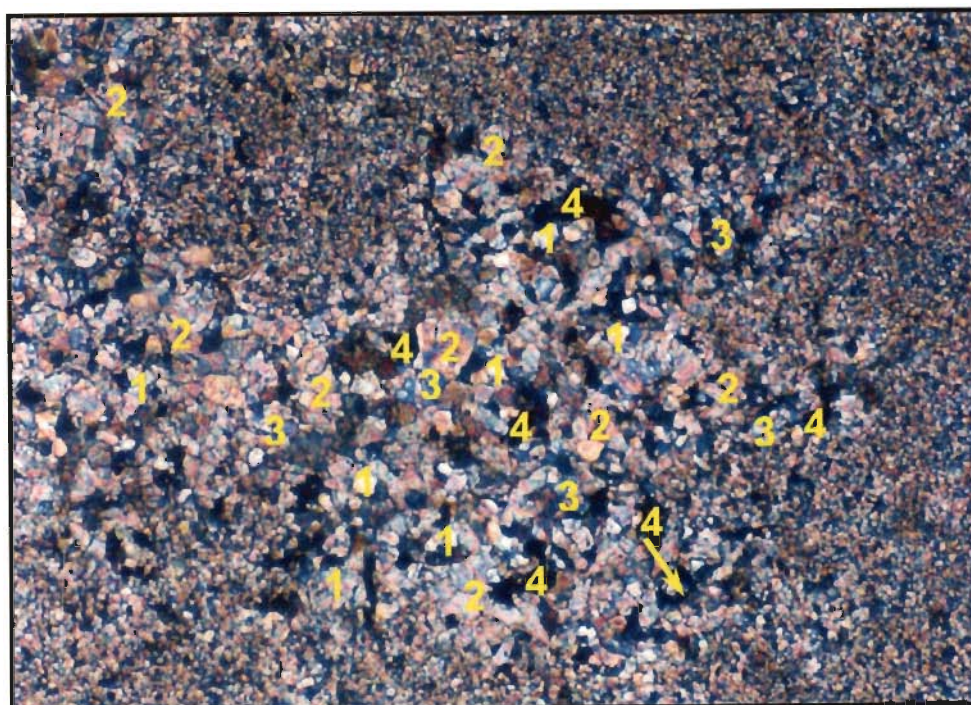


Fig. 4.19 : Photomicrograph Showing Clusters of Calcite and Dolomite and Grain size Variation in the Limestone of Lithounit B. (100 x. x - nicols)

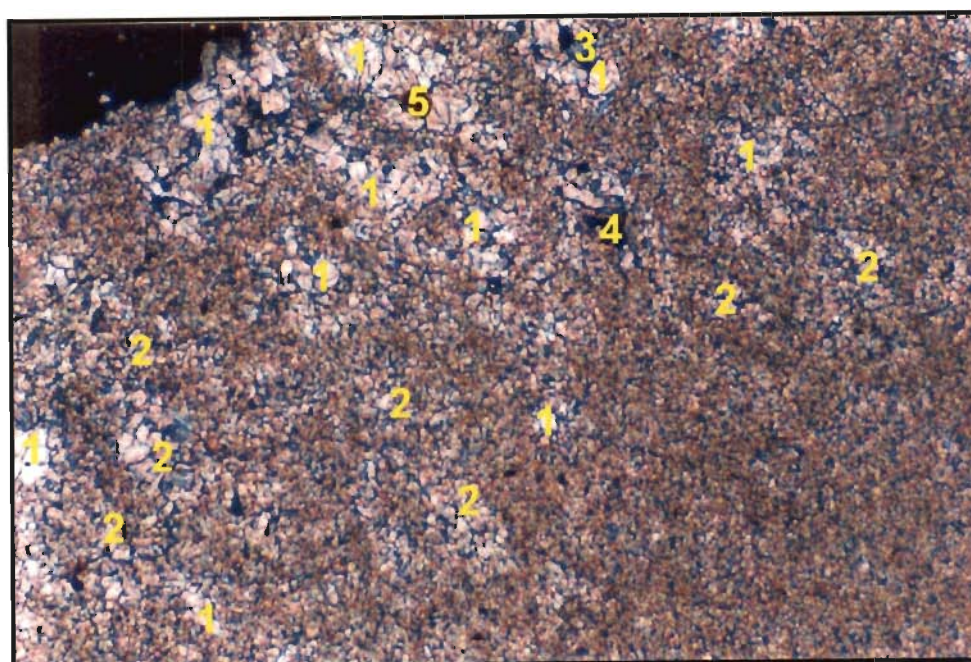


Fig. 4.20 : Photomicrograph Showing Clusters of Secondary Calcite and Dolomite in the Carbonate Matrix of Lithounit B. (100 x. x - nicols)

1 - CALCITE; 2 - DOLOMITE; 3 - QUARTZ; 4 - MAGNETITE; 5 - HEMATITE



Fig. 4.21 : Photomicrograph Showing Well Sorted and Evenly Distributed Calcite Grains with Poorly Oriented Magnetite Grains in Lithounit B (50 x, x - nicols)

4.2.3 Lithounit C

Overlying the Lithounit B, this Lithounit mainly comprises calcareous shales with occasional lenses of calcareous siltstones. The shales mostly olive but occasionally bright green, are massive as well as splintery, and show parallel lamination on weathered surfaces (Fig. 4.22). At several places, kink folds have also been observed in this Lithounit (Fig. 4.23 and 4.24). Occasional intercalations of red shales are present towards the top of the sequence. Grey to red calcareous siltstone lenses occasionally occur and are 2 cm to 2m thick. Their lateral extent ranges from a few meters to a few tens of meters. Stratification within these lenses consists of ripple lamination and micro-cross lamination and they often show disrupted bedding indicative of mud cracking. They contain small, 1.5 to 7 cm long, intraformational flat pebbles, which sometimes have an imbricate arrangement. Locally these may be sufficiently abundant in some of the lenses to form a breccia

Petrographically these are mostly clay rich with little calcitic constituents and silt size quartz.

Depositional Environment

These calcareous shales indicate their deposit in low-energy-environment, as is evident by their parallel lamination and general absence of current and wave formed structures. This low energy environment indicates their deposition mainly in the subtidal lagoon. However, the presence of mud cracks, flat pebbles and channels at certain levels in the sequence is suggestive of occasional exposure and intertidal conditions.

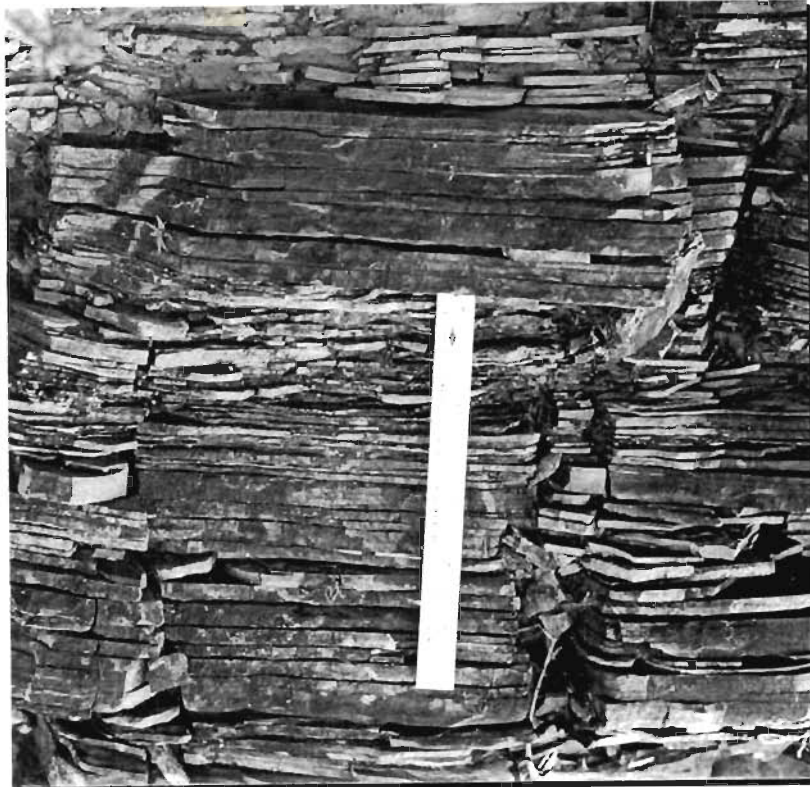


Fig. 4.22 : Lithounit C Showing Parallel Lamination in Jointed Olive Shale



Fig. 4.23 : Kink folds in Lithounit C



Fig. 4.24 : Kink folds in Splintery Olive Shales of Lithounit C

4.2.4 Lithounit D

Overlying the Lithounit C, this Lithounit D consists of grey black laminated to thin bedded micritic limestones (Fig. 4.25 and 4.26). The laminated beds show wavy and discontinuous laminae. Palisade structure is common but ripple lamination, flaser bedding, which signifies incomplete mud laminae trapped in ripple troughs and symmetrical ripple marks occur rarely. Domal structure is also observed in this lithounit (Fig. 4.27).

Petrography

Micrite occurs in the Lithounit D as dark grey to black micritic limestone. It consists of a homogeneous and structure less aggregate of calcite grains and some quartz silt grains, which show corrosion by the surrounding micrite. A delicate laminated structure is occasionally seen which appears as an anastomosing network of bedding. Most of the fabric shows dense to very dense interlocking of micritic grains. There are discontinuous micro veins of calcite within well sorted homogeneously distributed calcite grains (Fig. 4.28 and 4.29). Occasional magnetite and dolomite grains are also present in the fine grained calcite matrix (Fig. 4.30 - 4.32).

Depositional Environment

This Lithounits is almost entirely composed of micrite and neomorphosed micrite. The abundance of micrite suggests a low energy environment of deposition. Flat pebbles, mud cracks and channels are completely absent from this Lithounit. The other features that are suggestive of wave and current action and intermittent exposures are rare. This Lithounit is interpreted as a deposit of shallow subtidal lagoon on the basis of abundance of micrite, general absence of features suggestive of intermittent exposure and dark grey colour of sediment. The presence of algal mats in this Lithounit supports the interpretation of a low energy protected, shallow, subtidal environment, with poor clastic sediment supply.

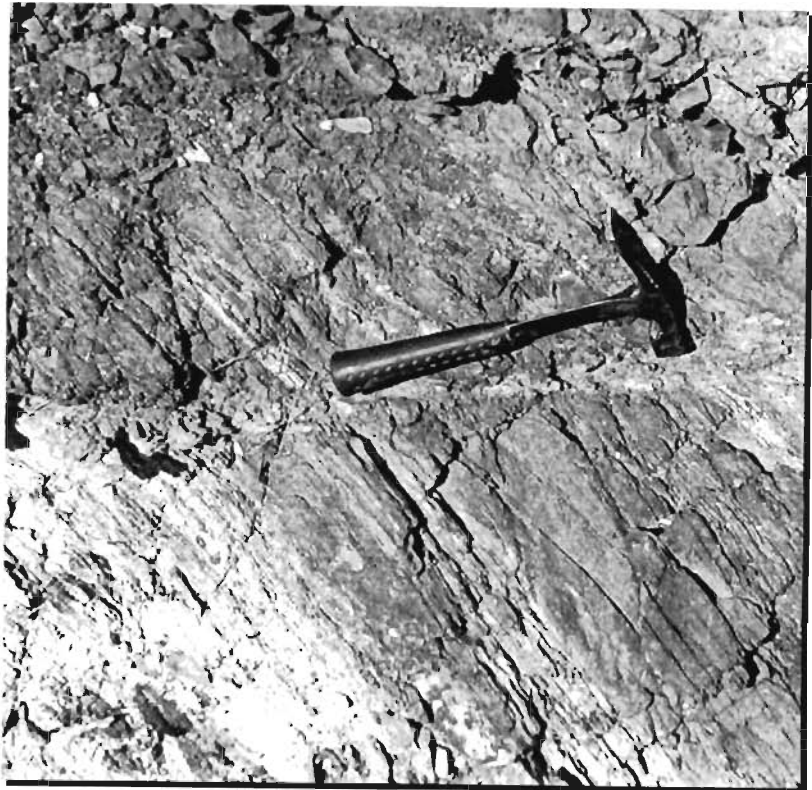


Fig. 4.25 :Lithounit D Consisting of Thinly Bedded Micritic Limestone



Fig. 4.26 : Vertical Section of Thickly Bedded Micritic Limestone of Lithounit D



Fig. 4.27 : Domal Structure in Thick to Thinly Bedded Lithounit D of Micritic Limestone



Fig. 4.28 : Photomicrograph Showing Well Sorted and Homogeneously Distributed Calcite Grains with Micro Fractures in Lithounit D (50 x, x - nicols)

1 - CALCITE; 2 - DOLOMITE; 3 - QUARTZ; 4 - MAGNETITE; 5 - HEMATITE

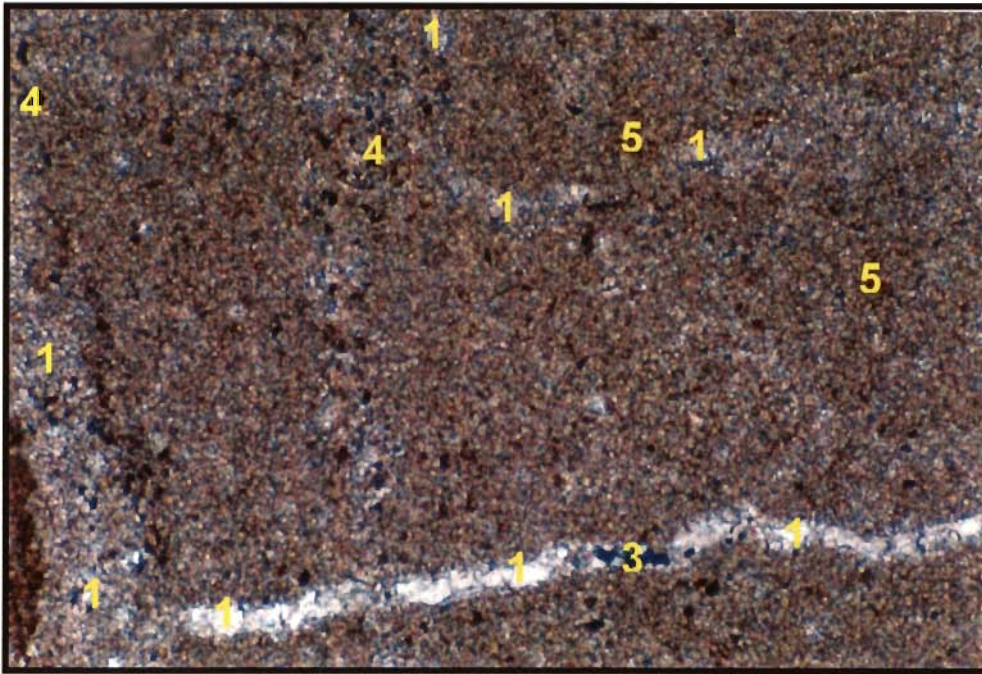


Fig. 4.29 : Photomicrograph Showing Three Sets of Discontinuous Calcite veins Cutting Across Each Other Within Fine Grained Lamination Plane of Lithounit D (50x, x - nicols)

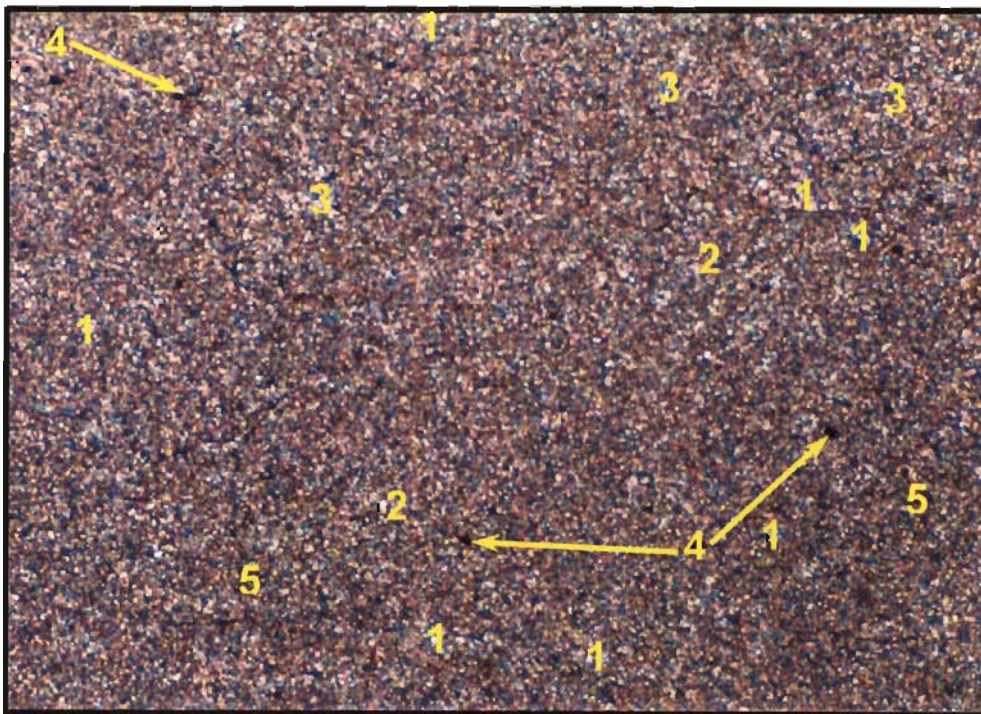


Fig 4.30 : Photomicrograph Showing Well Sorted and Homogeneously Distributed Calcite Grains in Lithounit D. Black Grains Represent Magnetite. (50 x, x - nicols)

1 - CALCITE; 2 - DOLOMITE; 3 - QUARTZ; 4 - MAGNETITE; 5 - HEMATITE

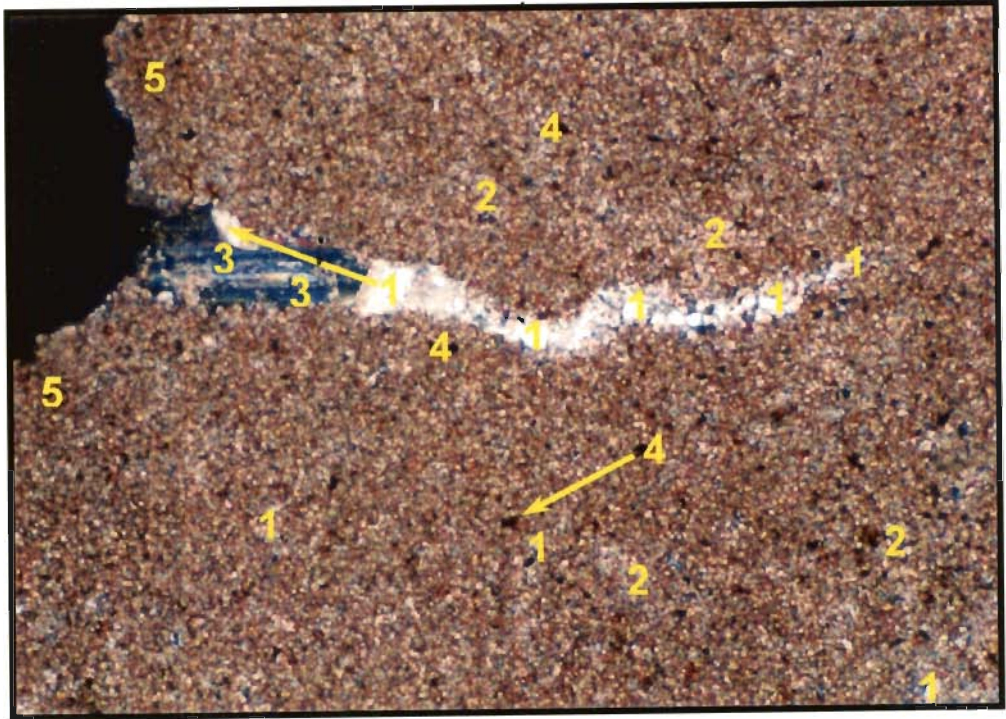


Fig. 4.31 : Photomicrograph Showing Discontinuous Micro Veins of Calcite in the Carbonate Matrix of Lithounit D. Micro Grains of Calcite and Magnetite are Present. A Well Developed Dolomite Grain is also Present (50 x, x - nicols)

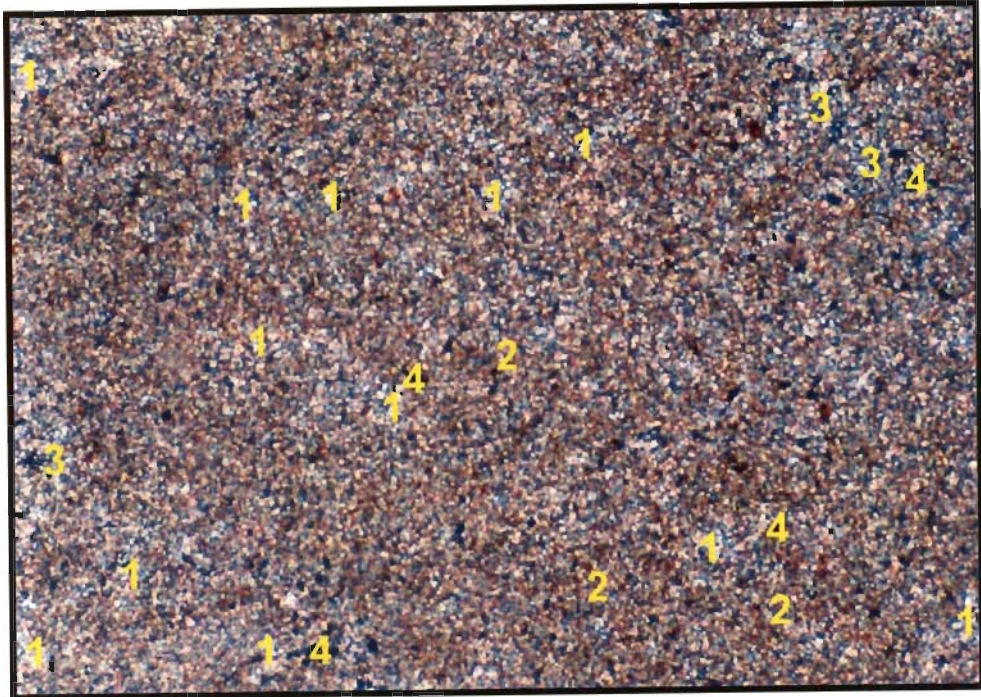


Fig. 4.32 : Photomicrograph Showing Well Sorted and Homogeneously Distributed Calcite Grains Relatively Finer in Size in Lithounit D (50 x, x - nicols)

1 - CALCITE; 2 - DOLOMITE; 3 - QUARTZ; 4 - MAGNETITE; 5 - HEMATITE

4.3 Spectral Response of Lithounits

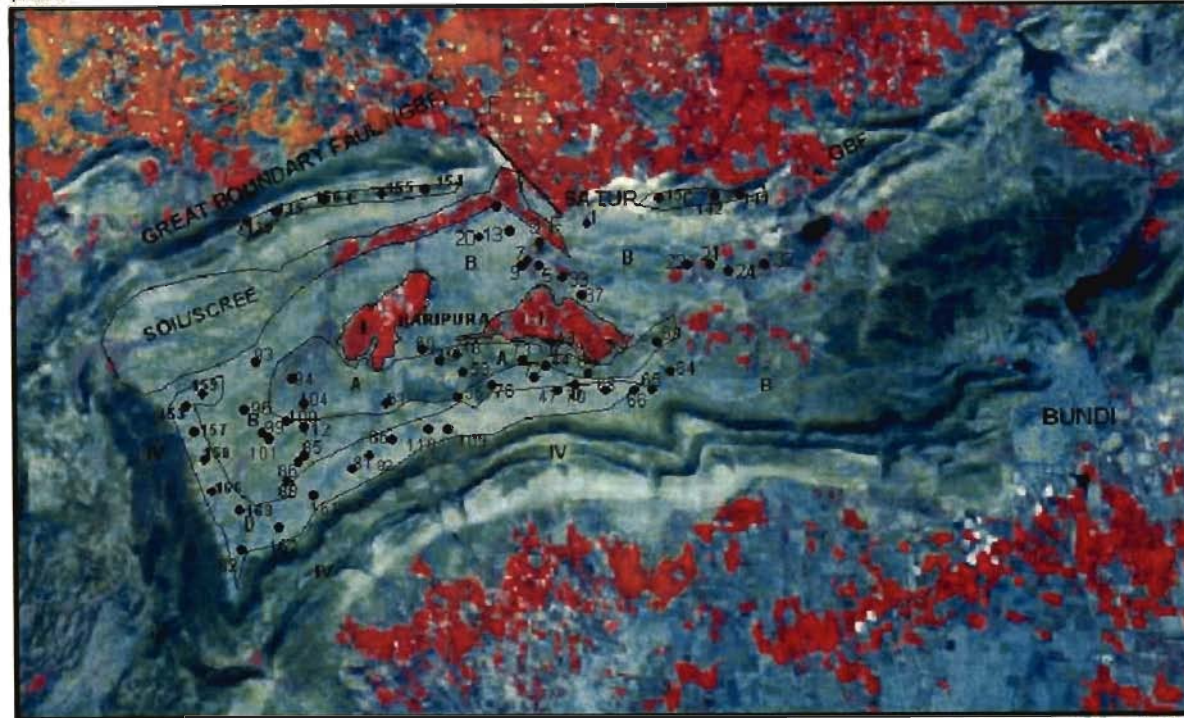
It has thus been observed that each Lithounit of Bhandar Limestone was born in its own depositional environment as evident from the physical imprints, bio-indicators and chemical make up of sediments. Accordingly, each Lithounits should have its own spectral response to various electromagnetic waves and therefore, can be differentiated from one another. With this premise, an attempt was made to identify various calcareous Lithounits of Bhandar limestone using remote sensing data.

The pixel values of IRS-LISS-III Data were determined with the help of ERDAS Imagine software for bands 2, 3, 4 and 5 in the wave length range of 0.52 – 0.59 μm (green), 0.62 – 0.68 μm (red), 0.77 – 0.86 μm , Near Infrared (NIR) and 1.55 – 1.70 μm , Short Wave Infrared (SWIR) respectively. The Lithounits were delineated on the standard FCC and Lithounit map was generated on the basis of pixel values and corresponding chemical analysis of limestone samples (Fig. 4.33).

With a view to identify various Lithounits, an attempt has been made to plot the pixel values in various bands of IRS-LISS-III Data (Fig. 4.34). The perusal of Fig. 4.34 indicates that the pixel values in bands 2, 3 and 4 of green, red and NIR could not be compared. However, in linear contrast image of band 5 (SWIR), the calcareous Lithounits A, B, and D with average pixel values of 152, 140 and 127 respectively could be distinctly identified.

75.47,25.51

75.67,25.51 N



75.47,25.39

75.67,25.39

LITHOUNITS	TYPE	CaO(%)	SiO2(%)
D	HIGH GRADE	>48	<10
C	OLIVE SHALE		
B	ACCEPTABLE GRADE	44-48	10-12
A	SUB GRADE	42-44	12-16
I	GANURGARH SHALE		
IV	SANDSTONE		

● Location of Sample Points

F
FAULT
F

(CO-ORDINATE IN DECIMAL DEGREES)

SCALE 1:1,06,810

Fig. No. 4.33 Map Showing Lithounits of Bhandar Limestone in the Study Area

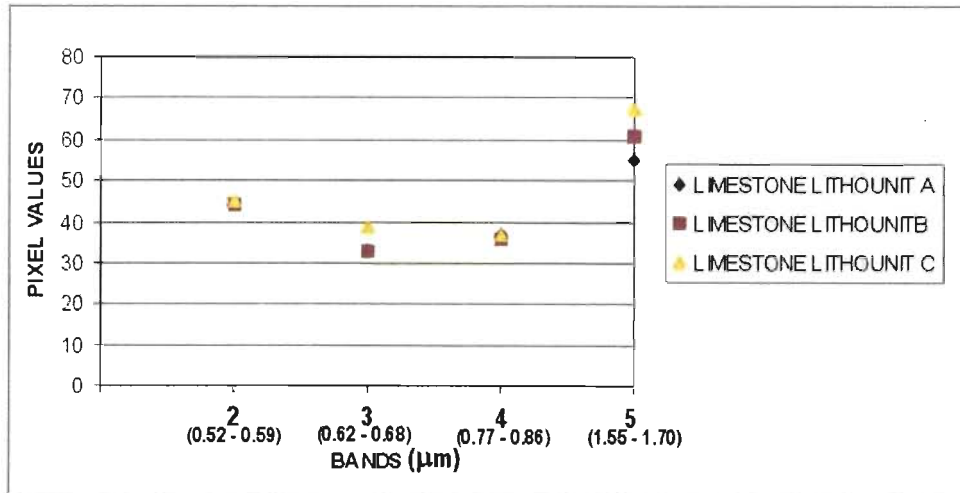


Fig. 4.34 : Pixel Values of Limestone Lithounits (in Linear contrast image of IRS LISS-III Satellite Data)

4.4 Summary

The Bhander Limestone locally known as Lakheri Limestone in this area has stratigraphically been classified into four Lithounits – A (the oldest, pink coloured) followed upward by B (bluish grey coloured), C (olive green coloured) and D (the youngest dark grey to black coloured).

The limestone of Lithounit D deposited in the low energy, subtidal lagoonal environment with poor clastic sediment that is entirely made up of calcitic (CaCO_3) mineral. It appears to be the best variety of limestone, which may be used as sweetener to upgrade the sub grade limestone of Lithounit A. The Lithounit C deposited mainly in the low kinetic energy conditions with fine grained clastic sediment supply. It is mainly calcareous shale, which may not be suitable as raw material for cement manufacturing.

The limestone bearing Lithounit B interpreted to be deposited mainly in the intertidal environment and is comprised of 80 % calcium carbonatic mineral calcite and, therefore, can be used as such in the cement industry.

The limestone of Lithounit A desposited in supratidal environment, has about 73 % calcite. Though inferior to Lithounit B, it may also be used in cement manufacturing alongwith Lithounit D

CHAPTER 5

EVALUATION OF BHANDER LIMESTONE AS SOURCE OF CEMENT

5.1 Introduction

Stratigraphically the Bhander limestone of Bundi district has been divided into Lithounit A (oldest), B, C and D (youngest). The Lithounits A, B and D are mainly calcareous and Lithounit C is mainly argillaceous. The limestones of these calcareous Lithounits broadly appear to be similar in terms of lithology and are micritic in nature. However their chemical make-up and terrigenous content in terms of nature and amount vary with variation in the physico-chemical environment of deposition of these shoreline sediments from mainly supratidal initially, through intertidal to subtidal- lagoonal in the end. In view of this, an attempt has been made in this chapter to analyse and work out chemical composition and relevant physical properties of these calcareous Lithounits and evaluate them for their suitability for utilization as raw material for cement generation. As discussed in chapter 3, the chemical constituents namely CaO, SiO₂, MgO, Fe₂O₃, Al₂O₃ and minor constituent such as Na₂O, K₂O, SO₃, Mn₂O₃, P₂O₅ and Cl are the most vital parameters. The effect of these parameters on the processing of raw materials and ultimately on the quality of cement has also been evaluated.

5.2 Geochemical Analysis

In order to carry out quality assessment of Bhander Limestone of Satur-Haripura area of Bundi District Rajasthan, 160 representative samples were collected from all the Lithounits. Geochemical analysis of limestone samples was carried out as per IS-1727-1967 and NCB standard method for determination of

Loss on Ignition (LOI), SiO_2 , Fe_2O_3 , Al_2O_3 , CaO and MgO , which are main controlling parameters for cement grade limestone.

5.2.1 Determination of Loss on Ignition

The loss on ignition of limestone indicates the superficially absorbed moisture besides release of carbon dioxide due to decomposition of calcium carbonate. It is determined by heating the sample in a muffle furnace at a temperature of 900 – 1000 °C .The detailed methodology of determination of LOI is given in Annexure I.

5.2.2 Determination of Silica

The soluble silicates are decomposed by hydrochloric acid. The insoluble silicates are rendered soluble by treating with fusion mixture (1 Part Na_2CO_3 + 1 Part K_2CO_3) in a platinum crucible. During heating at high temperature between 900-1000 °C for 15-20 minutes, all insoluble silicates get combined with alkalis rendering insoluble silicates to soluble silicate and are easily dissolved in hydrochloric acid, forming metasilicic acid in colloidal form. During evaporation, the meta-silicic acid gets converted into insoluble silica. The acidic solution is then filtered and the washed residue is ignited to give impure silica containing some of the impurities adsorbed like iron and alumina. Silicon dioxide is volatilised in the form of silicon tetrafluoride by hydrofluoric acid in the presence of sulphuric acid. The loss in weight is reported as pure silica. The detailed procedure of determination of silica is described in Annexure I. sample is titrated at pH of 10 against standard EDTA solution using triethanolamine for overcoming interference due to iron and aluminium and with thymol

5.2.3 Determination of Calcium Oxide and Magnesium Oxide

A suitable aliquot of the silica free solution of the sample is titrated at pH of 10 against standard EDTA solution using triethanolamine for overcoming interference due to iron and aluminium and with thymol phthalexone as indicator. The titre value gives the sum of calcium and magnesium present in the solution from which the value corresponding to magnesium is obtained by subtracting that of calcium. The details are given in Annexure I.

The average chemical analyses of Lithounit A, B and C is given in Tables 5.1, 5.2, 5.3 and 5.4 respectively. The low standard deviation for all the chemical parameters indicate that the individual lithounits have very low variation in their chemical quality and are chemically more or less homogeneous. The perusal of Table 5.1, 5.2 and 5.4 suggests that the average CaO in lithounit A, B and D are 42.88%, 46.24% and 49.9% respectively and average SiO₂ is 13.97%, 10.72% and 6.42% respectively. The data suggests that the Lithounit A has least CaO and maximum SiO₂. On the other hand, the Lithounit D has highest CaO and lowest SiO₂. On the basis of this, it is inferred that the limestone of Lithounit D appears to be of high grade and that of Lithounit A to be of relatively low grade. However, limestone of Lithounit B has optimum CaO and SiO₂ contents.

Keeping in view the quality requirement of cement grade, limestone has been grouped into following broad categories :

<u>Categories of Limestone</u>	<u>CaO (%)</u>	<u>SiO₂ (%)</u>
Sub-Grade (<i>Lithounit A</i>)	42 - 44	12 - 16
Acceptable Grade (<i>Lithounit B</i>)	44 - 48	10 - 12
High Grade (<i>Lithounit D</i>)	> 48	< 10

Table 5.1 : Chemical Constituents (%) of Limestone Samples of Lithounit A

SL. No.	Location	CaO	MgO	SiO ₂	Fe ₂ O ₃	Al ₂ O ₃	LOI
1	98	42.05	3.78	12.64	1.15	1.24	37.80
2	120	42.07	1.54	14.61	1.20	1.80	37.33
3	31	42.11	2.39	13.76	1.17	1.20	38.83
4	99	42.11	1.55	14.48	1.46	2.69	37.23
5	37	42.17	3.41	13.26	0.87	1.79	38.11
6	125	42.18	3.92	15.66	0.99	3.23	33.23
7	119	42.22	1.65	12.60	1.49	4.25	36.52
8	131	42.23	3.21	14.35	1.09	2.04	35.83
9	150	42.23	1.56	15.32	2.21	3.66	34.23
10	124	42.34	3.23	15.14	1.41	2.05	35.12
11	100	42.38	1.85	14.01	2.91	3.27	34.56
12	128	42.40	3.31	13.96	1.88	1.41	35.62
13	7	42.40	1.46	14.71	0.98	2.52	35.62
14	9	42.40	1.46	14.71	1.71	2.08	37.20
15	33	42.40	1.46	14.71	2.55	2.48	35.68
16	102	42.40	1.46	14.71	3.44	1.94	35.21
17	129	42.40	2.32	15.78	3.69	1.52	33.28
18	144	42.48	3.53	15.85	1.84	2.64	33.06
19	149	42.52	3.83	13.87	2.97	2.52	32.96
20	148	42.52	1.72	12.69	2.92	1.96	37.51
21	121	42.68	1.85	13.69	0.79	3.89	35.45
22	145	42.71	3.80	13.39	2.31	2.94	34.02
23	25	42.74	1.83	13.50	0.69	1.61	39.19
24	26	42.74	1.83	13.50	1.60	2.31	36.74
25	29	42.74	1.83	13.50	0.72	1.31	39.38
26	97	42.81	3.45	13.96	2.16	1.30	34.85
27	147	42.84	1.98	13.58	0.84	3.62	35.42
28	127	43.09	2.46	12.87	2.96	2.56	35.38
29	114	43.09	1.46	15.79	2.43	2.09	34.14
30	146	43.21	3.50	15.66	0.82	1.51	34.57
31	136	43.33	1.06	12.83	0.75	1.38	39.89
32	137	43.41	1.11	12.99	3.49	2.68	34.78
33	101	43.42	2.35	14.10	2.08	2.05	35.05
34	123	43.44	1.12	15.04	2.96	2.80	33.78
35	96	43.57	2.32	13.54	3.54	2.29	34.21
36	105	43.61	2.00	12.91	1.22	2.62	37.12
37	143	43.61	3.22	14.82	1.91	2.14	33.45
38	126	43.67	1.31	13.18	3.08	3.27	34.49
39	6	43.70	2.00	12.36	0.94	2.44	37.58
40	138	43.75	2.96	12.46	2.62	2.29	35.16
41	118	43.77	3.20	12.73	3.96	1.67	34.01
42	44	43.78	1.32	14.53	2.31	2.79	34.35
43	130	43.83	2.99	14.48	1.47	1.20	34.36
44	132	43.93	2.12	13.87	3.69	1.50	34.07
45	122	43.99	1.68	12.31	2.83	2.41	36.00
Mean		42.88	2.30	13.97	2.00	2.29	35.61
ST. Deviation		0.62	0.88	1.02	0.98	0.76	1.80

Table 5.2 : Chemical Constituents (%) of Limestone Samples of Lithounit B

SL. No.	Location	CaO	MgO	SiO ₂	Fe ₂ O ₃	Al ₂ O ₃	LOI
1	76	44.06	1.16	11.05	1.88	2.73	37.50
2	117	44.26	3.33	11.85	1.11	1.90	36.50
3	79	44.38	1.42	10.57	1.64	3.11	37.20
4	12	44.45	1.47	11.13	1.65	2.02	38.05
5	21	44.68	3.18	11.28	2.32	4.16	34.04
6	11	44.95	1.47	11.13	1.13	2.05	37.42
7	63	45.27	2.30	11.29	1.27	2.50	36.81
8	45	45.35	1.40	11.12	1.22	2.16	37.63
9	54	45.35	1.40	11.12	1.19	2.65	37.01
10	8	45.49	1.55	10.34	1.02	2.41	36.30
11	36	45.49	1.55	11.30	2.10	1.50	36.75
12	61	45.49	1.55	11.58	1.87	3.28	35.50
13	62	45.49	1.55	11.89	1.14	2.58	35.90
14	90	45.53	1.66	10.27	1.69	4.09	35.48
15	46	45.70	2.36	10.38	3.70	1.69	34.78
16	56	45.70	2.36	10.38	0.83	2.74	36.54
17	58	45.70	2.36	10.38	2.54	1.65	35.41
18	103	45.70	2.36	10.38	1.23	1.54	37.12
19	115	45.71	1.27	11.19	2.67	2.44	35.75
20	30	45.72	2.60	10.67	2.88	2.16	35.60
21	107	45.84	1.13	11.60	1.89	3.36	34.81
22	94	46.10	0.97	10.63	3.78	3.17	33.74
23	93	46.16	1.06	11.26	1.39	1.62	37.68
24	1	46.25	2.03	11.64	1.75	2.41	35.62
25	2	46.25	2.03	11.64	1.75	2.41	35.62
26	38	46.27	2.13	10.53	3.96	2.63	33.89
27	39	46.27	2.13	10.53	2.92	3.35	34.01
28	40	46.27	2.13	10.53	2.83	3.03	34.12
29	87	46.27	1.06	10.26	3.95	4.07	33.56
30	5	46.28	1.60	10.91	1.79	4.28	34.47
31	68	46.28	1.14	10.36	1.73	3.68	35.93
32	104	46.28	1.14	10.36	0.99	1.41	38.23
33	10	46.31	1.33	10.48	1.99	2.47	37.04
34	19	46.31	1.33	10.48	1.18	1.93	37.59
35	34	46.37	2.44	10.27	2.87	4.05	32.92
36	35	46.37	2.44	11.24	2.43	2.75	34.56
37	3	46.38	1.56	10.08	1.08	1.73	37.58
38	4	46.38	1.56	10.08	1.70	2.10	37.58
39	41	46.42	1.55	10.37	3.56	1.62	35.51
40	82	46.45	1.42	10.15	3.15	3.85	33.87
41	47	46.47	2.38	10.81	1.45	2.90	36.23
42	48	46.47	2.38	10.81	1.26	2.44	35.56
43	49	46.47	2.38	10.81	3.47	2.82	32.81

Contd.....

44	74	46.51	1.67	10.01	1.10	2.09	37.85
45	111	46.54	1.28	10.24	2.22	2.84	35.89
46	72	46.65	1.45	10.30	2.50	1.50	37.04
47	116	46.71	3.23	10.30	1.77	2.90	34.17
48	78	46.75	1.05	10.78	2.07	4.19	34.58
49	73	46.78	1.90	11.61	0.76	1.65	36.58
50	50	46.82	1.34	10.05	2.15	1.83	37.54
51	51	46.82	1.34	10.05	3.06	2.55	36.02
52	53	46.82	1.34	10.05	1.83	2.81	36.23
53	55	46.82	1.34	10.05	2.18	2.97	35.21
54	69	46.89	1.79	10.78	1.30	3.18	35.35
55	32	47.18	2.27	10.34	0.80	1.94	36.85
56	80	47.21	1.17	10.90	3.19	2.16	34.84
57	88	47.21	1.03	10.83	2.91	1.97	35.29
58	67	47.39	0.82	10.03	2.85	2.91	34.70
59	22	47.43	1.58	11.76	1.28	2.05	35.06
60	106	47.44	0.97	11.02	2.56	3.45	34.12
61	84	47.56	1.17	10.73	1.13	2.36	36.45
62	20	47.60	0.76	10.75	1.45	2.51	36.21
63	28	47.60	0.76	10.76	1.06	2.15	36.74
64	81	47.72	1.43	10.02	3.72	2.42	34.23
65	77	47.78	1.22	10.30	3.46	3.26	33.12
AVERAGE		46.24	1.67	10.72	2.05	2.60	35.76
STDEV		0.85	0.60	0.52	0.90	0.76	1.39

Table 5.3 : Chemical Constituents (%) of Lithounit C (Olive Shale) of Bhandar Limestone

SL. No.	Location	CaO	MgO	SiO ₂	Fe ₂ O ₃	Al ₂ O ₃	LOI
1	15	1.39	3.00	62.06	4.61	17.31	11.55
2	154	1.45	2.76	64.19	5.89	13.92	10.26
3	133	1.57	2.32	58.36	4.90	18.24	13.04
4	139	1.61	2.47	59.53	5.35	15.92	13.37
5	140	1.64	2.58	60.41	5.54	14.78	13.62
6	155	1.68	3.27	62.85	4.63	12.48	13.95
7	135	1.69	2.77	61.87	5.94	12.15	14.04
8	141	1.70	2.41	66.73	5.19	9.45	14.12
9	142	1.76	2.98	63.01	5.37	11.34	14.62
10	134	1.81	3.22	65.38	4.01	9.24	15.04
AVERAGE		1.63	2.78	62.44	5.14	13.48	13.36
STDEV		0.13	0.33	2.59	0.61	3.10	1.45

Table 5.4 : Chemical Constituents (%) of Limestone Samples of Lithounit D

SL. No.	Location	CaO	MgO	SiO ₂	Fe ₂ O ₃	Al ₂ O ₃	LOI
1	13	48.06	2.97	5.96	1.20	2.88	37.10
2	164	48.14	2.72	6.84	1.22	2.91	36.80
3	95	48.31	1.28	8.43	1.02	3.42	36.79
4	170	48.51	1.76	9.87	1.02	1.24	36.76
5	160	48.64	1.67	9.50	1.80	1.48	35.46
6	85	48.68	1.07	8.95	2.71	1.24	36.67
7	162	48.71	2.35	6.21	1.64	1.89	38.08
8	71	48.72	1.13	6.74	2.63	1.30	38.12
9	83	48.87	1.89	6.88	2.28	3.57	36.18
10	166	49.09	1.82	4.85	1.88	1.34	39.45
11	158	49.12	2.45	7.02	2.53	1.96	36.12
12	113	49.21	1.45	5.34	3.78	2.89	36.34
13	153	49.33	1.07	4.15	2.94	1.44	39.72
14	75	49.42	1.17	6.01	2.42	3.61	36.56
15	112	49.49	1.08	4.98	0.98	1.44	40.78
16	110	49.71	1.19	5.43	3.24	2.75	36.56
17	165	49.73	1.35	8.74	1.07	1.75	36.35
18	167	49.77	3.74	4.76	2.91	2.10	35.95
19	65	49.77	1.13	7.70	2.64	2.15	35.38
20	92	49.77	1.13	7.70	3.21	1.87	35.36
21	161	49.77	3.10	9.58	1.23	0.57	34.83
22	108	49.79	0.83	5.63	3.09	1.85	38.17
23	24	49.89	1.58	6.13	1.25	2.40	37.66
24	27	49.89	1.58	6.13	1.15	3.90	36.55
25	64	49.89	1.58	6.13	3.52	1.80	36.23
26	57	50.14	1.14	5.56	3.69	3.42	34.41
27	109	50.19	1.08	5.02	1.17	1.72	39.34
28	66	50.63	0.93	4.75	1.98	2.39	38.44
29	70	50.63	0.93	4.75	1.11	4.18	37.63
30	169	50.97	1.40	6.11	1.17	1.15	38.21
31	91	51.19	1.11	6.69	2.18	2.84	35.12
32	86	51.49	1.07	6.58	3.08	1.22	35.78
33	151	51.55	3.48	6.09	1.95	2.34	33.59
34	163	51.58	1.36	9.48	0.82	0.37	35.78
35	159	51.72	3.12	6.67	0.54	0.65	36.34
36	168	51.73	2.00	4.59	1.45	0.61	38.21
37	152	51.74	1.42	4.56	1.63	3.69	35.37
38	171	51.76	2.34	5.22	1.82	0.64	37.38
39	89	51.89	1.02	6.58	3.76	4.20	31.78
40	157	52.00	3.80	4.67	1.33	0.78	36.43
AVERAGE		49.99	1.73	6.42	2.03	2.10	36.69
STDEV		1.18	0.83	1.57	0.93	1.08	1.69

5.3 X-Ray Fluorescence Spectrometry

The X-ray fluorescence spectrometer was also used for determination of major oxides, alkalis and minor constituents in limestone. Some of the samples analysed by conventional technique as described in Annexure-I were also analysed by XRF as check samples analysis. The deviation was found to be well within the prescribed limits as indicated in Table 5.5. The methodology of XRF technique is described in Annexure-II.

Table 5.5 : Permissible Difference in Chemical Constituent of Limestone

Type of Limestone	Permissible difference in weight %						
	SiO ₂	Al ₂ O ₃	Fe ₂ O ₃	CaO	MgO	SO ₃	LOI
High Grade	0.20	0.1	0.1	0.50	0.20	0.04	0.5
Sub-Grade	0.50	0.3	0.15	0.40	0.20	0.04	0.5

The minor constituents such as Na₂O, K₂O, SO₃, P₂O₅, Mn₂O₃ and Cl, which have direct bearing on quality of cement were analysed for all Lithounits. The range of minor constituents in limestone, as analysed by XRF technique given in Table 5.6.

Table 5.6 : Minor Chemical Constituents of Bhandar Limestone of Study Area

Sr.No.	Minor Constituents	Range %	
		Minimum	Maximum
1.	Na ₂ O	0.13	0.56
2.	K ₂ O	0.11	0.42
3.	SO ₃	Traces	0.12
4.	P ₂ O ₅	Traces	0.040
5.	Mn ₂ O ₃	.021	.057
6.	Cl	.002	.006

All the minor constituents are well within the prescribed limits and they will not have any adverse effect either on cement manufacturing process or quality of cement.

5.4 Strength Parameters

In order to assess the amenability to crushing and grinding, the Crushing strength and Bond's index of five different types of limestone samples of Bundi area were determined as shown in Table 5.7.

Table 5.7 : Strength Parameters of Representative Samples of Limestone from Various Lithounits

Lithounits.	Chemical Composition					Crushing strength (Kg/cm ²)	Bond's Index (KwH / tonne)
	SiO ₂ (%)	Al ₂ O ₃ (%)	Fe ₂ O ₃ (%)	CaO (%)	MgO (%)		
D	7.8	1.0	1.7	49.1	0.8	1000	16.0
D	9.9	3.0	0.8	48.0	0.9	1000	16.0
B	12.3	3.2	2.4	45.2	1.5	900	11.3
A	16.2	2.2	1.01	43.7	0.9	850	13.8
A	14.5	3.4	1.3	44.1	0.6	1000	14.7

The above results indicate that the strength parameters in respect of crushing strength and Bond's index vary within the narrow range and are not corresponding to chemical composition of limestone. The higher values of Bond's index and crushing strength may be due presence of calcite crystals and free silica in the form of quartz.

5.5 Assessment of Limestone Reserves

The reserves refer to the known mineral assets, which are readily available for exploitation. Estimation of geological and mineable reserves along with their quality is the ultimate objective of an exploration programme.

5.5.1 Categorisation of Reserves

The Norms for Proving Limestone Deposits for cement manufacture evolved with the active participation of industry, R&D institutions, consultants, exploration agencies etc. where in the limestone reserves have been classified into proved, probable and possible categories (NCB norms 2001). These categories are defined in terms of the confidence level achieved on their estimation and has a direct bearing on complexity of the deposit vis-a-vis quantum of exploration. The different categories of reserves are described below :

- **Possible Reserves**

These shall refer to the first estimate of grade and quantity of limestone deposit calculated purely on the basis of data available, supplemented by surface continuity and width / thickness of the bed on geological evidence, which include information from first mining activity and comparison with similar deposit of the locality. Possible reserves are estimated after reconnaissance prospecting and should not vary by more than 4% in grade (CaO%) and 50% in quantity on actual mining.

- **Probable Reserves**

It refers to estimation carried out partly from actual prospecting work and partly from reasonable extrapolation on geological grounds. The grades and volumes of blocks are calculated on the basis of widely spaced drill holes, pits, trenches and exposed outcrop sections and should show less than 3% variation in grade (CaO%) and less than 30% variation in reserves on actual mining.

- **Proved Reserves**

It is estimated after detailed exploration and proving. This category of reserve is established on the basis of adequate number of closely spaced drill holes and excavation controlled by limited extent of exploratory mining, wherever necessary, with little or no extrapolation. Reserves estimated under this category should show less than 1% variation in CaO content and less than 10% variation in calculated reserves on actual mining.

In addition to the above categories of reserves, which are estimated during the different phases of prospecting and exploration, another category of reserves, designated as developed reserves is estimated only after the mining of deposit has started.

- **Developed Reserves**

This refers to portions, which are blocked or benched out and are ready for mining. The quantities and grades are based on mine development carried out preparatory to actual mining. This category takes into accounts the feed back from mining operations. Reserves estimated under this category should generally show less than 0.5% variation in CaO content and less than 5% variation in estimated reserves.

5.5.2 Method of Reserves Estimation

The reserves of various grades of limestone were estimated in the area using average factor and area method. In order to carry out quantitative assessment of various Lithounits of limestone, following parameters were considered :

- (i) The areal extent of Lithounits of limestone as measured on Lithounit map.
- (ii) The thickness of limestone was taken as 10 meters.

- (iii) The tonnage conversion factor of 2.5 tonnes of 1 cubic meter of limestone.
- (iv) Factor to account for mining and other losses 30%.

Table 5.8 : Estimation of Limestone Reserves in Bundi area

Lithounits	Type of Limestone	Areal Extent (sq.m.)	Volume (cubic meter)	Quantity (mt)	Reserves Considering 30% losses (mt)
Lithounit - D	High Grade	5530000	55300000	138.25	96.78
Lithounit - B	Cement Grade	25000000	250000000	625.00	437.50
Lithounit - A	Sub-Grade	3970000	39700000	99.25	69.475

The possible reserves of high grade, cement grade and blendable grade have been estimated as per details given in Table 5.8.

About 1.5 tonnes of limestone is required to manufacture one tone of cement. Accordingly, by taking 1.5 as limestone consumption factor, the acceptable grade limestone alone is good enough to manufacture 292 million tonnes of cement. The quantity of cement that can be produced by high grade and sub-grade limestone has been estimated as 65 and 46 million tonnes respectively. However, further detailed exploration through drilling as per NCB norms of complex deposits have to be carried out to assess sub-surface quality and proved category of reserves. The data generated after detailed exploration shall enable to estimate bench wise quality, preparation of bench wise slice plans, which is an essential pre-requisite for detailed mine planning for optimal and systematic utilisation of available reserves and grades.

5.6 Technical Classification of Bhander Limestone

The stratigraphy, structure and tectonics of the region have a direct bearing on the complexity of the deposit, which determines the quantum of exploration (boreholes spacing, drilling meterage, sample interval, number of samples etc.). Under the Norms for proving limestone deposit for cement manufacture, the limestone deposits have been classified into Simple, Complex and Intricate deposits. The simple deposits are horizontally bedded, continuous and uniform in quality. These are simple to explore with wide spaced drilling varying from 200 to 400 meter depending upon the stage of exploration. The complex deposits are folded, faulted, non-uniform in quality and the quantum of exploration required for proving the deposit is more than simple deposits. The drilling interval may vary from 50 to 200 meter depending upon the stage of prospecting. The intricate deposits are highly folded, faulted, highly variable in quality with lot of intercalations / impurities. The drilling interval cannot be generalised and may vary from 20 to 100 meter on case to case basis.

The Vindhyan limestone deposits by and large are horizontally bedded, uniform in quality and therefore easy to explore. However, in the area of study, these have undergone deformation in the form of folds and faults due to proximity of the Great Boundary Fault. As a result of mesofolds, beds are repeated at several places. The deposits may therefore be categorised as complex deposit.

5.7 Estimate of block capital cost and cost of production of cement

5.7.1 Estimate of Block Capital Cost

The total capital cost of the cement project has been estimated as Rs. 3400 million for a standard one million tonne per annum (MTPA) Greenfield Cement Project includes the cost of land and site development, building and civil work (including township cost) machinery and equipment, preliminary and pre-operative

expenses (including the interest on capital during construction period). A contingency provision of 10% on civil works, plant and machinery and on miscellaneous. fixed assets has been kept. The break up of the capital cost of Rs. 3400 million is given in Table 5.9.

Table 5.9 : Estimated Capital Cost for 1 MTPA Cement Plant

Sl. No.	Items	Cost (in Rs. Million)
1	Land and site development	50.00
2	Building and Civil Works	250.00
3	Plant and Machinery (as erected)	1900.00
4	Misc. fixed assets	350.00
5	Technical know-how fees and training expenses	100.00
6	Preliminary and capital issue expenses	120.00
7	Pre-operative expenses including interest during construction	300.00
8	Contingencies	255.00
9	Margin money	50.00
Total		3375.00

Say Rs. 3400.00 million

5.7.2 Estimate of Cost of Production

The unit cost of production for the proposed plant have been worked out with the following assumptions:

- Capacity utilization of the plant has been taken as 85%, total production works out to 0.85 million tonne per annum.
- Interest on term loan has been taken @ 12% p.a. and on short term @ 14% p.a.

The total cost of production per tonne of packed cement is estimated as Rs.1668.50 tonne, say Rs. 1670.00.

The selling price of cement varies from Rs. 130 to Rs. 150 per bag in Rajasthan. However, for working out the profitability, selling price of Rs. 140 per bag has been considered and the net realization has been worked out as Rs. 105 per bag, i. e. Rs. 2100.00 per tonne of cement. This gives a gross profit of Rs. 852.00 per tonne and payback period works out to be 4½ years. The details are given in Table 5.10.

Table 5.10 : Estimates of Production Cost

Sl. No.	Items	Consumption Factor/Tonne of Cement	Unit Rate (Rs.)	Cost of Cement (in Rs./Tonne)
1	Raw material and Consumables			
1.1	Limestone	1.30	120.00	156.00
1.2	Additives (Laterite / Bauxite / Red Ochre)	0.30	150.00	45.00
1.3	Gypsum	0.05	550.00	27.50
2	Utilities			
2.1	Power	80 kwh	4.00	320.00
2.2	Coal	0.18	2500.00	450.00
3	Stores & Consumables			10.00
4	Repairs & Maintenance			15.00
5	Salaries & Wages			50.00
6	Factory Overhead			20.00
7	Administrative Expenses			20.00
8	Depreciation			270.00
9	Interest on term loan @ 12% (average)			150.00
10	Interest on short term loan @ 14%			15.00
11	Packing Material			120.00
12	Cost of Production of Packed Cement			1668.50
13	Net Sales realization*			2100.00
14	Profit Margin Rs./Tonne			431.50
15	Profit before depreciation + interest			852.00
16	Payback Period			4½ years

* Rs. 2800.00 less Taxes and duties (Rs. 600.00) and selling expenses (Rs. 100.00)

5.8 Summary

The limestone of calcareous units A, B and D have been analysed for the relevant chemical and physical parameters. The limestone of youngest Lithounit D is richer in CaO (> 48 %) and low in SiO₂ (< 10 %) as compared to those of Lithounit B (CaO 44 - 48 %, SiO₂ 10 – 12 %) and Lithounit A (CaO 42 – 44 %, SiO₂ 12–16 %). On comparison with the standard chemical parameters (CaO, SiO₂ and MgO) for manufacturing of cement, these limestones have been categorized into three types- (i) High Grade Sweetener (Lithounit D), (ii) Acceptable Grade (Lithounit B) and (iii) Sub Grade (Lithounit A). T

The crushability and grindability indices of Limestone of various Lithounits indicate that it is amenable to crushing and grinding within the optimum level of energy consumptions. The quantity assessment of Lithounits D, B, and A have been made as 96.78, 437.50 and 69.50 million tonnes, respectively, from which 403 million tonnes of cement can be manufactured as per specification of Indian Standards profitably.

On the basis of techno-economic considerations and availability of sufficient limestone reserves, a cement plant of 3 million tonnes per annum capacity can be set up to cater to the requirement of nearby areas and the fast developing northern region.

CHAPTER 6

RAW MIX DESIGN FOR OPTIMAL UTILISATION OF MARGINAL GRADE LIMESTONE

6.1 Introduction

The designing of mixtures of specific proportion of raw material along with the limestone, forms a very important aspect called raw mix design for manufacturing of quality cement as per standard codes. The raw mix design and the kiln feed are considered to be the key for successful and profitable operation of cement plants. All the raw materials are naturally formed and they vary widely, chemically, mineralogically and physically. The raw mix design should, therefore, be made with an endeavour to optimise the utilisation of high grade limestone and maximise the use of subgrade (blendable) limestone.

Based on the Lithounits analyses as worked out in Chapter 4, the Bhandar limestones of Bundi are characterised by four Lithounits consisting of one with olive shales and the three grades of limestones mainly Blendable Grade, Cement Grade and High Grade quality. In the Chapter 5, an assessment of quality of limestone usable for cement manufacture has been made. In this Chapter, an attempt has been made to work out an optimum mix of blendable limestone with other two to use this important raw material for manufacture of cement.

The Portland cement clinker essentially contains the compounds of Tricalcium silicate (C_3S), Dicalcium silicates (C_2S), Tricalcium aluminate (C_3A) and Tetra calcium alumino ferrite (C_4AF). The limits of different oxide ratios (termed as moduli values) required in the raw meal to obtain an ideal raw mix for manufacturing of cement are given in Table 3.2.

The average chemical analysis of high grade limestone and sub-grade limestone of Bundi area, indicates that besides using both the grade of limestone in a suitable proportion, a small quantity of laterite, red ochre or bauxite is required to be added to achieve desired composition of raw meal for manufacture of cement. The laterite, bauxite and red ochre are found to occur in plenty in the near by areas, namely Pratapgarh near Chittorgarh and Iswal near Udaipur, located at a distance of 220 and 280 km from the area of study respectively (Fig 6.1). The average composition of limestones and other corrective materials- laterite, red ochre and bauxite used for raw mix design and chemical composition of coal ash used for manufacture of cement on laboratory scale is given in Table 6.1.

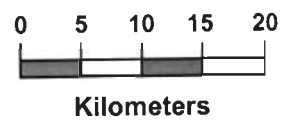
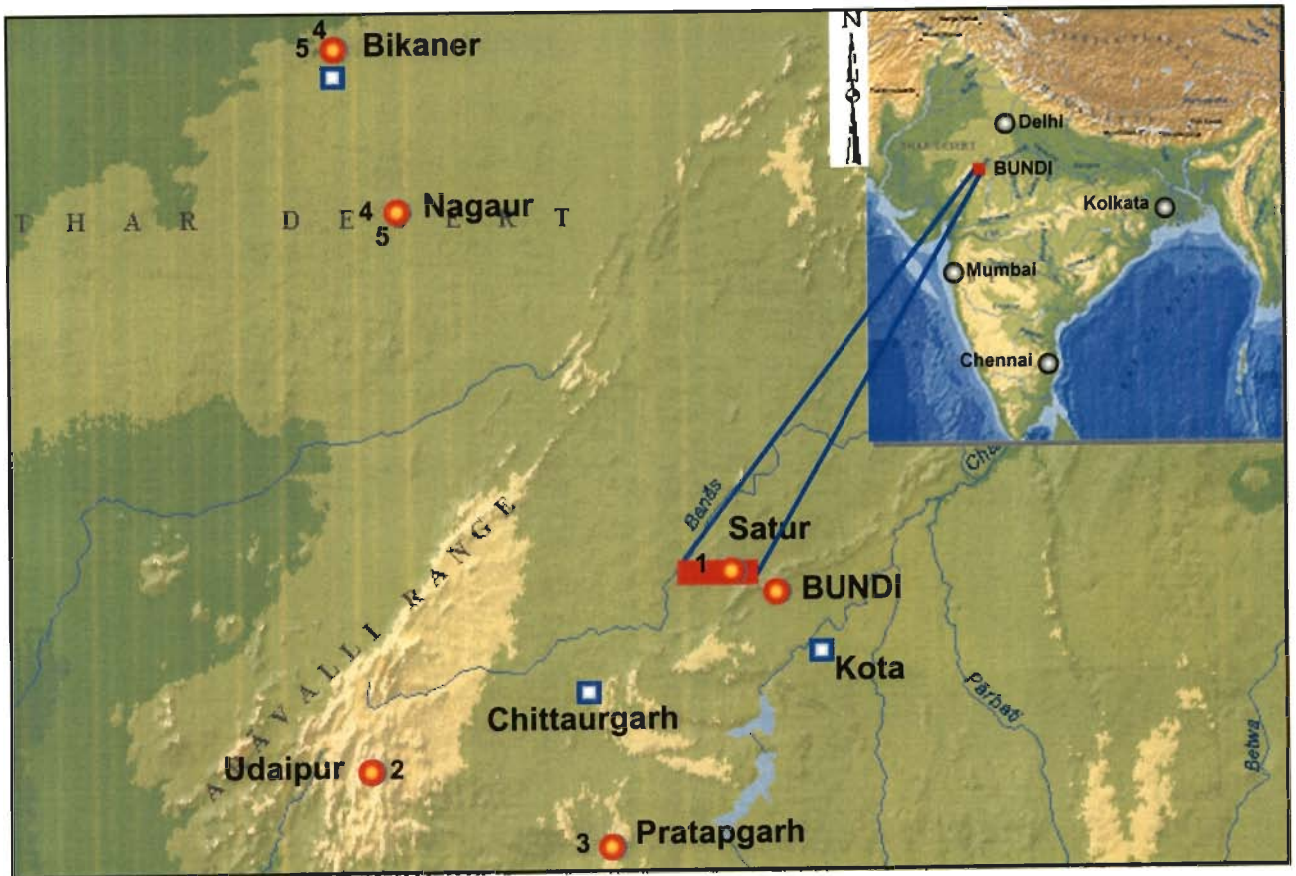
Table 6.1 : Average Chemical Constituents (%) of Bhander Limestone and Corrective Materials used for Raw Mix Design

Raw mix components	CaO	SiO ₂	Al ₂ O ₃	Fe ₂ O ₃	MgO	LOI*
High Grade Limestone	49.99	6.42	2.10	2.03	1.73	36.69
Sub-Grade Limestone	42.88	13.97	2.29	2.00	2.30	35.61
Laterite	2.50	19.49	15.90	49.66	0.37	10.58
Red Ochre	9.32	3.98	3.24	63.99	4.47	14.31
Bauxite	1.63	9.70	43.95	18.43	0.33	20.91
Coal Ash	7.80	58.90	21.22	6.67	1.65	0.51

* Loss on ignition

The proximate analysis of coal used for designing the raw mix and manufacture of clinker on laboratory scale is as follows :

Moisture (%)	2.91
Ash Content (%)	31.35
Calorific Value (Kcal/Kg)	4453



LEGEND

- 1 Location of Study Area - Satur (Bundi)
- 2 Source of Red Ochre - Iswal (Uaipur)
- 3 Source of Laterite and Bauxite - Pratapgarh
- 4 Source of Gypsum - Nagaur and Bikaner
- 5 Source of Lignite - Nagaur and Bikaner

Location of Industrial and mining wastes

- Flyash, Phospho Gypsum - Kota
- Lead Zinc Slag - Chittaurgarh
- Low Grade Mineral Gypsum - Bikaner

Fig. 6.1 : Sources of additives, lignite (fuel), industrial and Mining wastes with respect to study area

Based on the chemical composition of high grade and sub-grade limestone, additive materials and the limiting parameters of various modulii values, the raw mixes were designed and the clinker was manufactured on laboratory scale

The ratio of raw mix components and corresponding parameters of various raw mix design and phase composition of clinker is given in Table 6.2 and 6.3 respectively.

Table 6.2 : Raw Mix Proportions using Laterite and Red Ochre

Raw mix Components	Ratio of Raw Mix Components (%)		
	RM-1	RM-2	RM-3
High Grade Limestone	12.00	14.00	14.50
Sub-Grade Limestone	85.00	83.00	83.00
Laterite	2.00	2.50	2.50
Red Ochre	1.00	0.50	0.50
Coal Ash	5.50	5.50	6.50

Table 6.3 : Modulii Values and Phase Composition of various Raw Mix Designs

Parameters	RM-1	RM-2	RM-2
Modulii values			
LSF	0.87	0.87	0.86
S_m	2.78	2.68	2.69
A_m	1.14	1.14	1.19
Liquid	23.67	24.34	24.49
Phase Composition			
C_3S	49.46	48.93	46.14
C_2S	29.97	30.00	32.59
C_3A	5.27	5.44	5.85
C_4AF	11.92	12.30	12.08

In order to reduce the consumption of high grade limestone, a small quantity of bauxite was also added in the raw mix design. The design parameter of cement raw mixes and resultant clinker alongwith potential phase composition of various alternatives using bauxite are given in Table 6.4.

Table 6.4 : Design Parameters of Cement Raw Mixes and Resultant Clinker along with Potential Phase Composition using Bauxite

S. No.	Parameters	CL-1	CL-2	CL-3	CL-4
1.	Raw Materials				
	Sub-Grade Limestone	86.00	84.00	83.50	81.00
	High Grade Limestone	12.00	14.00	14.00	17.00
	Bauxite	1.00	0.50	0.50	0.50
	Red Ochre	1.00	1.50	--	--
	Laterite	--	--	2.00	1.50
	Ash Absorption	5.5	6.5	5.5	6.5
2.	Modulii Values				
	LSF	0.87	0.87	0.87	0.87
	SM	2.68	2.79	2.77	2.85
	AM	1.28	1.29	1.28	1.49
3.	Phase Composition				
	C ₃ S	48.66	49.17	49.07	49.04
	C ₂ S	29.89	29.97	30.07	30.17
	C ₃ A	6.49	6.34	6.32	7.46
	C ₄ AF	11.48	11.06	11.20	9.95
	Liquid Content	24.49	23.75	23.84	23.48

Based on the potential chemical composition of raw mix and clinker, RM-1 (without bauxite) and CL-1 (with bauxite) were used for preparation of lab scale clinker and subsequent investigation for qualitative assessment.

6.2 Burnability of the Selected Raw Mixes

Burnability studies of the raw mixes RM-1 without bauxite and CL-1 with bauxite were carried out at 1350⁰, 1400⁰ and 1450⁰C with a retention time of 20 minutes. The clinker sample prepared from raw mixes RM-1 & CL-1 respectively were room cooled and free lime determined and the results are given in Table 6.5. It is evident from the burnability studies that both the selected designs have better burnability and under plant conditions are capable of producing good quality clinker.

Table 6.5 : Burnability Studies of Raw Mixes

S. No.	Raw Mix	Temperature (°C)	Retention Time (min)	Free Lime (%)
1.	RM-1	1350	20	0.95
		1400	20	0.50
		1450	20	0.35
2.	CL-1	1350	20	0.80
		1400	20	0.43
		1450	20	0.29

6.3 Preparation and Evaluation of Bulk Clinker

In order to test the theoretically worked out designs, raw mixes RM-1 and CL-1 were prepared from weighted quantities of raw materials, ground in a ball mill at a fineness of 170 mesh sieve. The nodules were prepared in pan nodulizer and dried at 105⁰ ± 5⁰ for 2 hours and fired in an electric furnace at 1400 °C for 20 minutes. The resultant clinker RM-1 and CL-1 were studied for chemical, mineralogical and physical properties. The results of investigation are discussed below:

6.4 Chemical Analysis of Clinker

The clinker samples RM-1 and CL-1 were subjected to chemical analysis and results are presented in Table 6.6. The free lime content in the samples RM-1 and CL-1 were determined and found to be only 0.27 and 0.21 percent respectively.

Table 6.6 :Raw Mix and Clinker Composition of Raw Mix Designs

Constituents	RM-1		CL-1	
	Raw Mix	Clinker	Raw Mix	Clinker
LOI	35.43	--	35.44	--
SiO ₂	13.72	23.32	13.82	23.45
Fe ₂ O ₃	2.52	4.06	2.44	3.93
Al ₂ O ₃	2.38	4.64	2.28	4.50
CaO	43.88	64.65	43.93	64.74
MgO	0.80	1.26	0.82	1.29
Na ₂ O	0.13	0.20	0.13	0.20
K ₂ O	0.07	0.11	0.09	0.14

6.5 Optical Microscopic Studies of Clinker

The optical microscopic studied of polished section of clinker RM-1 and CL-1 indicates the presence of 46, 48 and 34, 32 percent of C₃S and C₂S respectively which matches closely with potential phase composition calculated by using Bogue' equation. The optical micrograph of RM-1 are given in Fig. 6.2 to 6.5 and for CL-1 in Fig. 6.6 to 6.9 respectively. The results of granulometry studies are given in Table 6.7.

Table 6.7 : Mineral Phase Analysis of Clinker Samples by Optical Microscopy

S. No.	Property	Granulometry			
		%	Min	Max	Average
1.	RM-1				
	C ₃ S	46	4	28	18
	C ₂ S	34	6	30	20
	C ₃ A	19	--	--	--
	C ₄ AF	19	--	--	--
2.	CL-1				
	C ₃ S	48	8	28	18
	C ₂ S	32	5	30	20
	C ₃ A	20	--	--	--
	C ₄ AF	20	--	--	--

6.6 Preparation and Evaluation of Ordinary Portland Cement

Ordinary Portland Cement sample OPC-A and OPC-1 were prepared by grinding clinker RM-1 and CL-1 with gypsum to a fineness of 301 and 310 m²/kg and tested for setting time, compressive strength, Le-Chatelier and autoclave expansion tests as per standard procedures (Table 6.8).

Table 6.8 : Performance of Ordinary Portland Cement prepared in Laboratory

S. No.	Property	Values	
		OPC-A	OPC-1
1.	Fineness (m²/kg)	301	310
2.	Setting Time (min)		
	(i) Initial	55	50
	(ii) Final	190	180
3.	Compressive Strength (N/mm²)		
	(i) 3 days	31.0	30.2
	(ii) 7 days	44.0	43.0
	(iii) 28 days	51.0	51.8
4.	Soundness		
	(i) Autoclave Expansion (%)	0.15	0.12
	(ii) Le-Chatelier Expansion (mm)	1.0	1.0

6.7 Setting Time of Cement

The initial and final setting time of laboratory prepared OPC-A and OPC-1 were determined as per IS: 4031-1988. The results indicate that initial and final setting time are of the order of 55 and 190 minutes for OPC-A and 50 and 180 minutes for OPC-1 respectively Table 6.8.

6.8 Compressive Strength

The compressive strength of cement samples of OPC-A and OPC-1 was determined as per IS:4031-1988 and found to be 31.0, 44.0 and 51.0 N/mm² for OPC-A and 30.2, 40.3 and 51.8 N/mm² for OPC-1 at 3, 7 and 28 days against the minimum values of 16.0, 22.0 and 33.0 N/mm² respectively (Table 6.8).

6.9 Soundness

Autoclave and Le-Chatelier expansion of cement sample OPC-A and OPC-1 as determined according to IS:4031-1988 was found to be 0.12 and 0.15 percent and 1 and 1 mm respectively. The results indicate high volume stability of the cement sample. From the above discussions it is observed that the cement sample OPC-A and OPC-1 prepared on laboratory scale using Bhandar limestone of Bundi passes all the requirements of IS: 269-1989 (Table 6.8).

6.10 Summary

Depending on the quality of limestone, various other raw materials such as laterite, red ochre and bauxite are used in small quantities for designing the raw mix. In order to optimally utilize the high grade limestone of Lithounit D with sub grade limestone of the Lithounit A, seven probable designs (three- laterite based and four-bauxite based) were found to satisfy the prescribed standard values of Silica modulus (1.7 - 3.5), Alumina Modulus (0.66 - 2.5), Lime Saturation Factor (0.66 -

1.02) and Phase Composition (C3S 40 - 60 %, C2S 15 – 35 %). Amongst these seven designs, two design (one from laterite based and one from bauxite based) characterized by minimum of high grade limestone were selected for laboratory testing.

The compressive strength of the cement produced from these two design (as detailed in the text) in the laboratory was found to be 31.0, 44.0 and 51.0 N/mm² for OPC – A and 30.2, 40.3 and 51.8 N/mm² for OPC – 1 at 3, 7 and 28 days against the minimum values of 16.0, 22.0 and 33.0 N/mm² respectively which qualify the norms as per IS: 269. These two designs have therefore, been proposed for manufacture of cement using sub grade limestone from Lithounit A alongwith high grade from Lithounit D. The limestone of Lithounit B can be used as such without requiring any blending.

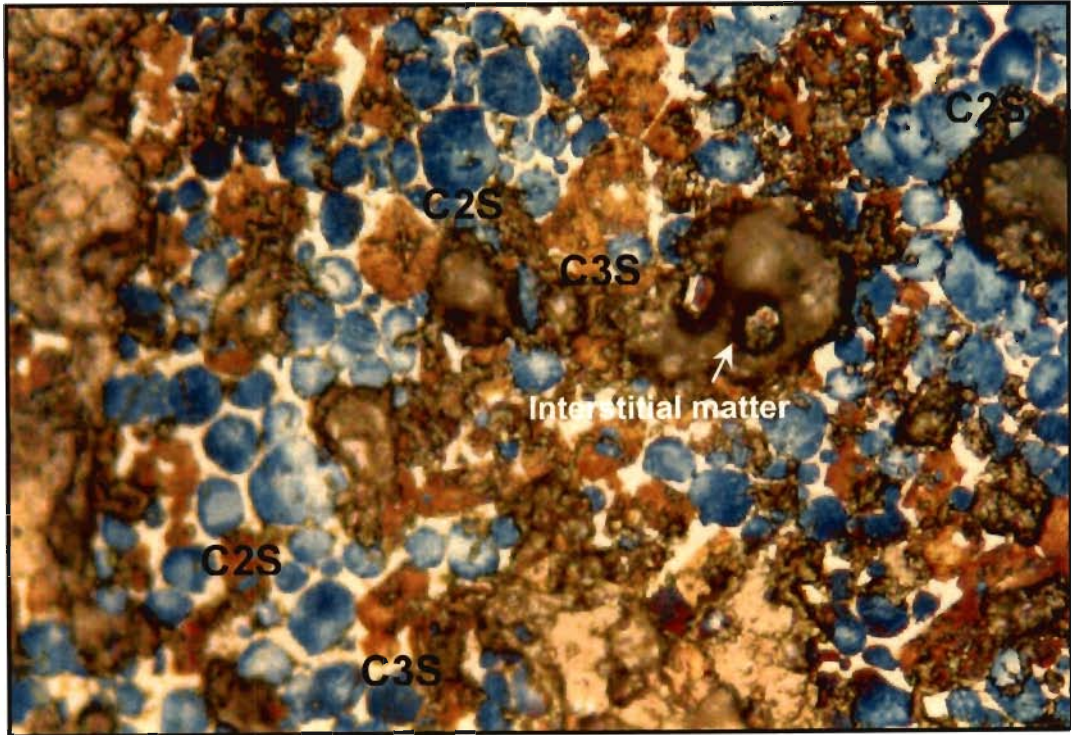


Fig. 6.2 : Photomicrograph of RM-1, showing clusters of C2S surrounded by lath shaped C3S grains on the periphery, 50 X

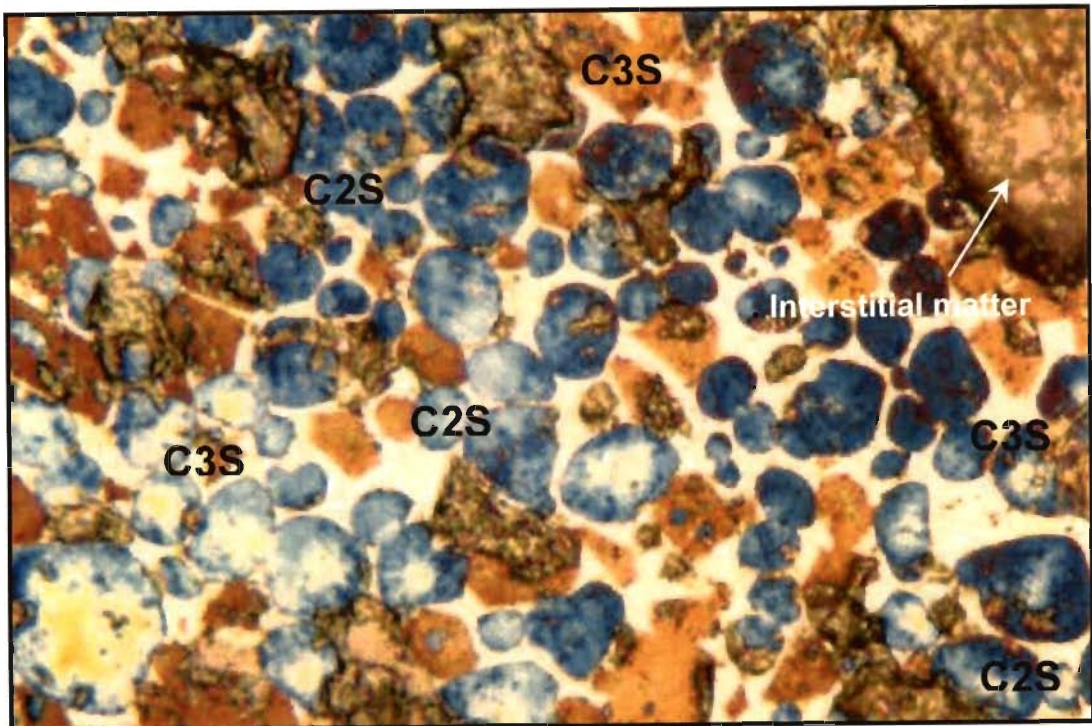


Fig. 6.3 : Photomicrograph of RM-1, showing Transformation of C2S in C3S, rounded C2S grains and lath shaped C3S grains with inclusions, 100 X

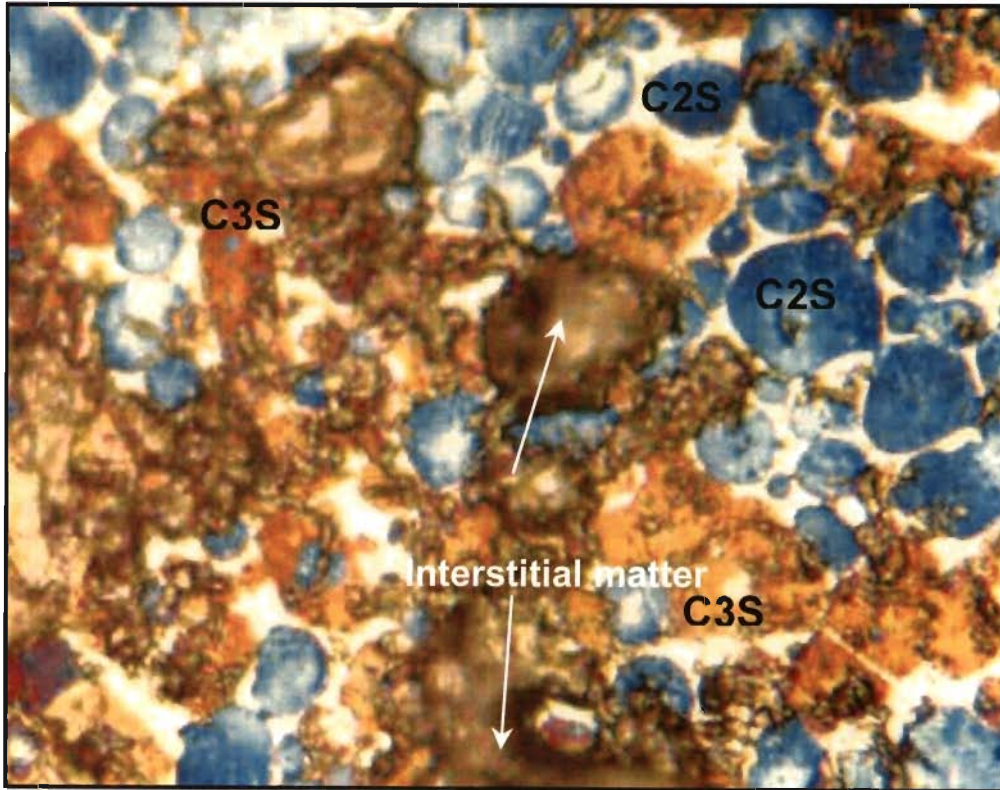


Fig. 6.4 : Photomicrograph of RM-1, showing fused grains of C3S, rounded C2S grains and clustered interstitial matter, 100 X

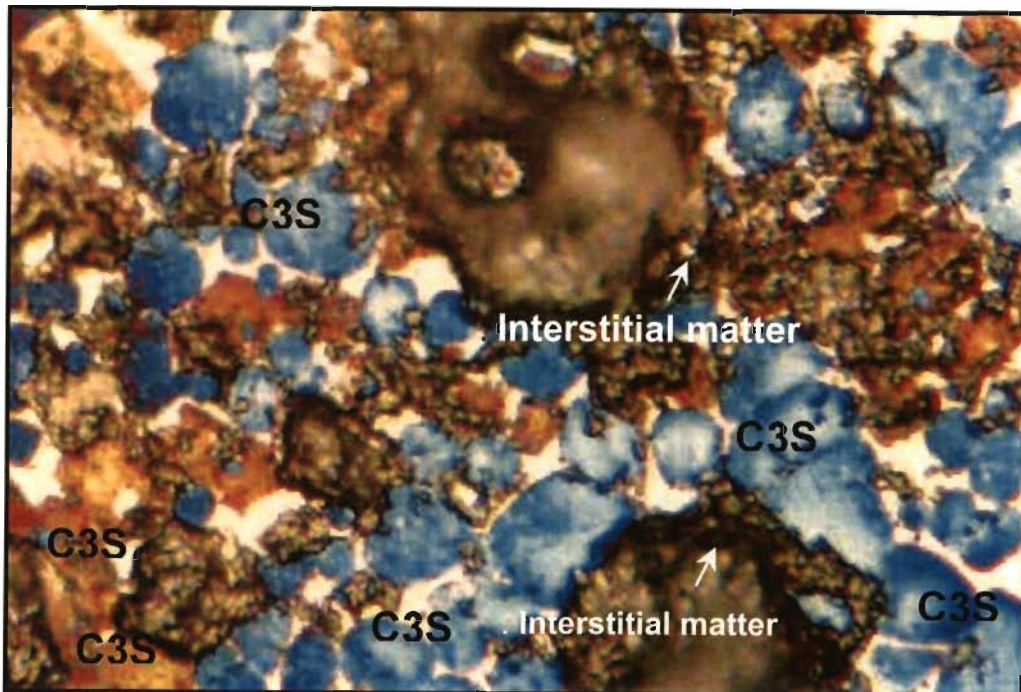


Fig. 6.5 : Photomicrograph of RM-1, showing transformation of clinker phases, 100 X

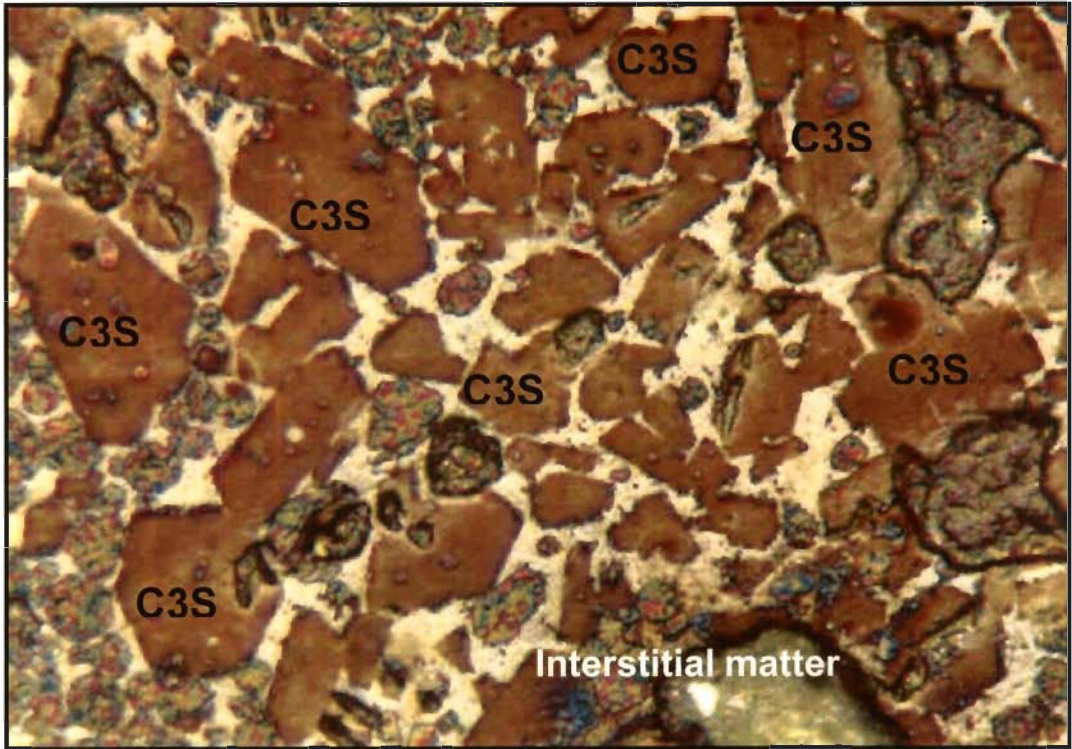


Fig. 6.6 :Photomicrograph of CL-1, showing hexagonal and pseudo-hexagonal grains of C3S within highly porous matrix, 100 X

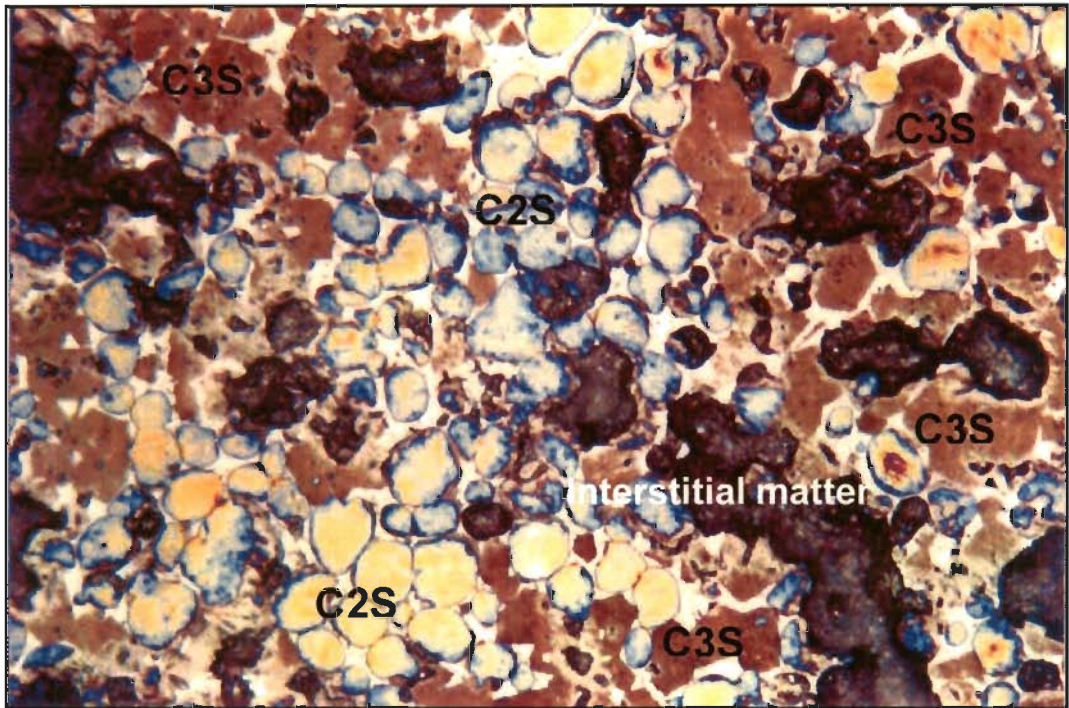


Fig. 6.7 : Photomicrograph of CL-1, showing C3S alongwith pre-dominant clusters of C2S alongwith interstitial matter, 100 X

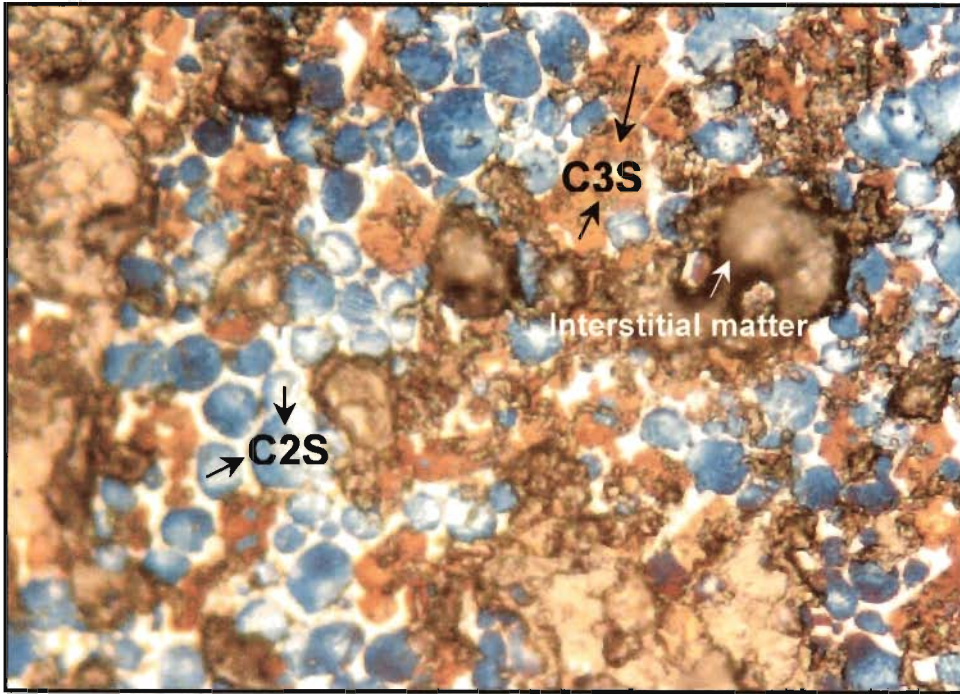


Fig. 6.8 : Photomicrograph of CL-1, showing homogeneous distribution of alite (C3S) and belite (C2S) grains with minor interstitial matter (C3A + C4AF), 50 X

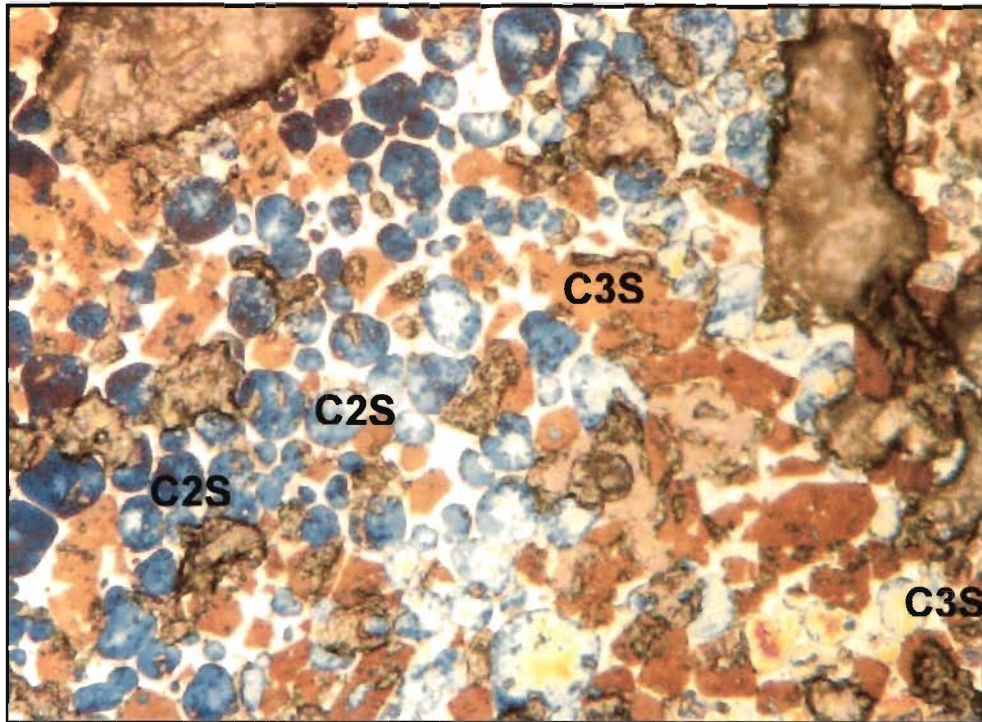


Fig. 6.9 : Photomicrograph of CL-1, showing pseudo-hexagonal alite (C3S) grains with inclusions of belite (C2S) and rounded C2S grains, clusters of minor interstitial matter (C3A + C4AF), 50 X

CHAPTER 7

SUMMARY AND CONCLUSION

A vast stretch of barren land occupied by extensive outcrops of limestone deposits occurs conspicuously in Bundi district of Rajasthan (Western India). This poorly and sparsely inhabited calcareous rock bearing terrain with the cultivable land, forms the locale of this study. This study is aimed at to assess possible use of these limestones as raw material to manufacture Portland Cement, the demand of which is continually increasing with increasing developmental activities in adjoining and nearby areas. Geographically, the area of study is located 10 km northwest of Bundi city along the National Highway No. 12, between the latitude $25^{\circ}25'$ to $25^{\circ}30'$ N and Longitude $75^{\circ}30'$ to $75^{\circ}40'$ E.

Geological Framework

Rocks exposed in the study area belong to the Lower Bhandar Group –a part of the Uppermost unit of the Vindhyan Super Group (Upper Proterozoic – Lower Cambrian ?). These rocks occur as sedimentary sequence juxtaposed to Great Boundary Fault (GBF). The GBF is the most conspicuous tectonic lineament in the pre-Cambrian terrain of western India and defines the boundary between Archaean metasediments of Hindoli Group and the sedimentary sequence of the Vindhyan Super Group (Prasad 1984, Srivastava et al., 1999). Stratigraphically, the Lower Bhandar formation consists of Ganurgarh Shale, Lakheri (Lower Bhandar) Limestone, Samaria Shale, Bundi Hill (Lower Bhandar Sandstone) and Sirbu Shale formations. The entire sequence except Sirbu Shale is exposed in this area

Based on field investigations and False Colour Composites (FCC) using IRS LISS-III Satellite data of the area of study, various lithological units – shales, limestones and sandstones have been mapped alongwith major and minor

structures. The ground reflectance data in the wavelength ranges of 485, 555, 650 and 815 Nm were also used for broad lithological discrimination.

In the area of study, the Vindhyan sedimentary sequence consisting of shale, limestone and sandstone is anticlinally folded into a macroscopic, non-plunging fold that trends ENE-WSW. The core of the fold is occupied by pink coloured Ganurgarh Shales forming the low lying terrain. The overlying pink and grey coloured Bhander Limestone exhibits gently undulating topography. It shows dendritic drainage pattern. The youngest pink, pale, grey, red brown to white coloured Bundi Hill Sandstone forms ridge like topographic feature.

Bhander Limestone

The Bhander Limestone, locally called Lakheri Limestone, occurs as calcareous sediments of pink, light grey and dark gery colours. Petrographic studies of these sediments, have indicated that they are micritic in nature. The Bhander Limestone in this area has been stratigraphically classified into the following four Lithounits on the basis of physical characteristics, petrography, stratification and internal structures.

Lithounit A

Overlying the Ganurgarh Shales (pre-Bhander Limestone), this oldest Lithounit of Bhander Limestone is characterised by pink to red coloured limestone and has gradational contact at the base. Generally these limestones are argillaceous and contain 10% or more terrigenous sediments- quartz, fine mica flakes and clays.

Intramicrodite occurs in the form of lenses of flat pebble breccia. It consists of intraclasts and matrix both of which are pink to red coloured micrite. The intraclasts range in size from a fraction of centimeter to more than a centimeter

and are poorly sorted and loosely packed. Their shape is variable and ranges from irregular to elongated with rounded edges.

Presence of features such as horizontal fenestrae, bird's eye structure, appreciable content of terrigenous admixture, general absence of algal mats, presence of micrite in the channels of small dimensions and predominant pink to red colour of sediments collectively indicate high to low supratidal environment for Lithounit A.

Lithounit B

Overlying the Lithounit A, the Lithounit B comprises alternate laminae of blue to grey coloured micritic limestone. They are wavy and discontinuous and extend laterally from few centimeters to few tens of meters. Lithounit B is generally devoid of sedimentary structures except for occasional symmetrical, straight crested ripple marks with wave lengths of 3 to 13 cm, mud cracks and exhibits profuse small domal stromatolites. This limestone shows alternate dark coloured lamination (0.5 to 1 mm) and light coloured lamination (4 to 5 mm thick).

The small lenses of flat pebble breccia (intrasparrudite) interbedded with the laminated micritic limestones, together with reversal of current direction, at places, indicate their depositional environment as intertidal flats with small shallow tidal channels.

Lithounit C

Lithounit C overlies Lithounit B and comprises mainly of calcareous shales with occasional lenses of calcareous siltstone. The shales are mostly olive green coloured but occasionally are bright green splintery and show parallel lamination on weathered surfaces. The intercalations of red shales are sometimes present towards the top of the sequence.

The parallel lamination and general absence of current and wave formed structures indicate that this olive coloured calcareous shale represents suspension deposits of a low energy environment of sedimentation. The low energy environment is interpreted as subtidal lagoons. However, the presence of, flat pebbles and channels and mud cracks at certain levels in the sequence are suggestive of occasional intertidal conditions, with subaerial exposures.

Lithounit D

This dark grey to black, laminated to thin bedded Lithounit of micritic limestones overlie the Lithounit C. The laminated beds show wavy and discontinuous laminae. The palisade structure is very common but ripple lamination, flaser bedding that signifies incomplete mud laminae trapped in ripple troughs during periods of slack water and symmetrical ripple marks occur rarely in this Lithounit.

The abundance of grey to dark grey coloured micritic sediments of this Lithounit suggests a low energy environment of deposition. Flat pebbles, mud cracks and channels are completely absent in this Lithounit and other features suggestive of wave and current action are rare. This Lithounit is therefore interpreted as shallow subtidal lagoonal deposits. The presence of algal mats in this Lithounit further supports the interpretation of a protected, shallow, subtidal environment in which this unit was deposited.

Spectral Response of Lithounits

The physical imprints, bio-indicators and chemical make up of sediments indicate that each Lithounit of Bhandar limestone was born in its own depositional environment. Accordingly, each Lithounit should have its own spectral response to various electromagnetic waves and therefore can be differentiated from one

another. With this premise, an attempt was made to identify various calcareous Lithounits of the Bhander Limestone using remote sensing data.

The pixel values of IRS LISS III data were determined with the help of ERDAS Imagine software for bands 2, 3, 4 and 5 in the wave length range of 0.52 - 0.59 μm (green), 0.62 - 0.68 μm (red), 0.77 - 0.86 μm Near Infrared (NIR) and 1.55 - 1.70 μm Short Wave Infrared (SWIR) respectively. Analysis of the data indicates that of all the four bands, only in linear contrast image of band 5 of SWIR, the calcareous Lithounits A, B, and D can be broadly identified.

Bhander Limestone as Raw Material for Cement

Portland cement is an active combination of silicates, aluminates and ferro-aluminates of lime, obtained by the preliminary grinding and mixing of the requisite quantities of lime, usually in the form of carbonates, silica, iron oxide and alumina, burning the mixture to incipient vitrification and grinding the resulting clinker to a fine powder with a small percentage of gypsum, to adjust the setting time. The limestone is, therefore, the basic raw material for cement manufacturing.

As per the norms evolved by National Council for Cement and Building Materials, India, cement grade limestone should have CaO 44 – 52%, SiO₂ <14%, MgO <3.5% and other major oxides such as Al₂O₃ and Fe₂O₃ should be able to satisfy the prescribed specifications of various modulli values.

Ideally, a limestone should be fine grained, organogenic, pelitic – amorphous or chemically precipitated (chemogenic) for cement manufactureping. It should have reactive silica in the form of alpha quartz and low crushability and grindibility indices. However, in nature, such limestones are rare and show variation in chemical and physical characteristics. Hence a detailed systematic analysis and evaluation of limestone is always carried out.

Keeping the above objective in view, representative samples of various Lithounits of Bhander limestone were collected from the area of study. A total of 160 samples were analysed for CaO, SiO₂, Al₂O₃, Fe₂O₃, MgO and loss on Ignition (LOI), besides other minor constituents such as Na₂O, K₂O, SO₃, Cl, P₂O₅ and Mn₂O₃.

The samples were analysed by X-Ray Fluorescence (XRF) technique and wet analysis following IS-1727-1967 and standard method evolved by National Council for Cement and Building Materials (NCB). The average chemical constituents as determined for various Lithounits of Bhander Limestone is given in Table 7.1, which indicate that the CaO content is lowest in Lithounit A as compared to Lithounit C and D. The corresponding SiO₂ content is maximum in Lithounit A, followed by Lithounit B and C respectively.

Table 7.1 : Average Chemical Composition of Lithounits of Bhander Limestone

Lithounits	No. of Samples	Average chemical composition (%)						
		CaO	MgO	SiO ₂	Fe ₂ O ₃	Al ₂ O ₃	LOI	Others*
A	45	42.88	2.30	13.97	2.00	2.29	35.61	0.95
B	65	46.24	1.67	10.72	2.05	2.60	35.76	0.96
C	10	1.63	2.78	62.44	5.14	13.48	13.36	1.17
D	40	49.99	1.73	6.42	2.03	2.1	36.69	1.04

* Includes the alkalis and other minor constituents such as Na₂O, K₂O, Cl, Mn₂O₃, SO₃ and P₂O₅.

The average compositions in terms of CaO, MgO and SiO₂ of various Lithounits of the Bhander Limestone (Table 7.1) when compared with the limiting values of prescribed specification of cement grade limestone, suggest the following:

- (i) The limestone of Lithounit B and D qualifies for use directly in the cement manufacturing. Lithounit D has highest CaO and least SiO₂ as compared to

- (ii) other Lithounit B, A and C and therefore provides the best variety of cement grade limestone.
- (iii) Lithounit B can be used directly as raw material for cement.
- (iv) The calcareous unit A is marginally sub-grade and can be used after blending with high grade Lithounit D.
- (v) The argillaceous unit C does not qualify for cement manufacturing.

Further, the low contents of Fe_2O_3 and Al_2O_3 in the limestone of Lithounits A, B and D suggest incorporation of red ochre and laterite, or bauxite in achieving the correct composition of raw mix.

On the basis of CaO and SiO_2 contents, the limestone of the area has been classified into three categories as shown in Table 7.2.

Table 7.2 : Categories of Limestone Based on Chemical Parameters

Categories of Limestone	CaO %	SiO_2 %	Remarks
High Grade Limestone	> 48	< 10	Mainly Lithounit D Recommended as sweetener to upgrade blendable grade limestone
Acceptable Grade Limestone	44 - 48	10 - 12	Mainly Lithounit B may be used directly
Sub-Grade Limestone	42 - 44	13 - 16	Mainly Lithounit A, can be upgraded by blending with high grade limestone

Besides CaO, SiO_2 , Al_2O_3 , Fe_2O_3 and MgO, the limestone may contain various sulphates, alkalis, phosphate, manganese, chlorides etc. in varying quantities, hence may affect the manufacturing process and quality of clinker, depending upon their concentration. The representative samples of limestone from Lithounit A, B and

D were analysed for such minor constituents. The maximum and minimum range in all the Lithounits are given in Table 7. 3 which indicates that these are well within the acceptable limits as per standard norms.

Table 7.3 : Minor Constituents in Bhander Limestone

Sr.No.	Minor Constituents	Range (%)		Acceptable rang (%)
		Minimum	Maximum	
1.	Na ₂ O	0.13	0.56	} 0.6
2.	K ₂ O	0.11	0.42	
3.	SO ₃	Traces	0.12	0.8
4.	P ₂ O ₅	Traces	0.040	0.6
5.	Mn ₂ O ₃	.021	.057	0.5
6.	Cl	.002	.006	0.05

The strength parameters of limestones namely, crushing strength and Bond's Index were determined for various lithounits. The crushing strength was found to be varying between 850 to 1000 kg/cm² and Bond's Index in the range of 11.3 to 16.0 kwh/tonne, thereby indicating amenability of these limestones for crushing and grinding under normal condition.

Raw Mix Design for Cement

The Lithounit B with acceptable grade of limestone can be utilized as such without any blending. However, in order to optimally utilise the high-grade limestone of the Lithounit D with sub-grade limestone, seven raw mix designs were made.

The two raw mix designs (Table 7.4) were selected on the basis of minimum consumption of high grade and maximum consumption of sub grade limestone for further evaluation, one with laterite and red ochre and the other one with red ochre and bauxite.

Table 7.4 : Raw Mix Proportion for Cement Production

Raw material components	Optimum Raw Mix Design	
	Type 1	Type 2
High Grade limestone (%)	12	12
Blendable Grade limestone (%)	85	86
Laterite (%)	2.0	-
Red Ochre (%)	1.0	1.0
Bauxite (%)	-	1.0

The potential composition of kiln feed and clinker were calculated based on the above theoretically worked out proportions. The moduli values (ratios of oxide components in clinker) and phase compositions of resultant clinker were then calculated and compared with the standard values prescribed for cement manufacture (Table 7.5). It is observed that all the moduli values and phase compositions are well within the prescribed limits, standardised for cement manufacturing.

Table 7.5 : Principal Moduli Values and Phase Composition of Raw Mixes

Moduli Values	Type 1	Type 2	Acceptable Range
Lime Saturation Factor (LSF)	0.87	0.87	0.66 - 1.02
Silica Modulus (SM)	2.78	2.68	1.7 - 3.5
Alumina Modulus (AM)	1.14	1.28	0.66 - 2.5
Phase Compositions			
C3S (Alite) %	49.46	48.66	40 - 60%
C2S (Belite) %	29.97	29.89	15 - 35%

Based on the theoretically worked out raw mixes, the cement was prepared on laboratory scale by grinding the laboratory fired clinker nodules with 5% gypsum. The cement thus prepared for both type 1 and type 2 designs have initial and final setting time as 55, 190 minutes and 50, 180 minutes respectively. The 28 days strength of the cements prepared were found to be 51 N/mm² and 51.8 N/mm², respectively, which are well above the minimum prescribed limit of 35 N/mm², thus conform to Indian Standard specification for Portland cement, thereby validating theoretically worked out proportions of various constituents in both types of Raw Mix Designs.

Feasibility of Setting of Cement Plant

In this area, on a conservative side, the possible reserve of limestone of Lithounits A, B and D have been estimated to be of the order of 69.5, 437.5 and 96.8 million tonnes respectively by average factor and area method. Taking 1.5 as limestone consumption factor, the Lithounits A, B and D are good enough to manufacture 403 million tonnes of cement (Table 7.6)

Considering all the parameters of fixed and variable costs, the cost to manufacture cement has been estimated as Rs. 1670/- per tonne at current rate. The profit margin as per current selling price of Rs 2100/- per tonne has been worked out to be Rs. 430/- per tonne.

Thus on the basis of techno- economic consideration and availability of limestone reserves, an eco-friendly three million tonnes per annum capacity cement plant can be set up in the area.

The barren area with well exposed limestone outcrops and negligible soil overburden, sparse habitation, little landuse, and availability of road and rail transport facilities, further make this limestone terrain attractive for such a venture.

As a spin off advantage, the proposed cement plant can use the industrial wastes of lead-zinc slag of Hindustan Zinc Ltd. Chittorgarh, fly ash from the Thermal Power Plant at Kota, Phospo Gypsum from fertilizer plant at Kota alongwith low grade mineral gypsum lying as a waste in Bikaner and Nagaur located at a distances of 250 km., 60 km., and 300 km. respectively to produce Pozzolana cement and slag cement (Fig. 6.1). (Panda and Goswami, 1985; Sharma et al. 1992; Ahluwalia and Page, 1992))

The typical spectral response of various lithounits of the Bhander Limestone and their chemical correlation may enable the application of this technique to explore the Bhander limestone of nearby areas. This would enable the savings in cost and time of initial exploration by avoiding reconnaissance survey and targeting the areas of interest.

In conclusion, it is surmised that the calcareous Lithounits, B, A and D of the Bhander limestone deposited in the physico chemical environment ranging from low energy to tidal (intertidal to supratidal), are qualitywise and quantitywise good enough to be used as raw material for commercial manufacturing of portland cement by adopting state-of-the-art environmentally friendly technology, A three million tonne per annum capacity cement plant can be set up in this area, which is characterized by easy availability and workability of limestone, besides requisite infrastructural facilities. In addition, the proposed plant can use the industrial and mines wastes of other nearby areas to manufacture Pozzolana and slag cements. The cement plant can cater to the requirement of nearby areas and also the fast developing northern region.

Table 7.6 : Bhander Limestone and its assessment for cement manufacturing

Lithounits of Bhander Limestone	Depositional Environment	Average Chemical Composition (% by weight)							Suitability of Limestone For Cement	Estimated Quantity (Million Tonnes)	
		CaO	MgO	SiO ₂	Fe ₂ O ₃	Al ₂ O ₃	LOI*	Others*		Limestone	Cement
Lithounit D. (Youngest) Dark Blue / Black Micritic Limestone	Protected, Shallow, Subtidal Environment	49.99	1.73	6.42	2.03	2.10	36.69	1.04	High Grade Limestone	96.8	65.0
Lithounit C. Olive Shales	Suspension Deposits of Low-Energy Environment	1.63	2.78	62.44	5.14	13.48	13.36	1.17	Not suitable for cement	--	--
Lithounit B. Inter laminated Blue Micritic Limestone	High Intratidal Flat Zone and in the Transitional Zone on to the Supratidal Flat	46.24	1.67	10.72	2.05	2.60	35.76	0.96	Acceptable Grade Limestone	437.5	292.0
Lithounit A. (Oldest) Red / Pink Argillaceous Micritic Limestone	High to Low Supratidal Environment	42.88	2.30	13.97	2.00	2.29	35.61	0.95	Sub-Grade Limestone	69.5	46.0 ***

* Loss on Ignition ** Includes the alkalis and minor constituents such as Na₂O, K₂O, P₂O₅, Cl, Mn₂O₃ and SO₃ *** based on optimum raw mix design

METHODOLOGY FOR THE DETERMINATION OF MAJOR OXIDES AND LOSS ON IGNITION IN LIMESTONE

I. Determination of Loss on Ignition

- **Principle**

The loss on ignition of limestone indicates the superficially absorbed moisture besides release of carbon dioxide due to decomposition of calcium carbonate.

- **Procedure**

Approximately 1.00g of sample (accurately weighed upto four decimal places) in a crucible of 25-30 ml capacity was heated in a muffle furnace maintained between 900-1000 °C for 20 minutes. After cooling it was again weighed. Checked for the loss in weight by second heating for 5 minutes and re-weighed. The experiment was repeated till constant weight was attained. The loss in weight is the loss on ignition and the percentage loss on ignition was calculated as given below :

$$\text{Loss on Ignition (\%)} = \frac{\text{Loss on Ignition} \times 100}{W}$$

where, W = weight of sample taken.

II. Determination of Silica

- **Principle**

The soluble silicates are decomposed by hydrochloric acid. The insoluble silicates are rendered soluble by treating with fusion mixture (1

$\text{Na}_2\text{CO}_3 + 1 \text{ Part } \text{K}_2\text{CO}_3$) in a platinum crucible. During heating at high temperature between $900\text{-}1000^\circ\text{C}$ for 15-20 minutes, all insoluble silicates get combined with alkalis rendering insoluble silicates to soluble silicate and are easily dissolved in hydrochloric acid, forming metasilicic acid in colloidal form. During evaporation, the meta-silicic acid gets converted into insoluble silica. The acidic solution is then filtered and the washed residue is ignited to give impure silica containing some of the impurities adsorbed like iron and alumina. Silicon dioxide is volatilised in the form of silicon tetrafluoride by hydrofluoric acid in the presence of sulphuric acid. The loss in weight is reported as pure silica.

- **Procedure**

About 0.5g sample (accurately weighed upto four decimal places) is taken in a beaker, moisten it with 10 ml of distilled water and 5-10 ml of hydrochloric acid is added and digested it until the sample is completely dissolved. Evaporated the solution on a steam bath to dryness.

For insoluble silicates the fused mass in a Platinum crucible is carefully placed in a beaker after cooling, 10-15 ml of hydrochloric acid is added and extracted the mass. Washed the crucible inside the beaker and digested the mass with the aid of gentle heat until it is completely dissolved. Evaporated the solution on a steam bath to dryness. Baked the residue in the oven at $105\text{-}110^\circ\text{C}$ for one hour. Added 5 ml of hydrochloric acid and diluted to 50-60 ml with water and heated it to just boiling, filtered it through Whatman No. 40 filter paper. Washed it with 1:99 HCl until it is free from chloride. The filtrate is again evaporated till dryness, baked the residue in an oven for one hour at $105 \pm 5^\circ\text{C}$ and treated the dry residue with 10-15 ml of dilute hydrochloric acid. The solution is then diluted with an equal amount of hot water, filtered and washed the small amount of silica with hot water until it is chloride free. The filtrate and washings are kept reserved for estimation of alumina and ferric oxide.

Placed the filter paper containing the precipitate in a weighed platinum crucible. The crucible is covered with its lid and heated gently to smoke off the filter paper without inflaming otherwise there may be chances of mechanical loss.

Finally, the residue was ignited at 1050-1100 °C in a muffle furnace. It was allowed to cool and weighed. Repeated the procedure till constant weight was attained. This gives the total silica contaminated with impurities mainly Fe₂O₃, Al₂O₃ etc. The ignited residue was treated with 1-2ml of water, 10-15ml of hydrofluoric acid and 1-2 drops of sulphuric acid and evaporated cautiously to dryness. Finally, the residue was heated at 1050-1100°C for five minutes, allowed to be cool and weighed, The difference between this weight and weight of the ignited residue represents the amount of pure silica. The silica recovered from the combined precipitate of alumina and ferric oxide was added to this amount. The residue was heated with 0.5 - 1.0 gm of potassium pyrosulphate and heated at below red heat until the residue is dissolved in the flux. Dissolved the fused mass in hot water and added to the filtrate and washings reserved for the determination of alumina and ferric oxide.

Calculations

$$\text{Silica (\%)} = \frac{(W_1 - W_2) + W_3}{W} \times 100,$$

where, W_1 = weight of silica and insoluble impurities;
 W_2 = weight of impurities;
 W_3 = weight of silica recovered from iron and aluminium oxide; and
 W = weight of sample taken.

III. Determination of Ferric Oxide

- **Principle**

A suitable aliquot of the silica-free acid solution of the sample is titrated against standard EDTA solution at pH 1 to 1.5 using sulphosalicylic acid indicator to a colourless or pale yellow solution.

- **Procedure**

- (i) The solution was made to 250 ml in a standard volumetric flask after removal of silica. The 25 ml of acid solution of the sample was measured through pipette in an Erlenmeyer flask. A very dilute, ammonium hydroxide (1:6) is added till turbidity appears.
- (ii) The turbidity was cleared with a minimum amount of dilute hydrochloric acid (1: 10) and added a few drops in excess to adjust the pH to 1 to 1.5. Shake well.
- (iii) Added 100 mg of sulphosalicylic acid and titrated with 0.01 M EDTA solution carefully to a colourless or pale yellow solution.

Calculations

1ml of 0.01 M EDTA = 0.7985 mg of Fe₂O₃

$$\text{Fe}_2\text{O}_3 (\%) = \frac{0.7985 \times V}{W},$$

where, V = volume of EDTA used; and

W = weight of the sample.

IV. Determination of Alumina

- Procedure

- (i) A quantity of 15 ml of standard EDTA solution was added to the same Erlenmeyer flask from burette after titrating iron, added 1.0 ml of phosphoric acid (1:3) and 5ml of sulphuric acid (1:3) and one drop of thymol blue into the Erlenmeyer flask.
- (ii) Added ammonium acetate solution by stirring until the colour changes from red to yellow. Added 25ml of ammonium acetate in excess to attain a pH of 5.5 - 6.
- (iii) Heated the solution to boiling for one minute and then allowed it to cool. Added 0.5 g solid xylenol orange indicator and bismuth nitrate solution slowly with constant stirring.
- (iv) Added 2-3 ml of bismuth nitrate solution in excess and titrated it with EDTA to a sharp yellow endpoint.

Calculations

$$V_1 = V_2 - V_3 - (V_4E),$$

- where, V_1 = volume of EDTA for aluminium;
 V_2 = total volume of EDTA used in titration;
 V_3 = volume of EDTA used for iron;
 V_4 = total volume of bismuth nitrate solution used in the titration; and
 E = equivalence of 1 ml of bismuth nitrate solution

$$1 \text{ ml of } 0.01 \text{ M EDTA} = 0.5098 \text{ mg Al}_2\text{O}_3$$

$$\text{Al}_2\text{O}_3 (\%) = \frac{0.5098 \times V_1}{W}$$

where, W = weight of sample,

V. Determination of Calcium Oxide

• Principle

A suitable aliquot of the silica-free acid solution is directly titrated against standard EDTA using Patton and Reeder's indicator at pH of 12 or slightly more. Magnesium gets precipitated as $Mg(OH)_2$ and does not interfere in the titration of calcium, The change of colour from wine red to blue indicates the end point.

• Procedure

- (i) A quantity of 10 ml of silica-free acid solution of the sample was measured into 250 ml Erlenmeyer flask, added 5 ml of 1:1 glycerol with constant stirring and then 1 ml triethanolamine.
- (ii) Added 1.0 ml of 4N NaOH solution and shaken well to adjust the pH to highly alkaline range of 12 or slightly more.
- (iii) Added approximately 50 ml of distilled water and 50 mg of solid Patton and Reeder's indicator.
- (iv) Titrated against 0.01 M EDTA solution. The end point of the titration was reached when one drop of EDTA produced a sharp change in colour from wine red to clear blue.

Calculations

1 ml of 0.01 M EDTA = 0.5608 mg CaO

$$\text{CaO(\%)} = \frac{0,5608 \times 25 \times V_1}{W}$$

where, V_1 = volume of EDTA used; and

W = weight of sample

VI. Determination of Magnesium Oxide

• Principle

A suitable aliquot of the silica free solution of the sample is titrated at pH of 10 against standard EDTA solution using triethanolamine for overcoming interference due to iron and aluminium and with thymol phthalexone as indicator. The titre value gives the sum of calcium and magnesium present in the solution from which the value corresponding to magnesium is obtained by subtracting that of calcium.

• Procedure

- (i) Measured 10ml of silica-free acid solution of the sample. Added 5 ml of 1:1 triethanolamine with constant shaking and 20-25 ml buffer solution of pH 10.
- (ii) Added 50 mg of solid thymol phthalexone indicator followed by 50 ml of distilled water.
- (iii) Titrated it against standard EDTA solution until the colour changes from blue to light pink or colourless.
- (iv) This titre value gives the sum of CaO + MgO present in the solution, Titre value of MgO is obtained by subtracting the titre value of CaO from the total titre value.

Calculations

1ml of 0.01 M EDTA = 0.4032 mg MgO

$$\text{MgO(\%)} = \frac{0.04032 \times 25 \times (V_2 - V_1)}{W}$$

where, V_1 = volume of EDTA used in calcium oxide titration;
 V_2 = total titre value used in this titration; and
 W = weight of sample

**METHODOLOGY FOR DETERMINATION OF MAJOR OXIDES AND MINOR
CONSTITUENTS IN LIMESTONE THROUGH X-RAY FLUORESCENCE
SPECTROMETRY**

I. X-Ray Fluorescence Spectrometry

• **Principle**

In this method the sample is irradiated by X-Ray beam from an X-Ray source. These X-Ray are absorbed by the elements present in the sample, which in turn emit X-Ray called secondary X-Ray or Fluorescence X-Ray. These X-Ray are characteristic of the elements present in the sample in terms of their wavelength (or energy) by way of their origin, that is transition amongst various energy states. Their intensities are directly proportional to the concentration of emitting element in the sample. Using suitable X-Ray wavelength dispersion and detection system, the intensities of various X-Ray lines are measured and correlated to elemental concentration.

• **Experimental Procedure**

Sample is converted into a suitable tablet form by using either pressed pellet or fused bead technique. Sample is exposed to primary X-Ray from the X-Ray tube. The Fluorescence X-Ray emitted by the element are analysed by using a set of collimating dispersing crystals, detectors and intensity measuring system. The intensities of secondary X-Ray are proportional to the concentration of element. A calibration is carried out using a set of suitable reference standard with varying range of oxide concentration. The concentration of elements are determined from the calibration curves.

In all cases check determinations (expressed in percent) have been made and repeated if satisfactory checks are not attained.

II XRF Instrument Used

X-Ray fluorescence spectrometer used for the elemental analysis of limestone samples in the present study was a simultaneous multi channel multi-dispersive system equipped with -

- (a) 11 fixed wavelength dispersive channels Na, Mg, Al, Si, P, S, Cl, K, Ca, Fe, Mn.
- (b) One energy dispersive channel for elements calcium onwards
- (c) Auto sampler with two sample trays. Each tray consisting of 36 sample positions.

Model Oxford MDX 1000 -

- (d) HP Computer Ultra VGA 1024
- (e) HP Printer Inkjet, Deskjet 690 C

III Sample Grinding Unit

The sample was ground with the help of Vibratory Cup Mill with digital grinding time control having Tungsten Carbide ring and puck vessel with 100 cm³ capacity.

IV Sample Pelletizing Unit

Sample pelletizing unit used for making pellets consisted Automatic Hydraulic Press having pressure range 0-40 tonnes with digital pressure control, pressure holding time, Stainless Steel Die and Non-breakable, Non-rusting Stainless Steel rings 40 mm dia.

V Sample Preparation and Testing

Pressed pellet technique was adopted for the sample preparation. All the limestone samples were oven dried first. About 50 g of sample was ground to 2 minutes to achieve $< 50 \mu\text{m}$ sample particle size. Grinding time was kept same in all the samples including calibration standards to maintain the uniformity in particle size and packing density of material.

About 15g of ground sample was poured into the die containing steel rings and pressed at 15 tonnes ram pressure. Pressure holding time was kept constant (i.e. 2 minutes), the care was taken to maintain the Pellet thickness not less than 2.5 mm. It was ensured that the analytical surface is smooth and shows no sign of crumbling or flaking. Pellets were checked carefully for any micro-crack present before analysis. In case the pellet is not conforming to any of the above guidelines, new pellets were made by ensuring that the die is clean.

Particle size of material, pressure and time of application of pressure was kept the same for limestone samples and calibration standards.

A portion of the ground sample was used to determine LOI in limestone samples. LOI was determined separately as per IS:1760 - 1991 and was reported alongwith concentration values, as per procedure described in Annexure I.

REFERENCES

Ahluwalia, S.C. and Page, C.H.; 1992, Effect of Low Grade Fuels, Combustible Wastes and Non-traditional Raw Materials, Proc. 9th International Congress on the Chemistry of Cement, Vol. I, P. 83-124.

Akhtar, K.; 1973, Petrology and Sedimentation Trends of the Bhandar Group (Upper Vindhyan) in the Singoli (Madhya Pradesh) - Mandalgarh (Rajasthan) area. Thesis Aligarh Muslim University, Aligarh, 219 P., Unpublished.

Akhtar, K.; 1975, Depositional Environments of the Proterozoic Bhandar Group, Mandalgarh - Singoli Area, Southeastern Rajasthan. In: Proc. Synmp. Sediment, Sedimentation and Sedimentary Environment, University of Delhi, Delhi, P. 91-99.

Akhtar, K. and Srivastava, V.K.; 1976, Ganurgarh Shale of Southeastern Rajasthan, India, a Precambrian Regressive Sequence of Lagoon - Tidal Flat Origin-. J. Sediment. Petrol, Vol. 45.

Akhtar Khurshieed; 1976, Facies Analysis and Depositional Environment of the Bhandar Limestone (Precambrian), Southeastern Rajasthan and adjoining Madhya Pradesh, India, Sedimentary Geology, Vol. 16, P. 299-318.

Albats, B.S; Shein, A.L.; 1997, High Quality Portland Cement Produced for Low Base Raw mix with Low Energy Consumption, 10th ICCG Gotegurg, li'015, P. 44.

Ali, M.M.; 1998, Long Term Performance Evaluation of High MgO Cement, Proc. 6th NCB International Seminar on Cement and Building Materials - New Delhi, P. X-3.

Balmiki Prasad; 1984, Geology, Sedimentation and Palaeogeography of the Vindhyan Supergroup, Southeastern Rajasthan, Memoirs of Geol. Surv. of India, Vol. 117, Part-I & II.

Barbanyagre, V.D.; 1997, Clinker Formation in High Silicate Low Temperature Melt, 10th ICCG Goteburg, li'011, P. 4.

Bissell,H.J. and Chilingar,G.V., 1967, Classification of Sedimentary Carbonate rocks, In:G.V. Chilingar,H.J.Bissell and R.W.Fairbridge(Editors) Carbonate Rocks,Elsevier, Amsterdam,pp,87-168

Black, M.; 1933, The Algal Sediments of Andros Island, Bahamas R. Soc. London Philos., Trans., Ser. B, Vol. 222, P. 165-192.

Boynton, R.S.; 1979, Chemistry and Technology of Lime and Limestone, Pub. John Wiley & Sons, P. 15.

Chatterjee, A.K.; 1979, Phase Composition, Microstructure, Quality and Burning of Portland Cement Clinker - A Review of Phenomenological Interrelations - Part 2, World Cement Technology, P. 165-172.

Coulson, A.L.; 1927, The Geology of Bundi State, Rajasthan, Rec. Geol. Sur. Ind. 60, P. 153-204.

Davies, G.R.; 1970a, Algal-laminated Sediments, Gladstone Embayment, Shark Bay, Western Australia. In: Carbonate Sedimentation and Environments, Shark Bay, Western Australia. Am. Assoc. Pet. Geol. Mem., Vol. 13, P. 169-205.

Davies, G.R.; 1970b, Carbonate Bank Sedimentation, Eastern Shark Bay, Western Australia, In: Carbonate Sedimentation and Environments, Shark Bay, Western Australia. Am. Assoc. Pet. Geol. Mem., vol. 13, P. 85-168.

Folk, R.L.; 1962, Spectral Subdivision of Limestone Types, In: W.E. Ham (Editor), Classification of Carbonate Rocks, Am. Assoc. Pet. Geol. Mem., Vol. 1, P. 62-84.

Folk, R.L.; 1959, Practical Petrographic Classification of Limestones - Assoc. Pet., Geol. Bull., Vol. 43, P. 1-38.

Friedman, G.M.; Amiel, A.J.; Braun, M. and Miller, D.S.; 1973, Generation of Carbonate Particles and Laminites in Algal Mats - Example from Sea-marginal Hyper saline pool, Gulf of Aqaba, Red Sea, Am. Assoc. Pet. Geol., Bull., Vol. 57, P. 541-557.

.Gebelein, C.D.; 1969, Distribution, Morphology and Accretion Rate of Recent Sub tidal Algal Stromatolites, Bermuda. J. Sediment. Petrol., Vol. 39, P. 49-69.

Gebelein, C.D. and Hoffman, P.; 1973, Algal Origin of Dolomitic Laminations in Stromatolitic Limestone. J. Sediment. Petrol., Vol. 43, P. 603-613.

Ghosh, S.P. and Imran, M; 1996, Raw Materials and Fuels, Present Scenario and Future Challenges, In Indian Cement Industry - The Challenges Ahead, CMA-NCB Publication, P. 9-17.

Ginsburg, R.N.; Isham, L.B.; Bein, S.J. and Kuperbug, Joel; 1954, Laminated Algal Sediments of South Florida and their Recognition in the Fossil Record. Univ. Miami Marine Lab., Coral Gables, Fla., Unpubl. Rept. No. 54-21, P. 33.

Gladwell, D.R.; Lett, R.E. and Lawrence, P.; 1983 Application of Reflectance Spectrometry to Mineral Exploration Using Portable Radiometers, Econ Geol. Vol 78, P 699-710.

Goetz, A.F.H.; Rock, N.B. and Rowan, C.L.; 1983, Remote Sensing for Exploration: An Overview , Econ. Geol., Vol. 78, No. 4, P. 573-590.

Gouda, G.R.; 1979, Raw Mix : the key for a Successful and Profitable Cement Plant Operation, World Cement Technology, P. 337-346.

Hacket,C.A.,1881,On the Geology of the Aravalli region,Central and Eastern.Rec. Geol.Surv.India,22,5.

Heron,A.M.,1917a, Geology of Northeastern Rajputana and adjacent districts. Mem. Geol. Surv.India,45(1),P128

Heron,A.M.,1922,Gowalior and Vindhyan System of South-eastern Rajputana,. Mem. Geol. Surv.India 45(2), P129-189.

Heron,A.M.,1936,Geology of South-eastern Rajputana and adjacent districts. Mem. Geol. Surv.India 68(1), P120

Hunt, G.R. and Salisbury, J.W.; 1970, Visible and Near Infrared Spectra of Minerals and Rocks, I., Silicate Materials, Modern Geology, Vol. 1, P. 283-300.

Hunt, G.R. and Salisbury, J.W.; 1971,Visible and near-infra-red Spectra of Minerals and Rocks II. Carbonates, Modern Geology, Vol. 2, P.23-30.

Hunt, G.R.; Salisbury, J.W. and Lenhoff, C.J.,1971, Visible and Near Infra Red Spectra of Minerals and Rocks, III. Oxides and Hydroxides, Modern Geology, Vol. 2, P. 195-205.

Hunt, G.R.; 1977, Spectral Signatures of Particular Minerals in the Visible and Near Infrared , Geophysics, Vol. 42, P. 501-513.

Imran, M.; Prasad, G.V.K and Panda, D.K.; 1989, Remote Sensing Applications in Evaluation of Limestone Deposits, Proc. Second NCB International Seminar on Cement and Building Materials, New Delhi, P. 1-14.

Imran, M.; Prasad, G.V.K. and Panda, D.K.; 1991, Remote Sensing Techniques for Limestone Exploration, Cement Industry-1991, P. 41-46.

Imran, M.; Panda, D.K. and Prasad, G.V.K.; 1992, Development of Remote Sensing Techniques for Prediction of Limestone Quality, Proc. 9th International Congress on Chem. of Cement, New Delhi, Vol. IV, P. 275-280.

Imran, M. and Panda, D.K.; 1995, Spectral Reflectance Studies in the Visible and near Infrared Range for Qualitative Assessment of Limestone - A case study, Proc. National Seminar on Raw Materials for Cement and Chemical Industry and Recent Trend in Mining, Veraval 24-25 January 1996, P. 45-54.

Imran, M.; 1998, Raw Materials Availability for the Growth of Indian Cement Industry in the next Millennium - In Challenges of 21st Century, CMA-NCB Special Publication, P. 8-18.

Indian Standard : Methods of Chemical Analysis of Limestone, Dolomite and Allied Materials IS : 1760 – 1991 (Part I to V).

Indian Standard, IS-269 - 1989 on Ordinary Portland Cement, 33 Grade.

Iqbaluddin; Prasad, B.; Sharma, S.S.; Mathur, R.K.; Gupta, S.N. and Sahai, T.N.; 1978, Genesis of the great boundary fault of Rajasthan, India, Proc third reg. conf. on geol. min. resources of Southeast Asia. Asian Instt of technology, Bangkok, P. 145-149.

.Kale, V.S. and Phansalkar, V.G.; 1985, Sedimentological Investigations of the Vindhyan Rocks of Taraj area, Jhalawer district, Rajasthan, Jour. Ind. Assoc., Sedum, Vol. 5, P. 34-46.

Kakali, G.; Kolovos, K. and Trvilis, S.; 2003, Incorporation of Minor Elements in Clinker : Their effect on the Reactivity of Raw Mix and the Microstructure of Clinker, 11th ICCC Durban, P. 98

Kedall, C.G. St.C. and Skipwith, P.A., d"E., 1968, Recent algal mats of a Persian Gulf lagoon. J. Sed. Pet. 38:P1040-1058.

Khursheed Akhtar; 1976, Facies Analysis and Depositional Environment of the Bhandar Limestone (Precambrian), Southeastern Rajasthan and Adjoining Madhya Pradesh, India, *Sedimentary Geology*, Vol. 16, P. 299-318.

Lea, F.M.; 1998, *Chemistry of Cement*, Pub. Arnold Publishers.

Logan, B.W., Rezak, R. and Ginsburg, R.N.; 1964, Classification and environmental significance of algal stromatolites, *Jour. Geol.*, 72: P68-83

Mallet, F.R.; 1869, On the Vindhyan Series in the Northeastern and Central Provinces. *Mem. Geol. Surv. Ind.* 7 (1).

Medlicott, H.B.; 1860, On the Vindhyan Rocks and their Associates in Bundelkhand. *Mem. Geol. Surv. Ind.*, Vol. 2 (2), P. 1-95.

Mehta, P.K.; 1980, Investigations on Energy - Saving Cements - World Cement Technology, P. 166-180.

Moranville, M.; Regourd and Boikova, A.I.; 1992, Chemistry, Structure, Properties and Quality of Clinker, *Proc. of 9th ICCG New Delhi*, Vol. 1, P. 20-22.

NCB Rapid EDTA methods for estimation of major constituents in Limestone, 1986, MS-11-86.

Neumann, A.C., Gebelein, C.D. and Scoffin, T.P., 1970, The composition structure, and erodability of subtidal mats, Abaco, Bahamas, *J. Sediment. Petrol.*, 40: P 274-297

Oldham, T.; 1856. *Jour. As. Soc. Beng.* Vol. 25, P. 253.

Panda, J.D. and Goswami, G; 1985. Utilisation of Slags from Defferent Metallurgical Industries, Proc.Nat. Seminar in Role of Building Materials Industries in Conversion of Waste into Wealth, New Delhi.

Prasad, B.; 1975. Lower Vindhyan Formations of Rajasthan. Rec., Geol., Surv. Ind., Vol. 106 (2), P. 33-53.

Prasad, B.; 1981. A Review of the Vindhyan Supergroup in Southeastern Rajasthan. Geol. Surv. Ind., Misc. Pub., No. 50, P. 31-40.

Prasad, B.; 1980. Vindhyan Stromatolites Stratigraphy in SE Rajasthan. Misc. Pub. Geol. Surv. Ind., No. 44, P. 201-206.

Prasad, B.; 1984, Geology, Sedimentation and Paleogeography of Vindhyan Supergroup, Southeastern Rajasthan, Geol. Sur. of India Mem116, P. 107.

Ramasamy, S.M.; 1995, Lineament Analysis and Stress Modeling of Vindhyan Basin, Rajasthan, India, In : Sinha Roy S and Gupta K R (Eds) Continental Crust of North West and Central India, Mem. Geol. Soc. Ind., Vol. 31, P. 279-310.

Roehl,P.O.,1967.Stony mountain (Ordovician) and Interlake (Silurian) facies analogs of Recent low energy marine and subaerial carbonates in the Bahamas.Am. Ass.Pet.Geol.Bull.51:1979-2032

Shuguang, H.U.; 1992, Studies on Rapid Burning Temperature, Time and Raw Meal Modulus Range in Portland Cement, Proc.9th ICC, New Delhi, Vol. II, P. 81-87.

Shah, H.U.; Bashir, A. and Zaka Uddin; 2003, Utilisation of Fluorospur, CaSO_4 and CaCl_2 for the Production of Low Energy Cement, Proc. 11th ICC, Vol. 1, P. 15.

Sharma, K.M.; Bhargava, R.; Yadava, D.; and Ahlywalia, S.C.; 1992, Metallurgical Slags as Blending Materials for Cement Manufacture. Proc. 9th International Congress on Chemistry of Cement, Vol. III, P. 121-127

Shinn, E.A., 1968, Practical significance of birdseye structures in carbonate rocks., J.Sed.Pet., 38, 215-223 .

Shinn, E.A. Lloyd, R.M. and Ginsburg, R.N., 1969, Anatomy of a modern carbonate tidal flat, Andros Island, Bahamas, J.Sed.Pet., 39, 1202-1228.

Sinha Roy, S.; Kirmani, I.R. and Sahu, R.L.; 1985. Limestone Resources of the Vindhyan sequence of Rajasthan, Indian Minerals, Vol. 39, P. 28-41.

Sinha Roy, S.; Kirmani, I.R.; Sahu, R.L. and Patel, S.N.; 1986. Fold Patterns of the Vindhyan Sequence in Relation to the Great Boundary Fault, Examples from Chittorgarh area, Rajasthan, Quat. Jour. Geol. Min. Met. Soc. Ind., Vol. 58(4), P. 244-251.

Sinha Roy, S.; Malhotra, G. and Mohanty, M.; 1998. Geology of Rajasthan, Pub. Geological Society of India. P. 157-178.

Srivastava, D.C.; Lisle, R.J.; Imran, M. and Kandpal, R.; 1999, A new approach for Paleostress Analysis from Kink Bands: Application of Fault-slip Methods, Jour. of Geol. Chicago, Vol 107, P. 165-166

.Srivastava, D.C.; Lisle, J. Richard, Imran, Mohd and Kandpal Rajeev; 1998, The Kink-Band Triangle: A Triangular Plot for Paleostress Analysis from Kink Bands, Journal of Structural Geology, Vol. 20, no. 11, P. 1579-1586.

Stuart E. Marsh and Timothy E. Townsend; Melvyn H. Podwysoki; Alexander, F.H.; Goetz; Gregg Vane; Philip N. Slater; 1983, Imaging Systems for the Delineation of Spectral Properties of Geologic Materials in the Visible and Near Infrared, Proc. Frontiers for Geological Remote sensing from Space, Pub. American Soc. of Photogrammetry. P.13-19.

Soni, M.K.; Chakraborty, S; Jain, V.K.; 1987, Vindhyan Supergroup – A review, Purana Basins of India, Ed. B P Radhakrishna Pub., Geol. Society of India, Bangalore, P. 87-138.

Tiwari, S., 1995, Extension of Great Boundary Fault (GBF) of Rajasthan in the Ganga Valley, Mem. of Geol. Society of India, 31, 311-328.

Wajdorvies, A.A. and Magnesite, S.A.; 1994, Correlation of Basic Refractory Brick Development with the Evolution of Cement Kilns-World Cement, Vol. 25, No. 2, P. 28-37

West, W.D., 1981. Vindhyan of Central India, Misc. Pub. Geol. Sur. Of India, 50, 1-4.

Van Straaten, L.M.J.U. 1961, Sedimentation in tidal flat areas Alberta, Soc. Pet. Geol. Jour., 9, P203-226